NPS ARCHIVE
1959
GATES, H.

PLASMA JET
ELECTRICAL CHARACTERISTICS

HERBERT K. GATES, JR.
JOHN K. THOMAS

PLASMA JET ELECTRICAL
CHARACTERISTICS

* * * * *

Herbert K. Gates, Jr.

and

John K. Thomas

PLASMA JET ELECTRICAL CHARACTERISTICS

by

Herbert K. Gates, Jr.

Lieutenant, United States Navy

and

John K. Thomas

Lieutenant, United States Navy

Submitted in partial fulfillment of
the requirements for the degree of

MASTER OF SCIENCE
IN
ELECTRICAL ENGINEERING

United States Naval Postgraduate School
Monterey, California

1 9 5 9

NPS ARCHIVE
1969
GATES, H.

Thesis
~~G253~~

PLASMA JET ELECTRICAL
CHARACTERISTICS

by

Herbert K. Gates, Jr.

and

John K. Thomas

This work is accepted as fulfilling
the thesis requirements for the degree of
MASTER OF SCIENCE
IN
ELECTRICAL ENGINEERING
from the
United States Naval Postgraduate School

ACKNOWLEDGEMENTS

The authors wish to express their sincere gratitude to Doctor Richard M. Head of the United States Naval Postgraduate School, who suggested this research topic, and whose guidance, assistance, and constructive criticism throughout the course of this investigation have been a constant source of inspiration; and to Doctor Allen E. Vivell of the United States Naval Postgraduate School for his cooperation, helpful advice, and constructive criticism. Many stimulating and helpful discussions with members of the Physics, Aeronautics, and Electrical Engineering Departments of the United States Naval Postgraduate School were held during the course of the investigation, and this aid is gratefully acknowledged.

During the design phase of this work, the authors were extremely fortunate in having the aid, advice, and direction of Doctor Milton U. Clauser and his staff, namely Doctor Rudolph Meyer and Mr. George Bronson, at the Physical Research Laboratories of Space Technology Incorporated, Los Angeles, California. Particular gratitude is felt to this group for their invaluable assistance.

The authors also wish to thank the Commanding Officer, United States Naval Shipyard, Hunter's Point, San Francisco, California, for the generous hardware and facility contributions made by his command.

ABSTRACT

The plasma jet has recently become the subject of considerable interest, particularly as a research tool for the production of extremely high temperatures, and as a source of high temperature, high Mach number flows for laboratory investigations.

The authors have been primarily concerned with the development of such a device and its associated hardware, for use at electrical energy levels in the order of three megawatts. Basic emphasis in this investigation was placed upon certain of the electrical parameters, in particular voltage and current variation with changing electrode separation. As a result of this investigation, a working method for adjusting the power level of the plasma jet was evolved.

As a by-product of the design calculations and investigations made, considerable information has been obtained on the flow parameters of the swirling fluid media used to contain the arc, and on the fluid and electrical parameters of the internally cooled coils used to obtain the magnetic field necessary for magnetic confinement attempts.

TABLE OF CONTENTS

Section	Title	Page
1.	Introduction	1
2.	Notation	2
3.	Plasma Jet Design	3
4.	Experimental Set-Up	11
5.	Volt-Ampere Characteristic	15
6.	Arc Resistance	42
7.	Temperature and Pressure	44
8.	Conclusions and Recommendations	47
Appendices		
A	Chamber Burst Pressure Calculation	50
B	Magnetic Field	57
C	Conclusions Based Upon Model Swirl Chamber Investigation	74
D	Power Generation Facilities	77
Bibliography		90

LIST OF ILLUSTRATIONS

Figure		Page
1a	Plasma Jet Design Cross Sectional View	4
1b	Component Parts, Plasma Jet	5
1c	Component Parts, Plasma Jet	6
1d	Simplified Circuit Diagram, Plasma Jet	16
2.	Stability Point Location on the Arc Volt-Ampere Characteristic	17
3.	Oscillographic Record of Brass Cathode-Copper Anode Run	20
4.	Oscillographic Record of Tungsten Cathode-Copper Anode Run	22
5.	Voltage versus Current, Tungsten Cathode-Copper Anode Run	23
6.	Operating Point Change Resulting from Change in Electrode Separation	25
7.	Electrode Insert Configuration	27
8.	Oscillographic Record of Tungsten Cathode-Tungsten Anode Run	28
8a	Anode Erosion for Asymmetrical Lead Configurations	30
8b	Anode Erosion for Asymmetrical Lead Configurations	31
9.	Volt-Ampere Characteristic, Two Inch Gap, in Helium	33
10a	Volt Ampere Characteristic, Sundry Gaps in Helium	35
10b	Volt Ampere Characteristic, Sundry Gaps in Helium	36
11.	Helium and Argon Runs, Oscillographis Comparison	38
12.	Volt-Ampere Characteristic, Two Inch Gap in Argon	41
13.	Arc Resistance Time Variation	43
14.	Pressure Variation Oscillograph	45

Figure Page

1B Temperature Change versus Power and Current for Water-Cooled 24 Gage Wire 59

2B Temperature-Flow Ratio versus Current for Water-Cooled 24 Gage Wire 60

3B Computed Values of Magnetic Flux Density versus Current 62

4B Computed Values of Magnetic Flux Density versus Current Density 63

5B Current versus Current Density for Various Tube Sizes 64

6B Comparison of Computed and Measured Values of Flux Density 66

7B Temperature-Flow Ratio versus Current for Refrigeration Tubing 67

8B Pressure Characteristic of Water through 3/16 Inch Refrigeration Tubing 69

9B Pressure Drop versus Flow Rate for Single Coil, 3/16 Inch Refrigeration Tubing 70

10B Coil Test Set Up 71

11B Coil Test Set Up 72

12B Coil Test Set Up 73

1C Swirl Chamber Pressure Distribution 76

1D Wiring Diagram, Postgraduate School Power Plant 78

2D Volt-Ampere Characteristic, Postgraduate School Power Plant 80

3D Volt-Ampere Characteristic, Hunter's Point Generator 81

4D Postgraduate School Power Plant 82

5D Resistor Banks and Inductors, Postgraduate School Plant 83

6D Instrumentation, Postgraduate School Plant 84

Figure Page

7D Plasma Jet in Gaseous Operation Configuration 85

8D Hunter's Point Power Plant 86

9D Resistor Banks, Water Pump, Plasma Jet at Hunter's Point 87

10D Plasma Jet in Water Operation Configuration 88

11D Plasma Jet in Water Operation Configuration 89

1. INTRODUCTION.

The plasma jet, or arc jet, is a relatively new device. Within recent years aerodynamicists, and others interested in space and re-entry problems, have become increasingly interested in the plasma jet as a device for the production of re-entry conditions, e.g. high temperature, high Mach number flows. The basic purpose of this investigation was the production and test of such a device.

The plasma jet consists, essentially, of a electric arc constricted, by a vortex core of swirling fluid, to a small diameter path between anode and cathode. This fluid column, by confining the arc, increases the current density and temperature within the arc. The temperature causes the fluid in and near the arc to vaporize and partially ionize, forming a plasma. The plasma is then released, or forced, through an orifice, or jet.

The intense heat generated in the arc is prevented from reaching the wall of the arc chamber by the swirling fluid formed by the tangential influx of fluid media. This fluid absorbs the major portion of the heat produced, and the gradient across it is such that the walls receive a minor portion of the generated heat.

This swirl also tends to stabilize the arc by restricting its path; that is, any tendency of the arc to increase its length is forestalled by a wall of water. In this device, in addition to the swirl, an axially directed magnetic field may be introduced between the electrodes in order to determine the practicability of magnetic containment.

2. NOTATION.

The symbols and notations used in this report are those commonly used in the fields of Electrical Engineering, and Gas Dynamics. The notation is as follows:

p_o = static pressure at chamber wall, pounds per square inch

P = electrical power in watts

h = enthalpy BTU/# mass

R = gas constant in gas equations, $ft^2/sec^2/^oK$; ohmic resistance in electrical equations

T = temperature in degrees Kelvin

γ = ratio of specific heats C_p/C_v

C_p = specific heat at constant pressure

C_v = specific heat at constant volume

MW = molecular weight

Z = compressibility

S = entropy

E = voltage rise in volts

V = voltage drop in volts

I, i = current in amperes

L = inductance in Henries

3. PLASMA JET DESIGN.

During the initial design phase, the works of numerous investigators in the field of plasma jets were carefully studied.[1] Perusal of these papers provided the basic requirements for design; however, specific design parameters were not provided. As a consequence, these required determination.

It was desired to produce a plasma jet capable of withstanding the temperatures and pressures produced by the expenditure of approximately three megawatts of electrical energy. Since this was to be a research tool, it was deemed desirable to incorporate provisions for the use of both gaseous and liquid media as cooling agents. It was further desired to provide an axially directed magnetic field between the electrodes so that the effect of magnetic confinement could be observed. A final consideration was the desire to make the overall design as simple as possible to facilitate manufacture and repair.

Fig. 1a presents a cross-section sketch of the final design. Figs. 1b and 1c are photographs of the component parts of the plasma jet.

The first parameter to be determined was the pressure which could be expected within the arc chamber. Since the device was to be used with both gaseous and liquid media, design calculations were based upon water as the cooling and plasma agent. It is to be expected that, through a liquid-swirl containment, maximum pressures would be encountered. Calculations of the expected pressure within the chamber were based upon the heat of vaporization versus the

[1] See references following Appendices.

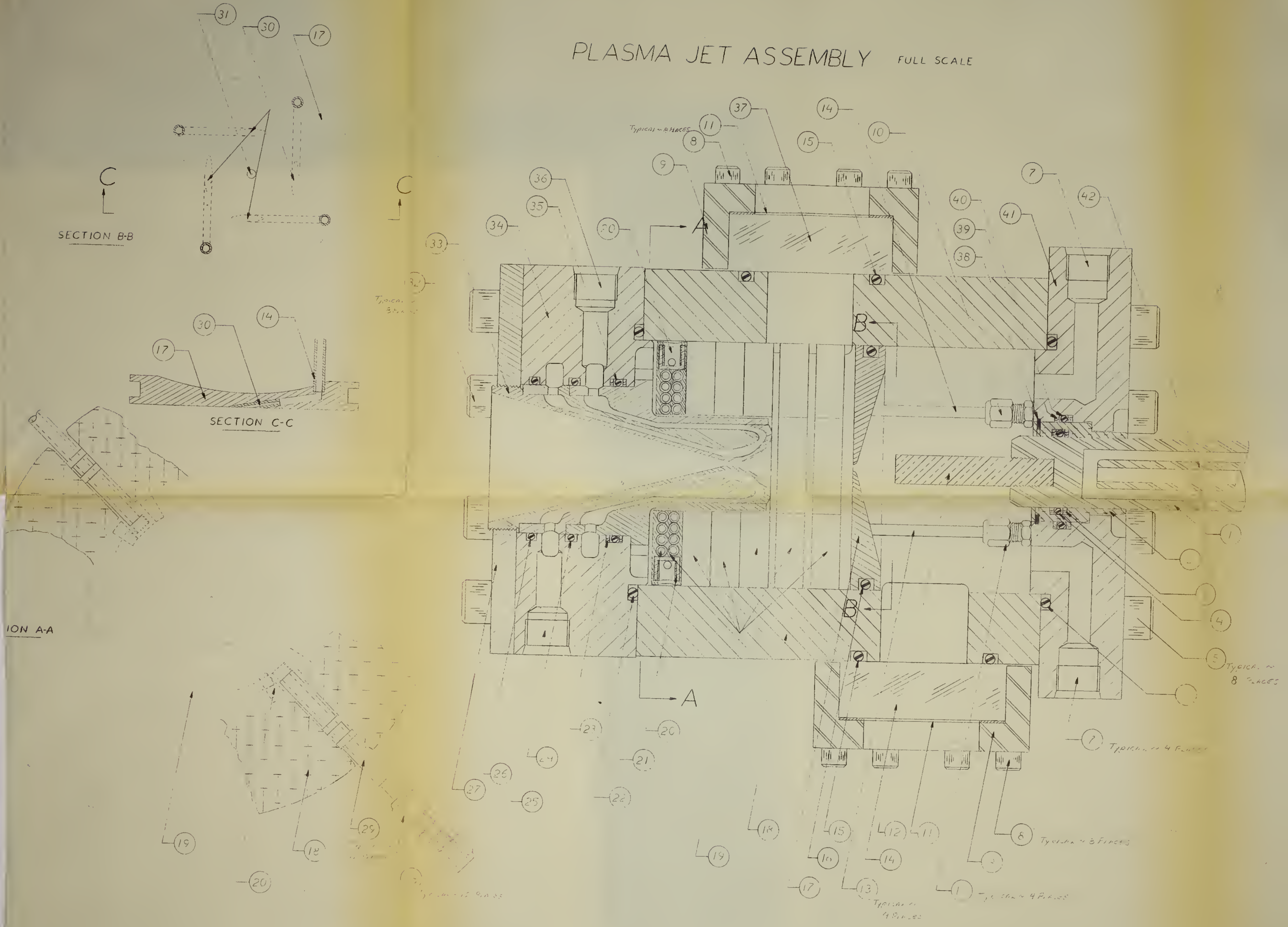

PLASMA JET ASSEMBLY FULL SCALE

PLASMA JET ASSEMBLY FULL SCALE

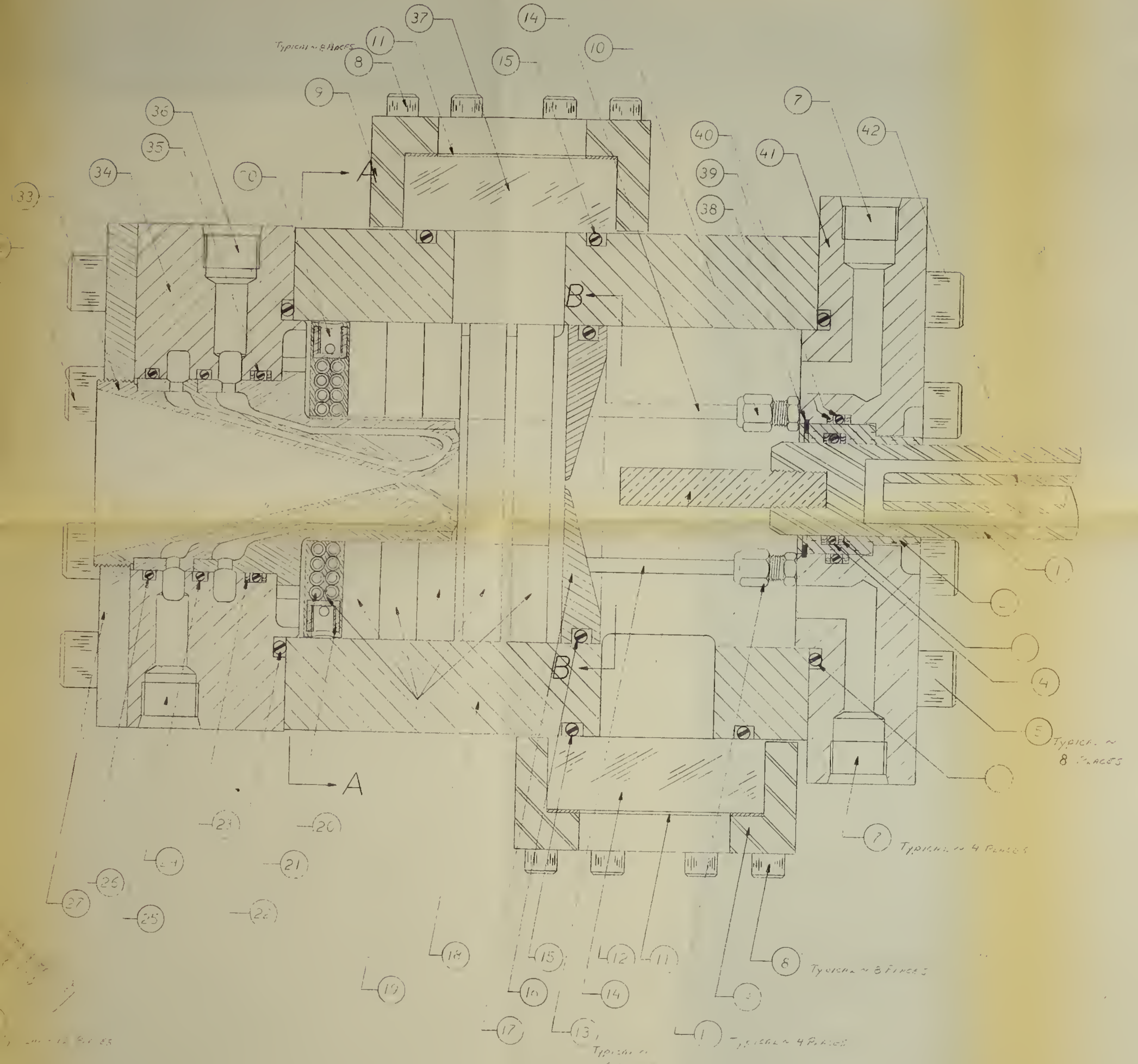

42	WATER COOLED CATHODE INNER SLEEVE - BRASS
41	LOWER END CAP - ALUMINUM
40	GLAND - LOWER END CAP "O" RING SEAL
39	GLAND - LOWER END CAP BACK-UP RING
38	GLAND RETAINING RING
37	FUSED QUARTZ WINDOW
36	WATER DRAIN PORT FOR WATER COOLED ANODE NOZZLE
35	UPPER END CAP - ANODE NOZZLE "O" RING SEAL
34	UPPER END CAP - ALUMINUM
33	WATER COOLED ANODE (ANNULAR) NOZZLE - COPPER
32	ALLEN HEAD SCREW - 1/2-13 THREAD × 3 1/2 LONG
31	JET ORIFICE DRAIN HOLE
30	JET ORIFICE NOZZLE - 1/64, 1/32, [illegible] DIAMETER ORIFICES
29	MAGNETIC COIL WATER FEED TUBE - BRASS
28	SWAGELOK NYLON UNION
27	ANODE NOZZLE LOCKING NUT - COPPER
26	LOWER END CAP - ANODE NOZZLE "O" RING SEAL
25	WATER INLET PORT FOR WATER COOLED ANODE NOZZLE
24	UPPER END CAP - ANODE NOZZLE "O" RING SEAL
23	UPPER END CAP - ANODE NOZZLE BACK-UP RING
22	LOWER END CAP CHAMBER BODY "O" RING SEAL
21	MAGNETIC COIL - 3/16 COPPER TUBING
20	MAGNETIC COIL END COLLECTOR - BRASS
19	MAGNETIC COIL ASSEMBLY - COPPER TUBING IN EPOXY RESIN
18	CHAMBER BODY - ALUMINUM
17	JET ORIFICE PLATE - COPPER
16	JET ORIFICE PLATE - CHAMBER BODY "O" RING SEAL
15	WINDOW - CHAMBER BODY "O" RING SEAL
14	PYREX GLASS WINDOW
13	JET ORIFICE WATER INLET TUBE - COPPER TUBING
12	SOLID CATHODE - COPPER, BRASS, CARBON, ZIRCONIUM AND TUNGSTEN
11	MICARTA SHEET WINDOW SHIM
10	SWAGELOK NYLON UNION
9	WINDOW RETAINING RING - CHROME-MOLY STEEL
8	ALLEN HEAD SCREW - 5/16-18 THREAD × 2 1/2 LONG
7	CHAMBER DRAIN OUTLET
6	LOWER END CAP - CHAMBER BODY "O" RING SEAL
5	ALLEN HEAD SCREW - 1/2-13 THREAD × 2 1/2 LONG
4	GLAND - CATHODE "O" RING SEAL
3	GLAND - CATHODE BACK-UP RING
2	PHENOLIC INSULATING CATHODE GLAND
1	WATER COOLED CATHODE OUTER SLEEVE - BRASS

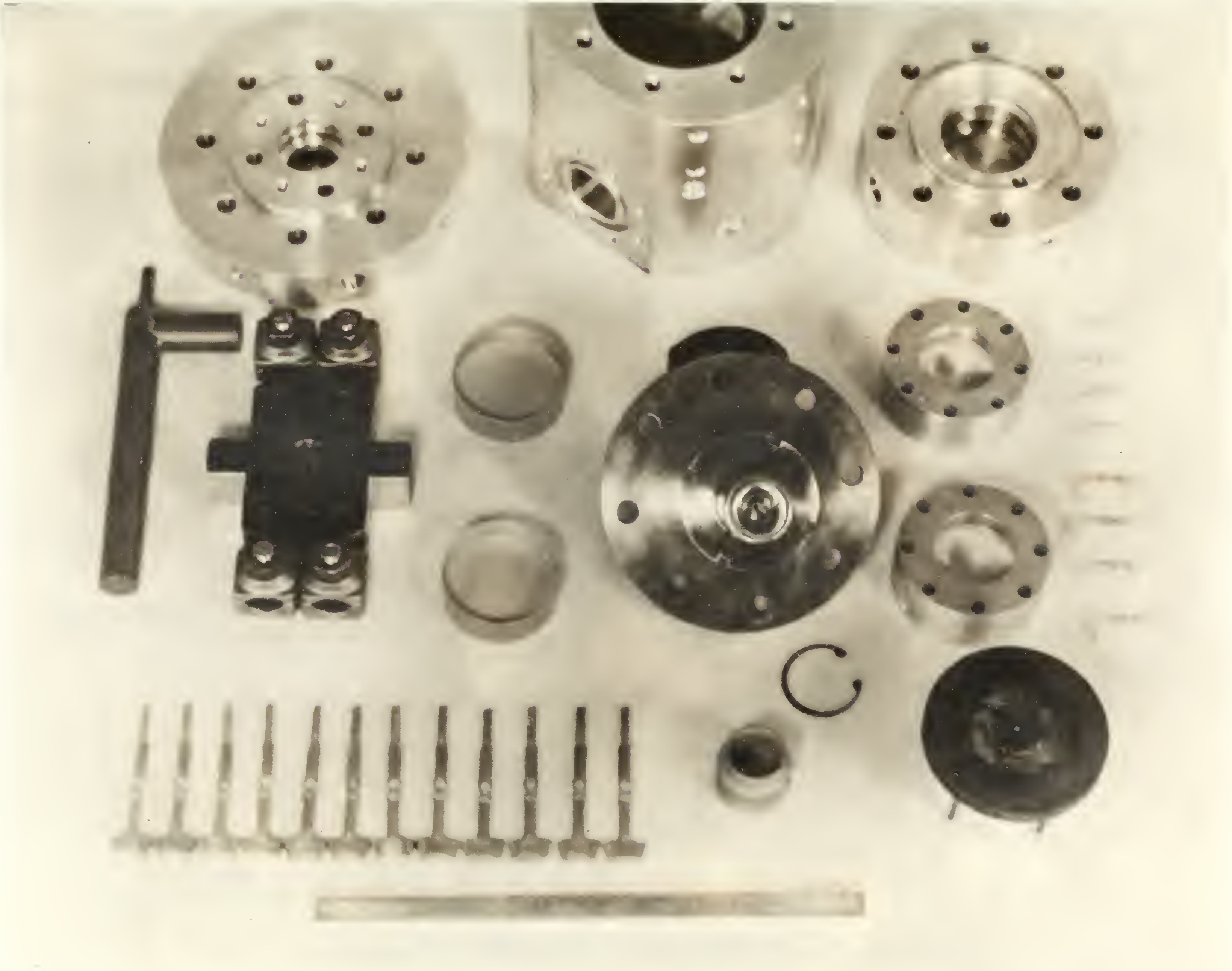

Fig. 1b Component Parts, Plasma Jet

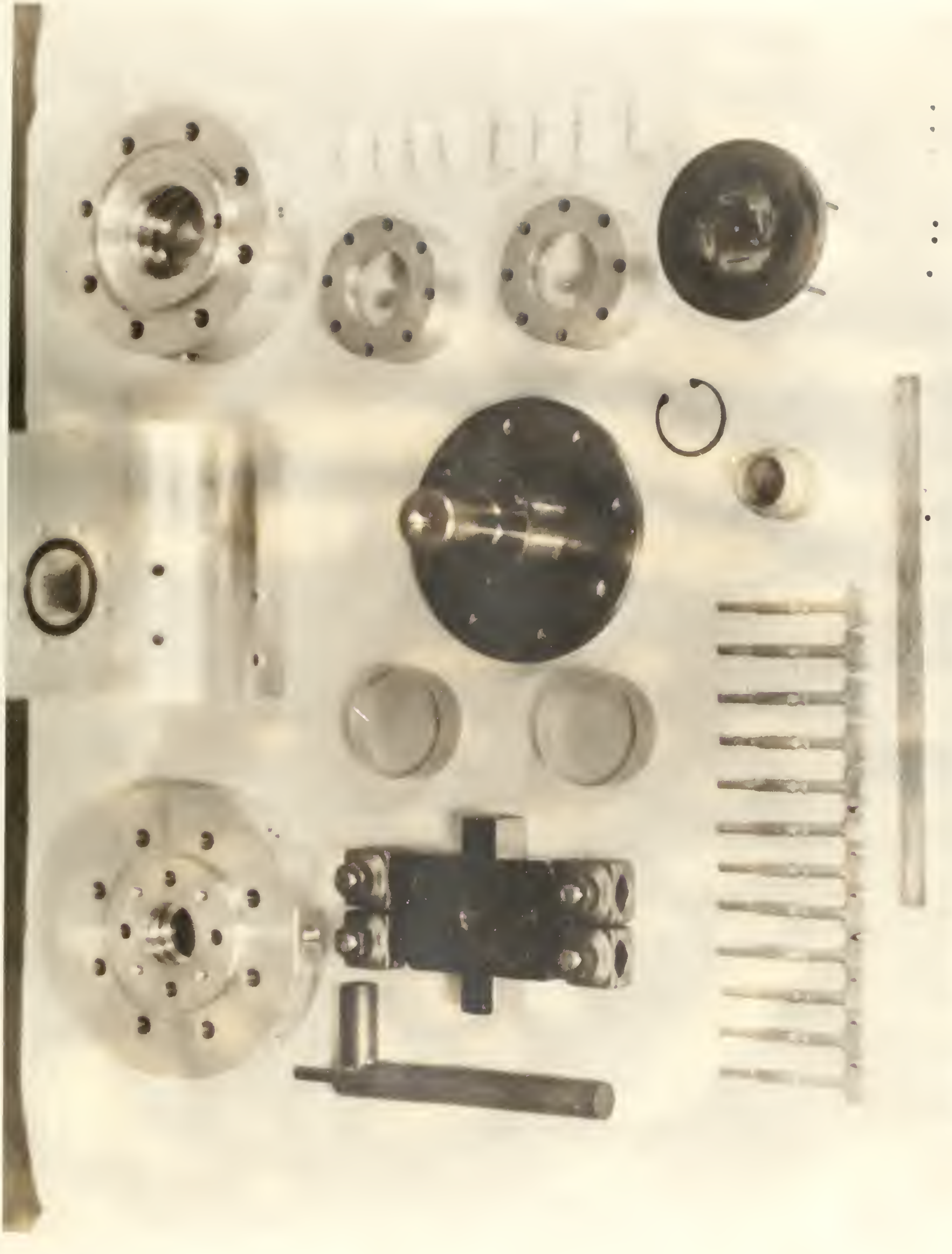

Fig. 1c Component Parts, Plasma Jet

dissociative equilibrium of water. It was necessary to make certain assumptions concerning flow through the nozzle:

1. Frozen composition: d (MW) = 0
2. Temperature gradient from chamber to throat would not vary appreciably: d (C_p) = 0
3. Pressure and temperature would be sufficiently high so that compressibility, Z, could be considered essentially unity: Z = 1
4. Isentropic flow in the nozzle: d (S) = 0

Under these conditions the flow can be treated as a perfect, isentropic gas. The problem which remains to be solved before pressure and flow can be specified is that of values of molecular weight, MW, and the ratio of the specific heats, γ. Instead of actually determining these values, approximations of extreme values were made to see if the problem was strongly dependent upon an accurate determination. It was found that the more accurate determination was not necessary. Under the conditions here stated, the problem was solvable. Appendix A contains the method, and actual solution, of this problem.

From the solutions obtained, it was felt that the maximum pressure which would be encountered in the chamber would be 5,000 pounds per square inch. A safety factor of 1.5 was incorporated when it became obvious that this would not produce any dimensional absurdities in the final design. Since a vortex was to be formed by a tangentially introduced fluid, the inner cross section of the chamber necessarily needed to be circular. For obvious reasons, stresswise, the overall shape of the chamber was cylindrical in nature.

It was decided to mount the chamber vertically. In this position gravity would not interfere with core formation, and any thrust developed by the device would be transmitted to the ground, eliminating any need for side thrust bracing. Furthermore, the discharge from the nozzle would be directed upward, eliminating a personnel hazard.

An arbitrary decision was made to make the nozzle the anode end of the device, and to provide cathode mounting in the base. It was desired, however, to make provision for reversal of polarity to study the effect of so doing. Since high Mach number flows were desired, the anode was constructed in the form of a supersonic nozzle. Heat transfer calculations conducted at this time indicated the need for water cooling of the anode and, further, that the walls of the anode should be as thin as practicable. This posed an electrical problem, in that sufficient cross sectional area was needed to prevent high local electrical resistance. As a compromise between these requirements, it was decided to construct the walls of one-sixteenth inch copper. The cathode posed no problem. A cathode holder was constructed of brass and internally cooled. The cathode was a cylindrical rod provided with threads for attaching to the cathode holder.

It was desired to incorporate in the design an axially directed magnetic field between the anode and cathode so that investigations could be conducted of magnetic containment and stabilization of the arc. From preliminary estimates of the degree of ionization within the arc it was felt that this field should be as strong as

possible. High magnetic field strengths, however, are normally associated with considerable bulk, and yet it was hoped that field strengths of from 15 to 60 thousand gauss could be obtained within the limited space of the cylinder interior. After considerable investigation it was found that water cooled conductors were quite capable of solving this problem. In order to provide for field strength variation and adequate cooling, the field was produced by several coils rather than by a single coil. Six of these coils, helically would in pancake form, were provided for in the design. These were to be constructed of refrigeration tubing. Field strengths in the desired range could be obtained with seven and one-half turns of three-sixteenths inch diameter refrigeration tubing, and considerably stronger fields are attainable with more turns of smaller tubing. To provide for ease of insertion and turbulence reduction in the swirl, the coils were encased in an epoxy resin. Appendix B contains considerable data illustrating the ability of these small tubes to carry currents of extremely high densities, when adequately cooled.

Provision was made in the design for enclosing a portion of the anode in this magnetic field.

The optimum position for the swirl plate, or diaphragm, was considered to be directly below the field coils. Previous investigators had shown that water introduced tangentially into a cylinder provided with axially located holes in its end plates produced a core of air along the axis of the vortex. To determine the actual mechanism of this phenomenon, a model of the plasma jet chamber was

manufactured and the different parameters varied to determine the controlling factors. Data and conclusions based upon this investigation can be found in Appendix C. As a result of this investigation, the suitability of vertical mounting, flow rates and hole sizes were determined. It was also determined that the contemplated diaphragm design produced a satisfactory core. It was necessary that the diaphragm be electrically neutral. Isolation from the base was provided by nylon unions; other portions of the diaphragm assembly which required electrical insulation were wrapped with teflon tape.

The base of the device was provided with drainage exits and water inlets. The cathode holder projected through a hole located axially in the base plate. Adequate insulation was provided at this point to prevent flashover between the oppositely polarized base and cathode.

Windows were provided in the chamber, as were pressure and temperature probe ports.

4. EXPERIMENTAL SET-UP.

The plasma jet was designed expressly for the expenditure of large quantities of electrical energy. Although it was desired to study the effects of both alternating and direct currents, it was decided to operate initially with direct current in view of the considerably greater work that had already been done on direct current arcs. The authors were fortunate in locating a motor-generator set capable of delivering 3,000 amperes at 80 volts continuously, which was then set up at the Naval Postgraduate School. This machine could deliver, for short periods, currents up to 5,500 amperes from a starting voltage of 100 volts. A second plant, at the San Francisco Naval Shipyard, Hunter's Point, was made available. At this installation, two motor-generator sets having a per unit rating of 4,000 amperes at 360 volts were used. These units could be used either singly, in series, or in parallel.

Due to the initially negative slope of the volt-ampere characteristic curve of electric arcs, it was necessary to control the current through an external resistance. At the Postgraduate School installation, a sufficient number of degaussing-grid resistors were placed in parallel to provide the required capacity. At the Hunter's Point facility, water cooled resistors were made available and used successfully.

It was felt that a certain amount of inductive reactance would be beneficial in stabilizing the arc. It was reasoned that an inductance in series with the arc would act in opposition to any violent changes in current magnitude. This inductance was provided

at the Postgraduate School plant by three 50 KVA transformers. These transformers were connected in parallel with their secondaries open-circuited. This transformer group was then placed in series with the arc. With this arrangement a considerable inductance existed in the circuit at low current magnitudes; however at high current magnitudes the transformer iron saturated, and the transformers served mainly as an energy storing device. In order to determine whether or not this introduction of inductance into the circuit was beneficial, the electrical circuit of the Hunter's Point facility was not provided with a series reactor.

Water having the proper pressure and mass flow rate for use in the swirl chamber was provided for by standard high-pressure, positive displacement, piston type pumps. During gaseous operation, helium and argon bottles were regulated to the desired inlet pressure.

Appendix D contains photographs and wiring diagrams of the two plants used.

Voltage and current measurements of the arc were made utilizing direct current amplifiers and pen oscillographs. Pressure measurements were obtained using a pressure pickup which utilized a frequency modulated oscillator in conjunction with a decade counter, presenting the pressure information in digital form. Temperature measurements within the arc were not attempted. Static temperature at the walls was obtained in several cases using thermocouple pickups which fed into a self-balancing recording potentiometer. Additional electrical meters were incorporated in the circuit as shown

in Appendix D.

Considerable effort was made to obtain an arc in the core of the water swirl. Sundry types and sizes of fuse wire were used for shorting the electrodes, various values of external resistance were tried, and the gap between electrodes was varied from the design value to nearly touching, but with no success. It was concluded that the 100 volts available was insufficient to produce the necessary degree of ionization to sustain an arc in the water configuration. Consequently, it was decided to utilize a gaseous medium.

Inasmuch as water provides considerable protection for the chamber walls which is lacking when gas is used as the cooling agent, it was decided to determine the effect of gas operation on the chamber walls by constructing an inexpensive model of the plasma jet out of pipe fittings. Toward this end, a standard two inch pipe nipple was provided with a cap at each end. These caps were drilled so that a nozzle could be force-fitted into one end and an insulator-cathode-holder combination fitted into the other. A pressure fitting was secured to the cathode end so that a gas could be introduced. It was felt that the heat generated would be a maximum if air were used as the cooling agent, since the use of noble gases, as contemplated, involves much lower ionization potentials. Operation of this device was attempted using a number 26 nichrome wire as the shorting agent.[1] Light-off was immediate and

---

[1] This wire was used throughout subsequent investigations with complete success. A possible detrimental property associated with the use of this material, however, is the finely powdered black residue resulting from the vaporization. This powder contributes to severe contamination within the chamber.

spectacular.[1] No severe damage to the chamber wall resulted from these tests, although a certain amount of pitting was evident. Consequently an aluminum sleeve was manufactured to protect the chamber wall of the large jet during gas operation. Utilizing the information obtained in the above test, operation of the designed configuration proceeded, using helium as the cooling medium and plasma agent.[2] No difficulty was encountered in obtaining light-off in the helium atmosphere. Normal operation throughout the subsequent investigations was as follows:

1. The inter-electrode spacing was decided upon and set.
2. The nichrome wire used for shorting the electrode gap was inserted.
3. The desired initial voltage and external values of resistance were set.
4. The recording instruments were calibrated.
5. The main breaker was closed and then reopened upon completion of the run.

It should be stated here that the authors were wary of using the water-cooled anode with other than a water swirl. The cost of this anode was such as to preclude replacement if it were destroyed. Consequently, solid copper anodes were constructed which had the same outside dimensions, but no provision for internal cooling. These anodes were used throughout the initial investigations.

---

[1] It is felt that, for educational institutions which do not have the desire to invest in a more sophisticated plasma jet, this simple device provides a fairly dramatic demonstration of plasma jet operation. All that is required is a suitable source of direct current power, say 100-150 volts and 1-2,000 amperes.

[2] Several of the noble gases were considered for use. Argon seemed to be the choice of most investigators in the field. Helium was chosen solely for economical reasons.

5. VOLT-AMPERE CHARACTERISTIC.

An enormous amount of work has been done in the general field of gaseous conduction of electric currents. The major portion of this work, however, has been concerned with low intensity currents. As early as 1929 evidence existed that the initially negative slope of the volt-ampere characteristic curve decreased and then became positive at high currents.[1]

Fig. 1d shows a simplified diagram of the electric circuit. Writing the voltage summation around the circuit, where lower case letters indicate instantaneous values:

$$E_g - i(R) - L\, di/dt - v_a = 0 \qquad (1)$$

For the purpose of this analysis, let it be assumed that the inductance is small and that the time rate of change of current is also a small quantity. In this event, the product of these two small quantities can be neglected when compared with the remaining quantities, and equation (1) reduces to:

$$E_g - i(R) = v_a \qquad (2)$$

Equation (2) defines the voltage drop across the arc. Furthermore, if the volt-ampere characteristic of the generated voltage, E_g , is linear, and the external resistance is constant, the left-hand

---

[1] J. D. Cobine, Gaseous Conductors, Ref. 1, page 299 refers to F. Kesselring, E. T. Z., 50, 1005, 1929 as corroboration for this statement.

Fig. 1d

Simplified Circuit Diagram

Plasma Jet

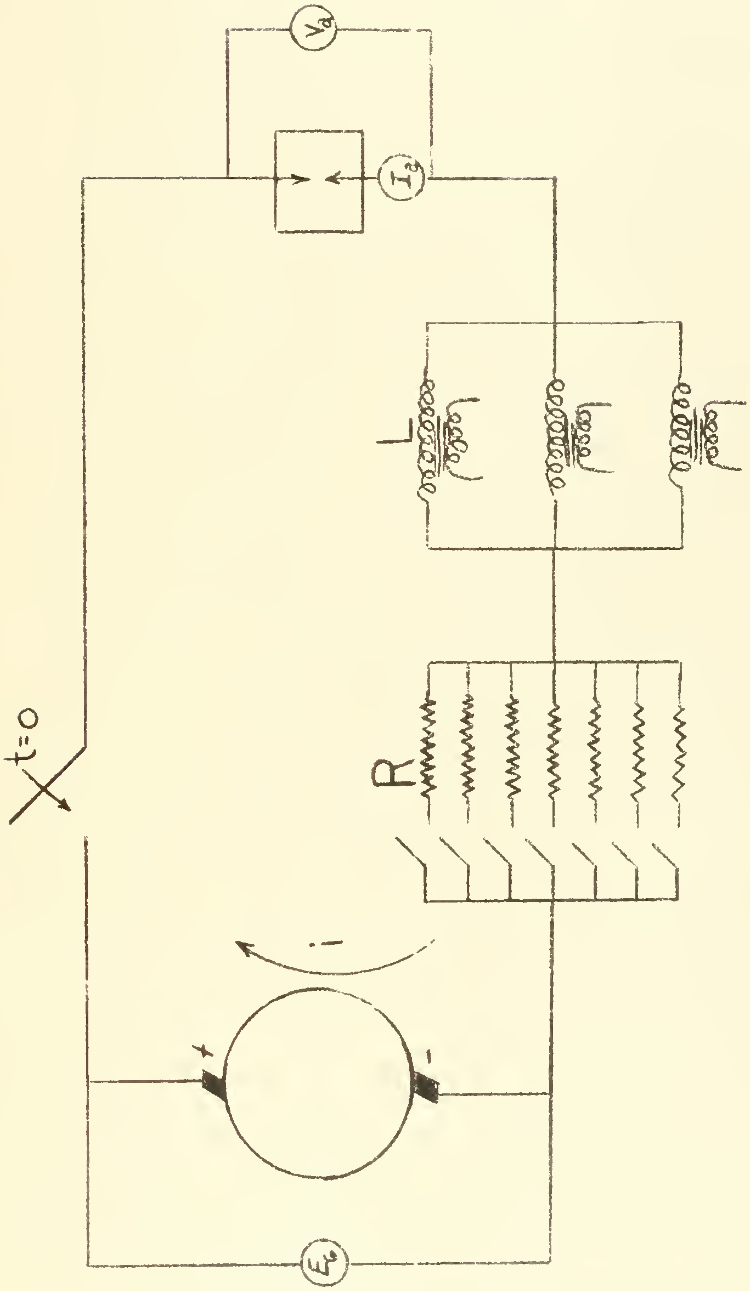

portion of equation (2) establishes a straight line on the volt-ampere plot. It is convenient in the analysis to plot the line thus defined and to term it the external resistance load line, or, simply, the load line.[1] The position of this load line may be varied by adjusting the value of the external resistance. It is to be noted that this line defines the voltage available to the arc; i.e., the arc voltage must lie somewhere on this load line.

A second equation is needed in order to locate the operating point on the load line. Assuming a voltage variation with current for the arc of the type mentioned in the initial paragraph of this section, and plotting this curve in such fashion that it intersects the load line, a diagram such as Fig. 2 is obtained. Referring to this diagram, it can be seen that equation (2) will be satisfied only at points A and C. Suppose that operation be at point C initially. If, due to some perturbation, the current decreases to I_x amperes, an increment of voltage E exists. This incremental voltage will drive the current back to I_c amperes. Any tendency for the current to continue to increase to some value greater than I_c amperes is prevented by the decremental voltage which would exist beyond I_c amperes. From this it can be seen that point C is one of stability. Examining point A in similar fashion, it can be seen that any perturbation to the right will cause the current to increase to the value I_c . Any perturbation to the left of point A

---

[1] If the reader will refer to Appendix D it will be noted that both generators used had volt-ampere characteristics which were essentially linear. Adequate cooling of the external resistance was provided, so that little change in the ohmic value occurred with changing current.

Fig. 2

Stability Point Location on the

Arc Volt-Ampere Characteristic

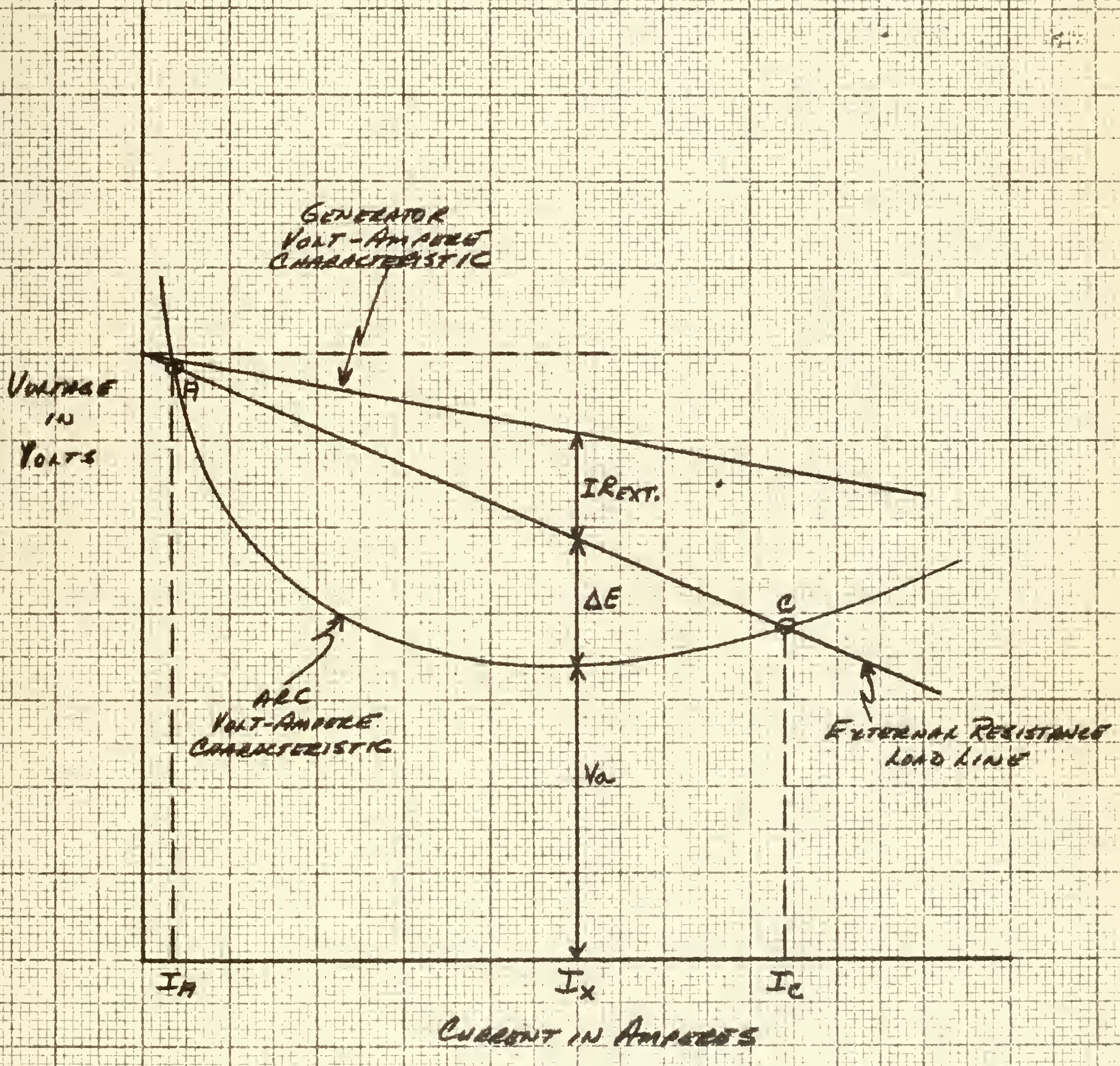
GENERATOR VOLT-AMPERE CHARACTERISTIC
VOLTAGE IN VOLTS
A
$IR_{EXT.}$
ΔE
C
ARC VOLT-AMPERE CHARACTERISTIC
EXTERNAL RESISTANCE LOAD LINE
V_a
I_A
I_X
I_C
CURRENT IN AMPERES

will cause the arc to extinguish, since more voltage is required by the arc than exists in the circuit. Consequently, the point A is one of instability. The arc is capable of operation at point A, but the slightest disturbance will cause a large change in the power level.

In view of the foregoing analysis, it would seem that definition of the volt-ampere characteristic would be a relatively simple project. If the external resistance is varied through increments, and the individual points "C" recorded, a smooth curve through these points will give the arc characteristic. The statement of method, and accomplishment of this end proved to be different matters, however.

Initial attempts at defining the characteristic curve were made using the solid copper anode previously described, in conjunction with a brass cathode, in an atmosphere of helium. This proved to be a very poor choice. The erosion rate was very high, and the molten metal in the arc stream produced severe instabilities.[1] Fig. 3 is an oscillographic record of voltage and current on a typical run. It was impossible to obtain useful information from this configuration.

Various attempts were made to reduce this erosion rate. Zirconium, carbon and tungsten were tried as electrode materials. Zirconium proved poor. Carbon seemed to resist erosion very well, but consistently shattered under the sudden application of high

[1] The erosion occurred principally at the cathode. As much as two inches per second of one-half inch diameter brass rod vaporized or melted during the runs made.

Brass Cathode Voltage and Current Time Variation

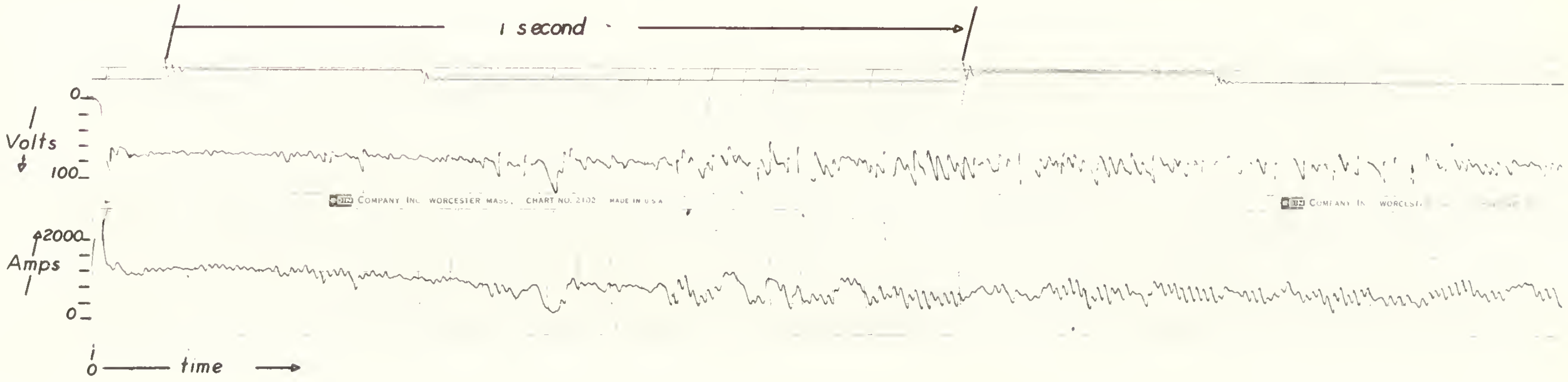

Fig. 3

current densities.[1] Tungsten showed good erosion and mechanical properties, and this material was decided upon for use as electrodes. The cost and difficulty of machining seemed to preclude manufacturing a complete nozzle of this material, and hence an initial series of tests was made with a tungsten cathode only.

Use of tungsten for the cathode erased the major instabilities. Fig. 4 shows a typical run using the above combination of electrodes. If the voltages and currents from these curves are plotted against each other, the curve of Fig. 5 is obtained. On this curve the timewise position of points has been indicated by increasing numbers. It will be noted that with increasing time the current increases to a maximum and then decreases. This variation is apparently linear. To analyze this result, consider the increasing and decreasing current regimes separately.

An explanation of those points which move toward increasing currents becomes apparent when it is noted that they lie on, or near, the external resistance load line. Thus during the period in which the arc is becoming established, equation (2) is satisfied. Since all voltage supplied by the generator which is not dissipated in the external resistance appears across the arc, the assumption that the product $L\, di/dt$ is approximately zero is seen to be valid.

---

[1] Various types of carbon were tried, from commercially available electrodes to brush carbon. It is known that other investigators have had considerable success with carbon electrodes. It would seem, therefore, that the difficulties encountered by the authors could be traced to a design deficiency. However, H. P. Furth, Strong Magnetic Fields, Scientific American, Vol. 198, No. 2, Feb., 1958, p. 28, has an interesting article which might be an explanation of the rupturing encountered.

Tungsten Cathode Voltage and Current Time Variation

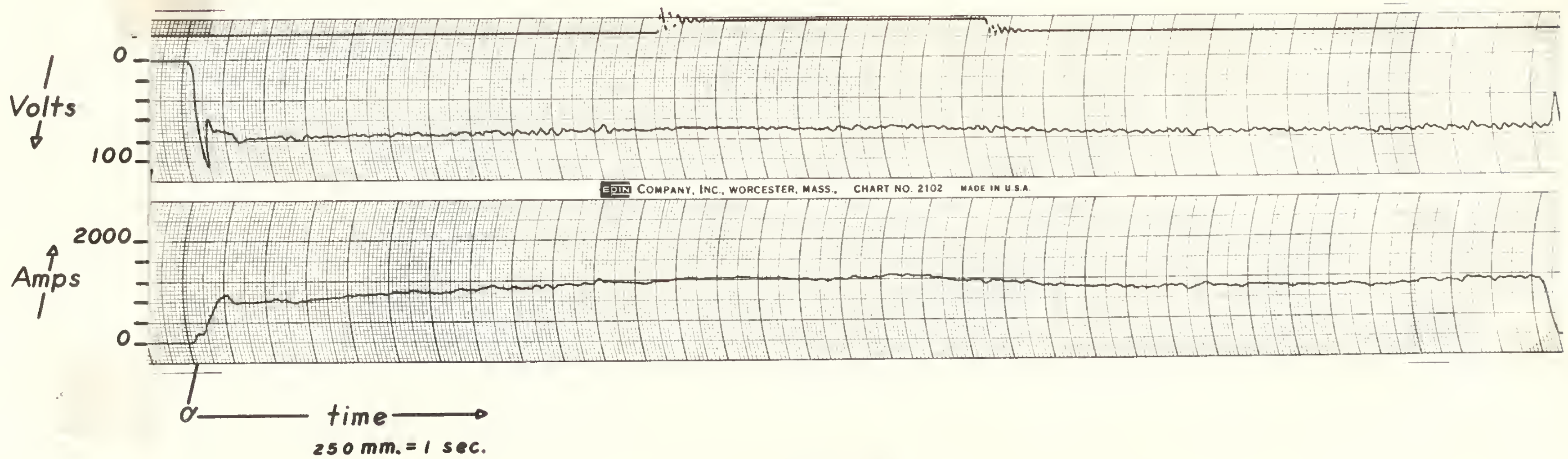

Fig. 4

Fig. 5

Voltage Versus Current

Tungsten Cathode, Solid Copper Anode

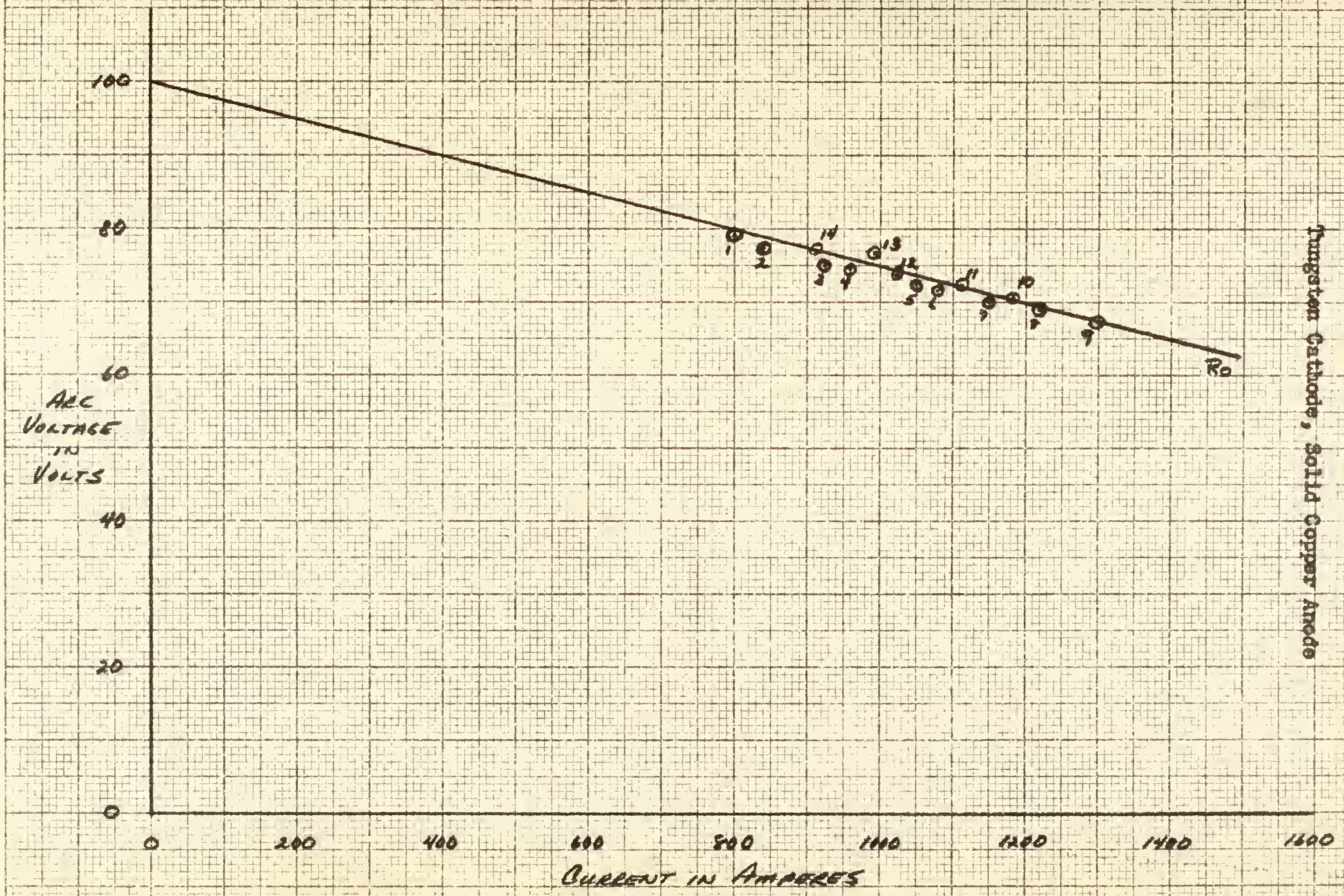

The resistance of the arc during the running period can be found by dividing the voltage at any point on the load line by the current at that point. If a series of such points were plotted, it would be seen that as the arc is forming the resistance variation with time is exponential and has a negative slope. Let the linear variation of current with voltage, during this period in which the arc is becoming established, be called the DYNAMIC ARC CHARACTERISTIC.

In explanation of those points which move toward decreasing currents, consider Fig. 6. On this curve, portions of several arc characteristic curves have been plotted. It has been assumed in so doing that for each gap spacing between electrodes a separate characteristic curve exists. Such a condition has been proven to exist at low current intensities, and the assumption that this is true at high current intensities is reasonable. Suppose that initially the electrode separation is L_1, and that the mechanism of the preceding paragraph has occurred. Operation will then be at point C_1. Accordingly, if the separation remains constant, the voltage and current will remain constant. That this did not occur can be traced to anode erosion, which lengthened the gap. As the gap increased through separations L_2, L_3, ..., points C_2, C_3, ... were defined and recorded.[1]

---

[1] As an interesting aside, it can be seen from Fig. 6 that the arc will extinguish at the point where the external resistance load line becomes tangent to the L_{co} characteristic curve. An arc cannot exist for separations greater than L_{co}, since this would require more voltage than exists in the circuit.

Fig.6

Operating Point Change Resulting from Change in Electrode Separation, ΔL

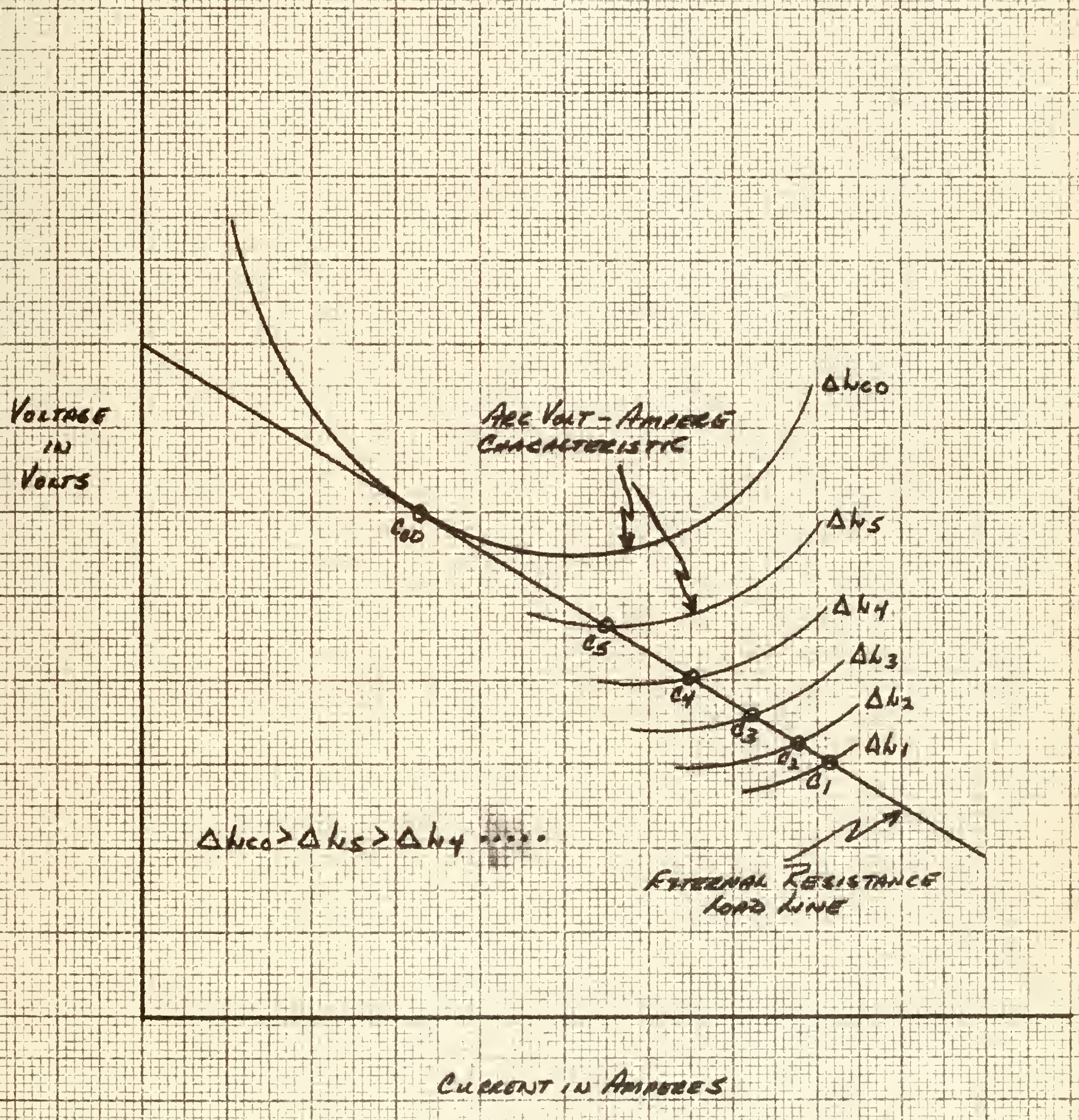

Hence it was clear that both electrodes had to be erosion resistant. A tungsten insert was provided for the anode, giving the electrodes the appearance of Fig. 7. In this drawing the tungsten inserts have been darkly cross-hatched. This combination proved to be resistant to erosion at low current densities, but was far from being proof against high intensity currents.

A typical run using the electrode combination of Fig. 7 is shown as it appeared on the oscillograph, Fig. 8. An initial oscillation exists which is probably related to the transient response of the R , L , C circuit to a step input of voltage. Although the general nature of this transient is the same from run to run, no two runs are identical. The current intensity has a marked effect on this transient condition. For high currents the damping of this transient is materially faster than for low current intensities. Following this transient oscillation, a period of rising current and falling voltage typical of the dynamic characteristic is observed.[1] Finally, a nearly constant level of maximum current and minimum voltage is reached. This value defines a point of stability on the arc characteristic curve.

The tungsten-tungsten electrode combination held the erosion to a sufficiently low level that definition of the volt-ampere

---

[1] The time of rise of current is a direct function of the inductance in the circuit. If the reader will compare the rise time of current in Fig. 8, where an external inductance was incorporated in the circuit, with the current rise time for helium in Fig. 11 where no external inductance existed, the difference will be obvious. Care must be taken in making this comparison to note the difference in time scales.

Fig. 7

Electrode Insert Configuration

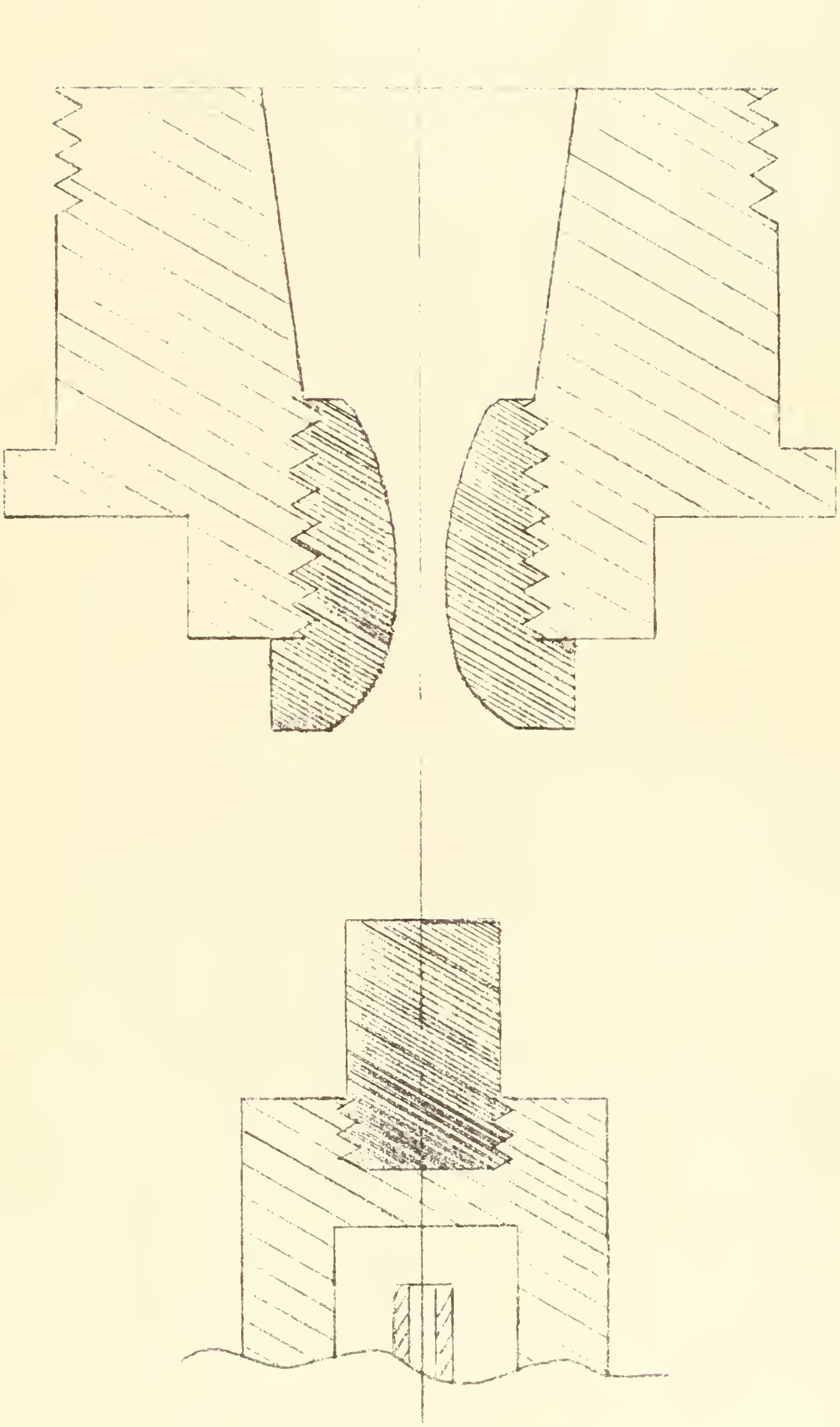

Tungsten Anode- Cathode Voltage and Current Time Variation

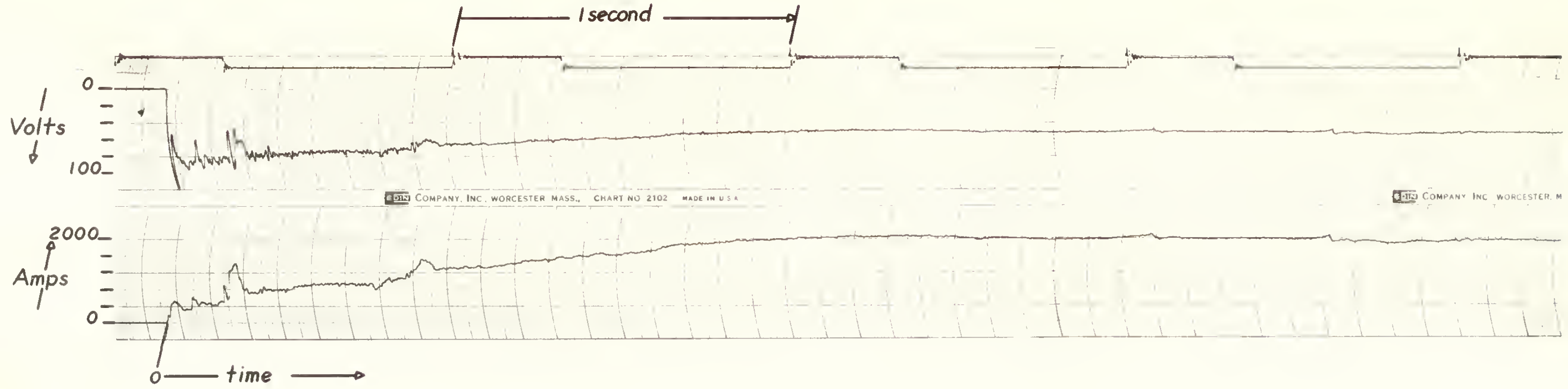

Fig. 8

characteristic was possible. Local erosion still existed, however, making duplication of a run difficult. This local erosion tended to change the local length of path during a run, causing scatter to exist. It would seem on analysis that the erosion should be uniform. The arc should tend to fire across the minimum separation point, e.g. at the point where the field intensity is greatest. If this were so, as erosion occurred, the arc would move from point to point maintaining the surfaces of the electrodes plane and parallel. That this was not the case, especially at low current intensities, was adequately demonstrated. The arc tended to fire between the electrodes in a random fashion, subsequent to fuse wire vaporization. No point on the surface seemed to be more predominant than any other.[1] For low intensities, where the arc tends to be a single line as opposed to the fuzzy, many fingered, high intensity arc, the current density is very high. Judging by erosion patterns on the anode, this current density may be in the order of 10^6 amperes per square inch. Consequently the flux of power through this small area is very high, quickly raising the metal to the boiling point. Ions

[1] This statement is true only if the resultant magnetic field normal to the arc stream is zero. Even a small magnetic field intensity will cause the arc to have a preferred direction. This is due to the Lorentz force, $(\overline{J} \times \overline{B})$. This was noted during the course of the investigation by deliberately arranging the anode leads, which were parallel to the arc stream, in an asymmetrical configuration. Figs. 8a and 8b illustrate this effect and for two different lead configurations. The position at which the arc attached at the anode could be varied by varying the position of the conductors. The field due to these conductors was effectively cancelled by placing the four leads ninety degrees apart at the same radial distance from the arc stream.

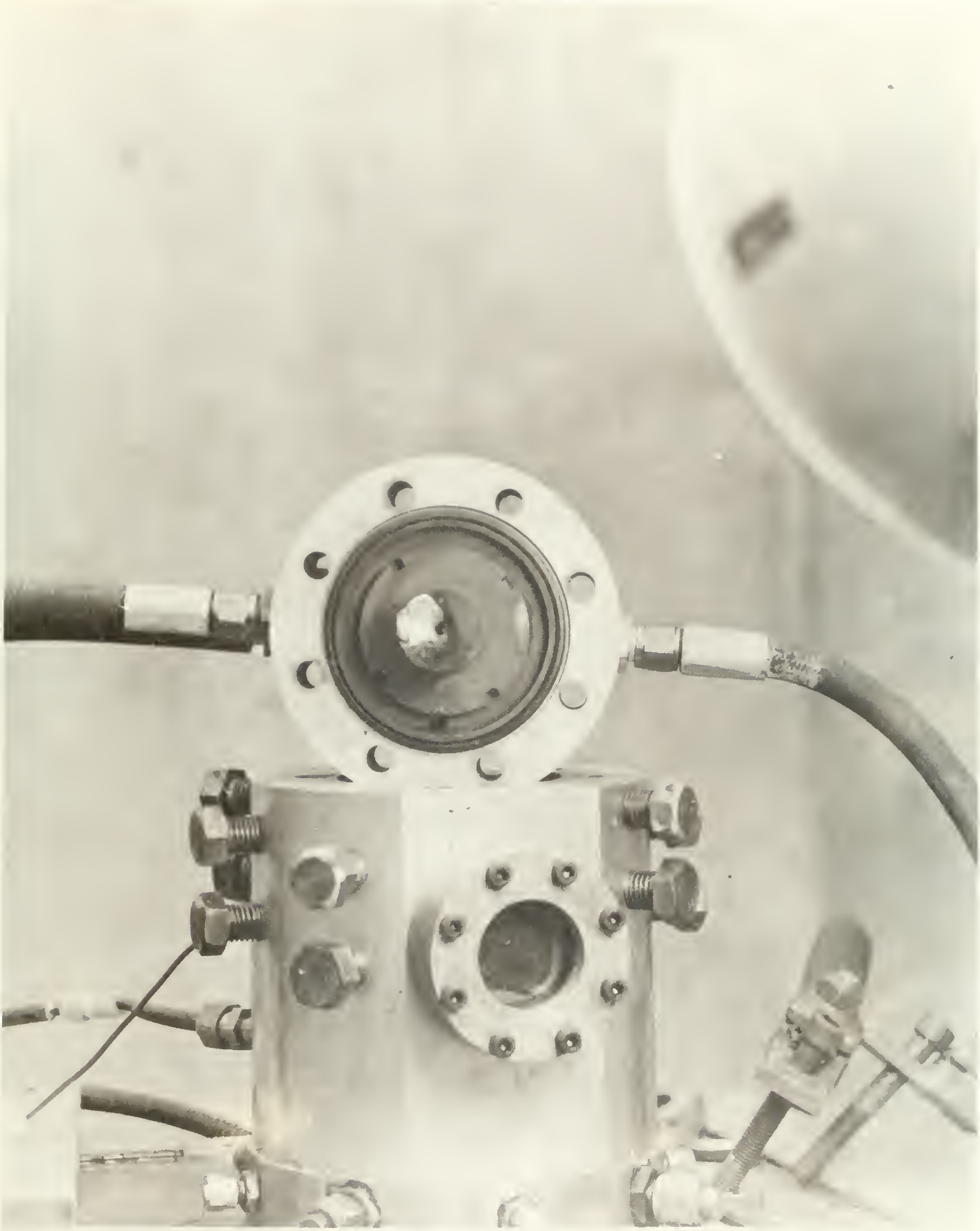

Fig. 8a Anode Erosion for Asymmetrical Lead Configuration, Case 1.

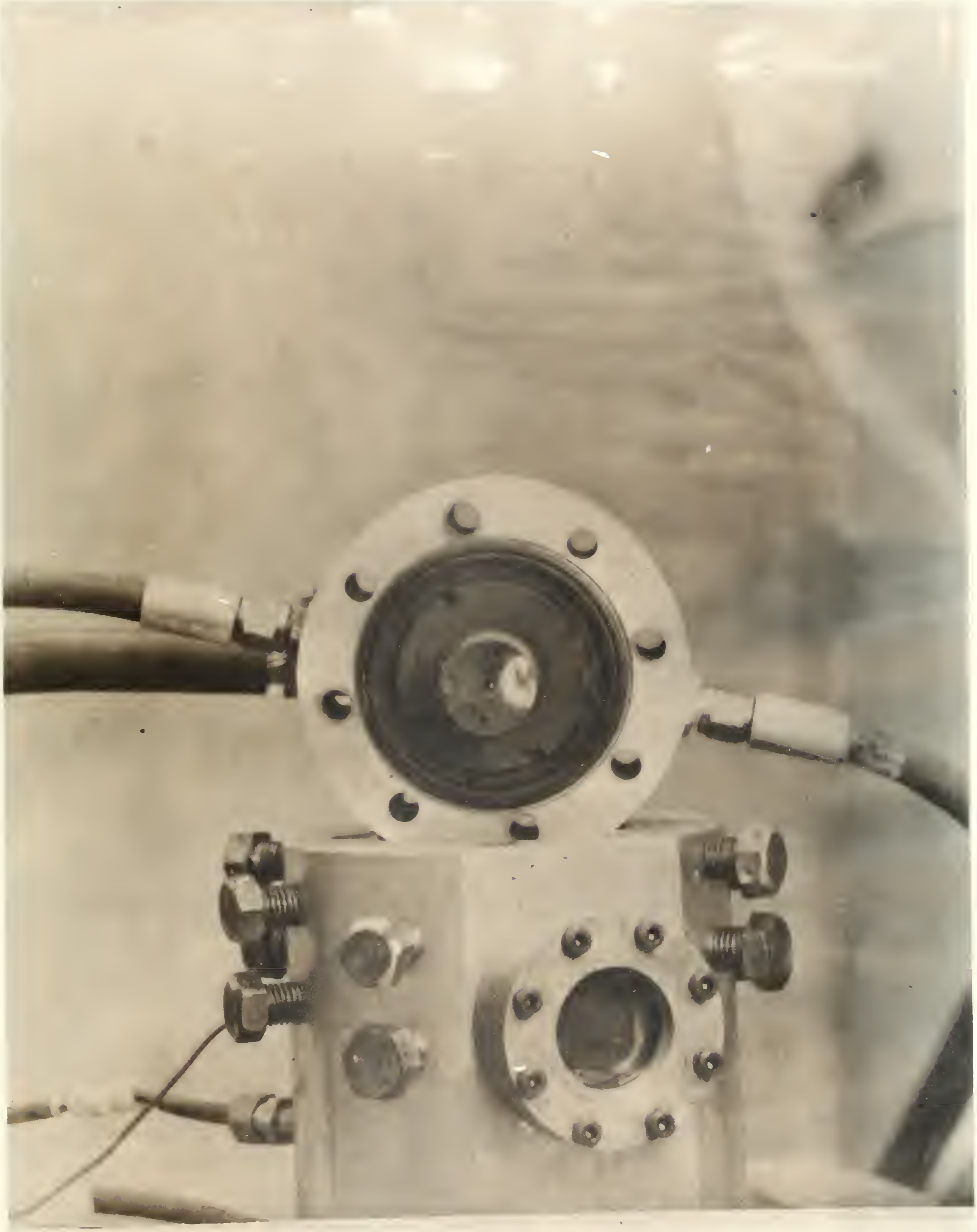

Fig. 8b Anode Erosion for Asymmetrical Lead Configuration, Case 2.

of the metal produced by this vaporization will effectively reduce the local resistance and the arc tends to remain at this point. Hence the surface erodes at that point, and not elsewhere, causing a lengthening of the local path. It is not possible to lessen the gap on succeeding runs in order to take this increased local separation into account, since the arc may or may not return to this point. In order to ensure a constant gap from run to run, it would be necessary to change electrodes after each run, an extremely expensive operation when working with machined tungsten. As a result of the foregoing, successive runs at the same gap setting did not produce exactly the same information.

Fig. 9 shows the scatter resulting from the effect described in the previous paragraph. Runs were made at each value of external resistance several times, with the initial conditions held constant. The location of the stability point on an individual load line would seem to be problematical with scatter of this magnitude. This problem was resolved by taking a statistical average position of the points along an individual load line. A smooth curve connecting these averaged points produces the characteristic curve, as shown. A characteristic curve having a large scatter was deliberately chosen for demonstration. Quite often, however, a series of runs would have so little scatter as to make the location of the stability point obvious, giving a check as to the accuracy of the points estimated by statistical average. The curve defined is the STATIC ARC CHARACTERISTIC. It is the locus of points where stable operation is possible.

Fig. 9

Volt-Ampere Characteristic, Two Inch Gap, in Helium

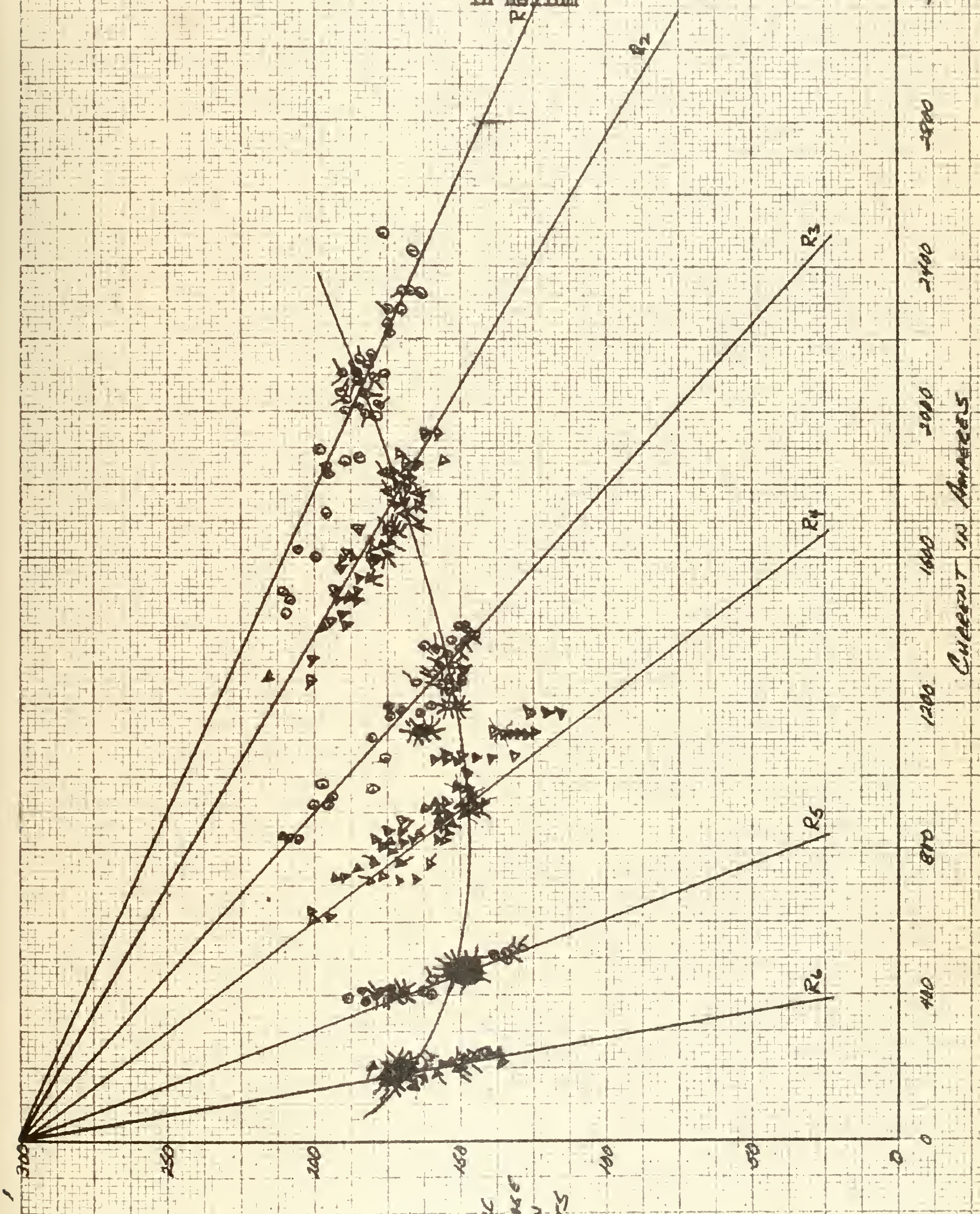

The curves resulting from the investigation of the change in the static arc characteristic location with changing gap setting appear as Fig. 10a and 10b. Fig. 10a shows the starting voltages and load lines used in obtaining these curves, while in Fig. 10b the load lines have been eliminated. These curves cannot be said to be exact, due to the erosion difficulties mention above. The curves actually arrived at through experiment are shown as solid lines. The two curves indicated by dotted lines were only partially defined experimentally, and the remaining values estimated. The assumption made earlier, that for each gap setting between electrodes a separate characteristic curve exists, is seen to be valid. The variation of voltage with separation, at a given current, is not linear but changes from point to point. It is possible to predict from these curves that at larger gap spacings, say three to four inches, a major change in the gap setting will produce a minor change in the voltage.

It should be borne in mind that these curves apply to this particular arc jet configuration. Future experimenters using this type of arc jet with helium, initially at atmospheric pressure, can determine the operating point for a given run by the following method:

1. Determine the value of external resistance.
2. Using this value, plot a volt-ampere curve.
3. On this same plot, draw the volt-ampere characteristic of the generator in use, for the voltage to be used.
4. Subtract the two curves thus obtained. The line thus formed is the load line for operation.

Fig. 10a

Volt-Ampere Characteristics, Sundry Gaps, in Helium

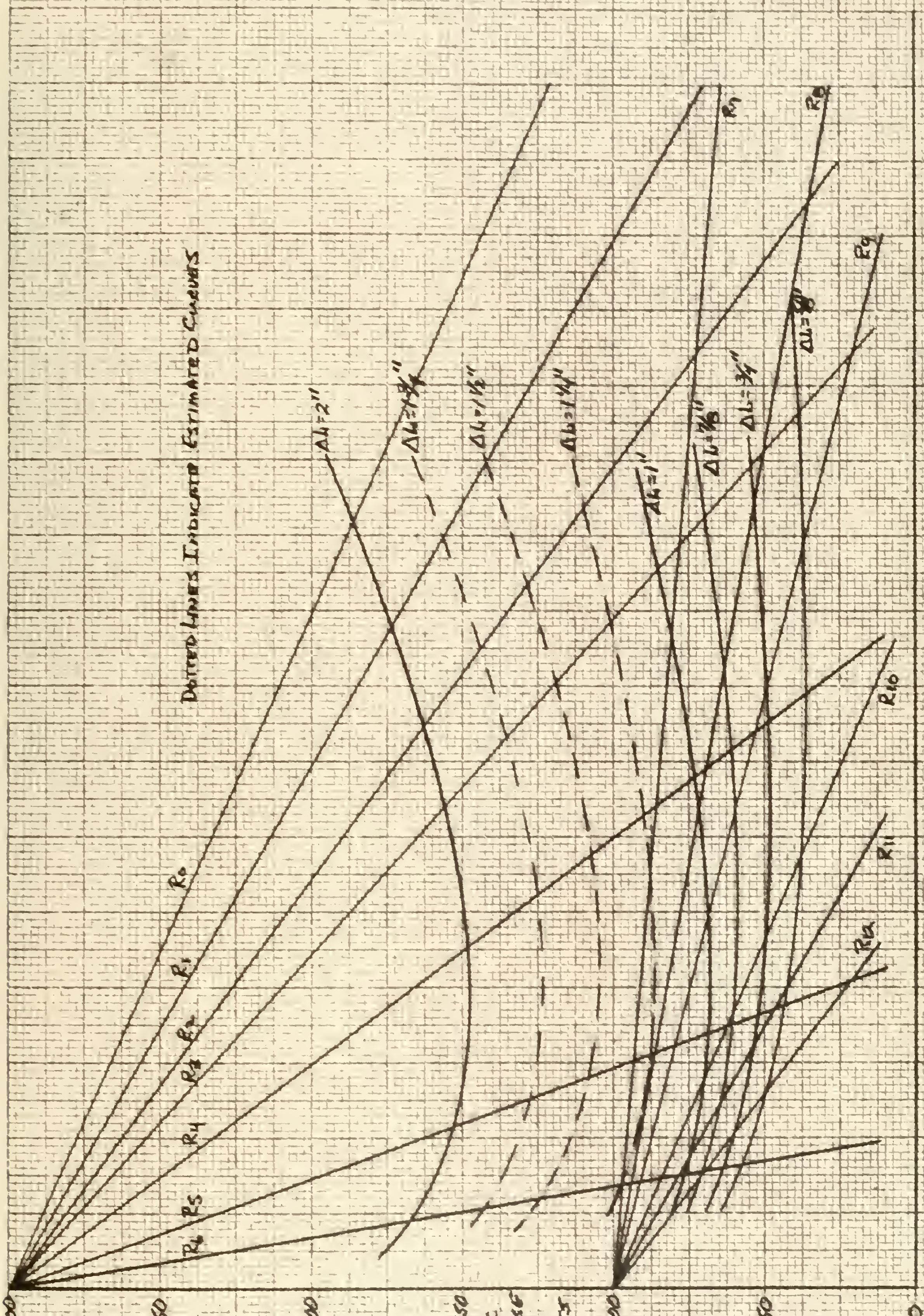

Fig. 10b

Volt-Ampere Characteristics, Sundry Gaps, in Helium

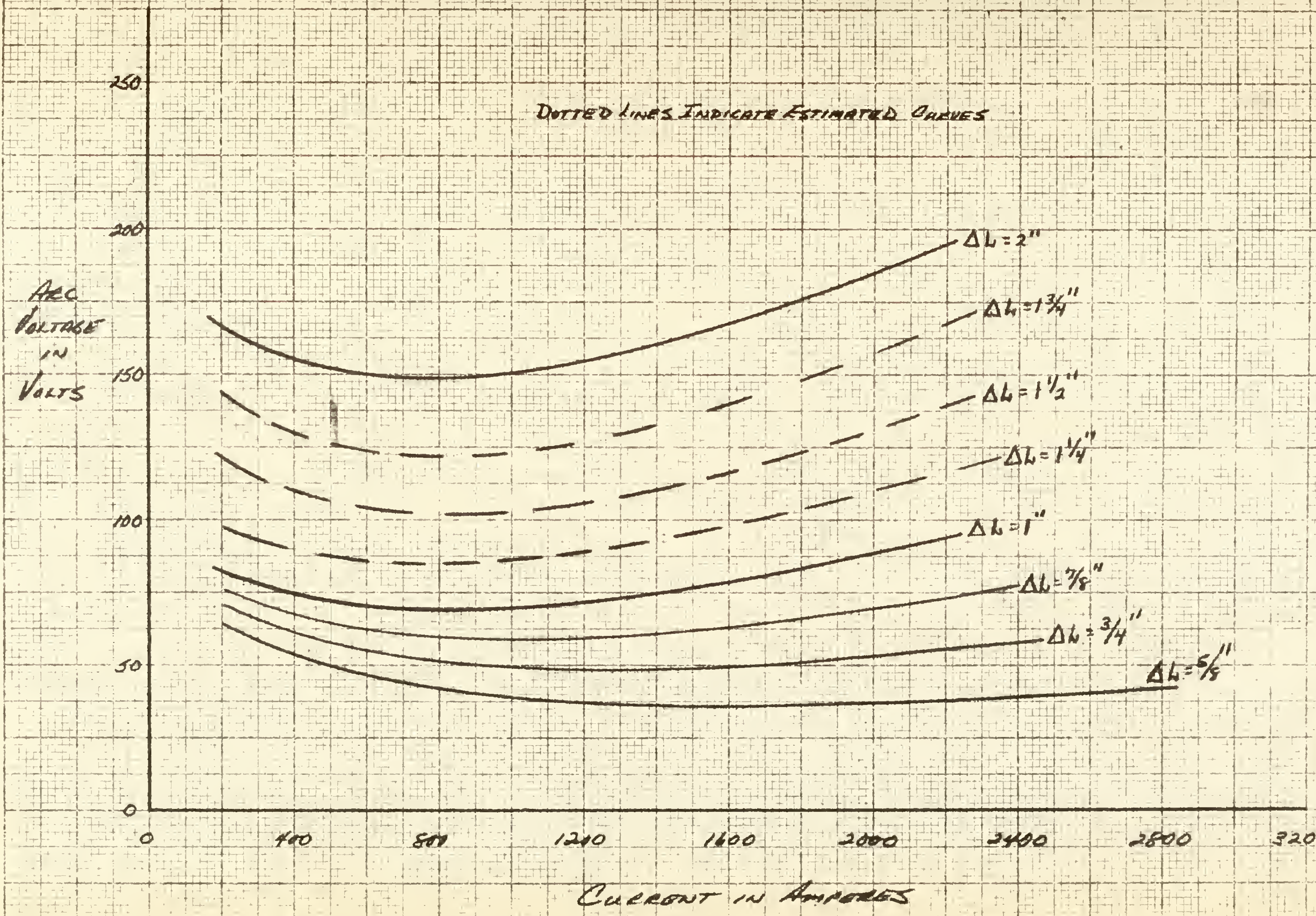

5. The intersection of this load line with the static characteristic curve corresponding to the electrode separation to be used is the operating point.

The point thus defined will be well within ten-percent of maximum values which will be reached during the run.

Having developed the volt-ampere characteristic curves for helium, it was felt that it would be of interest to compare these curves with those for another of the noble gases. Argon was chosen, not only for its chemical inertness, but because the physical characteristics of the gas are known moderately well up to extremely high temperatures. Fig. 11 is an oscillographic record of a helium run and an argon run, each made under identical operating conditions. The traces differ in several respects. The voltage drop across the arc is greatly reduced in argon. The voltage fluctuations in the helium are completely eliminated in argon, and there is less fluctuation in general.[1] The current intensity in the argon is nearly double that which exists in the helium. Further, the stability point is reached much more swiftly in argon, and there is less scatter. Although not shown in the portion of the traces reproduced, unmistakable signs of local erosion existed in the latter portion of the helium run, whereas in the argon trace the erosion

---

[1] If the voltage trace of the helium run in Fig. 11 is compared with that of Fig. 8, it will be seen that considerably more oscillation of voltage exists in the trace of Fig. 11. This can be traced to the lack of external inductance in the run of Fig. 11. From this it was concluded that the original estimate of stabilization through external inductance was justified.

Two Inch Gap in Helium

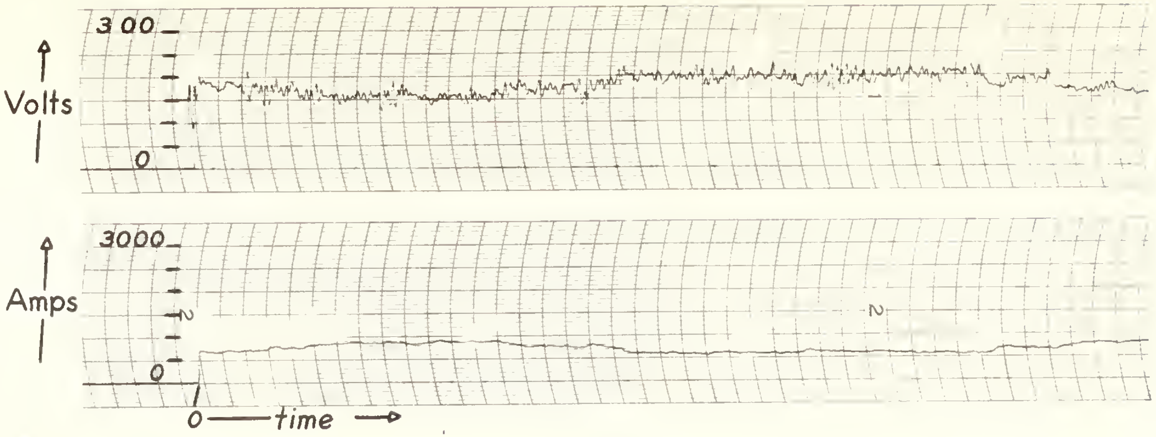

Two Inch Gap in Argon

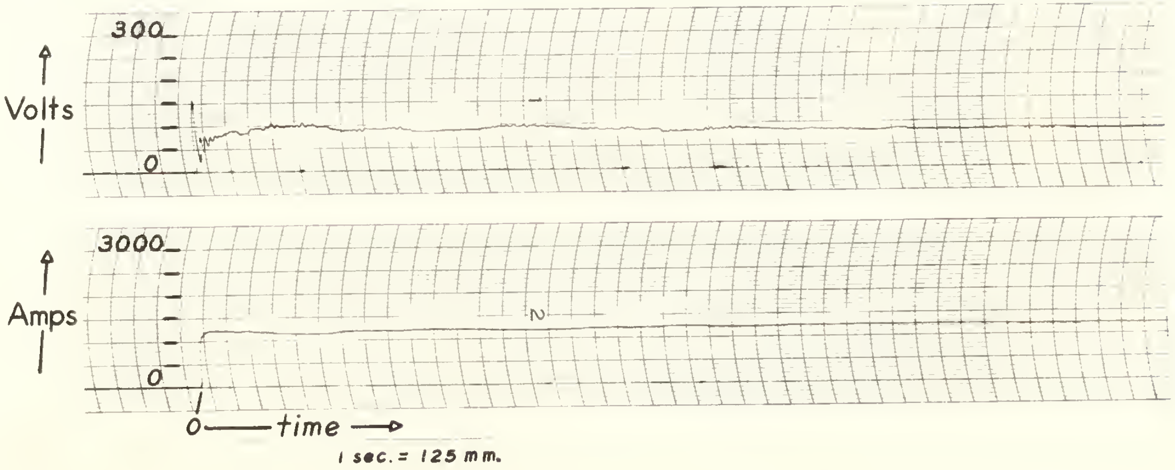

Fig. 11

was nearly uniform.[1] Furthermore, the initial and final values on the agron trace differed little, indicating slight erosion.

From the foregoing it would seem that argon would be a more suitable medium for use in an arc jet than would helium. On the other hand, as can be noted from a comparison of the characteristic for argon, Fig. 12, and the corresponding helium characteristic of Fig. 9, the power level in the helium is nearly double that of the argon. At a given current level of operation, more power is dissipated in the helium than in the argon. If the helium retains this energy through the nozzle, and a high energy plasma is the main consideration, helium could easily be more satisfactory than argon. The question of retention of energy is problematical, however. It is felt that the losses within the chamber would be much higher with helium than with argon. A comparison of the ionization levels of the two gases at the nozzle exit would be necessary in order to resolve this question.

As was stated previously, the scatter observed in the argon runs was small compared to that which existed in the helium runs. The stability point is well defined. Fig. 12 is, however, the result of only a single series of runs. Time did not permit re-running each individual point. It is felt that a certain amount of scatter would appear on plotting re-runs, but it is almost

---

[1] From this it can be concluded that in the argon runs the arc stream was of the high intensity type.

certain that no error of any magnitude exists.

Fig. 12

Volt-Ampere Characteristic, Two Inch Gap,

in Argon

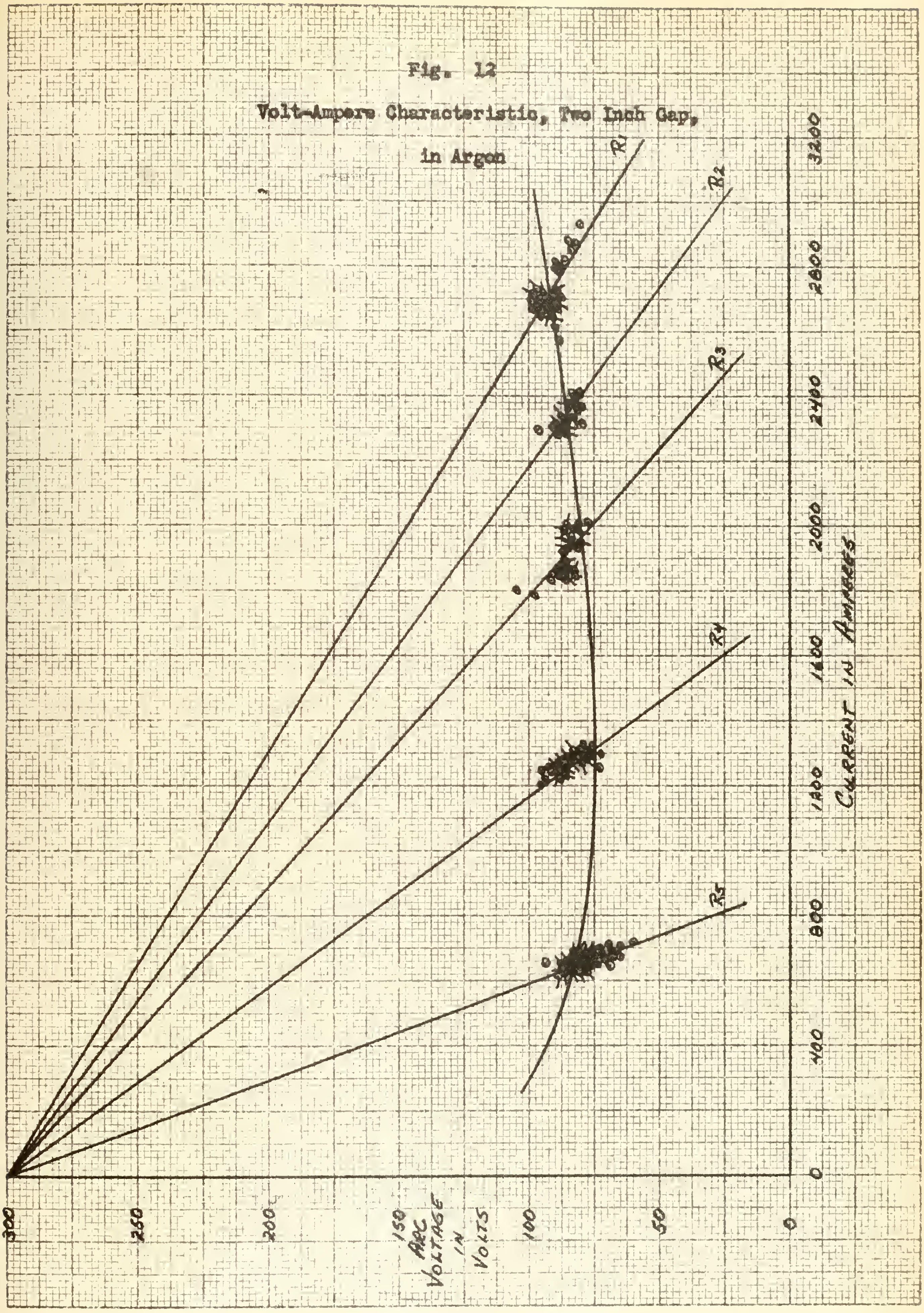

6. ARC RESISTANCE.

The resistance of the arc as a function of time may be determined from the time history of voltage and current; e.g. as presented in Fig. 8. This variation, shown in Fig. 13, is what would be expected from a rational investigation of the sequence of events that occurs after the switch is closed to start the arc.

Initially the fuse wire vaporizes. The combustion products of this vaporization will continue to constitute a path for current flow for a short period of time. Then, due to diffusion and to flow through the nozzle, these vaporization products will no longer constitute a significant current carrying path. This initial arc will continue, however, if it contains sufficient energy to partially ionize the helium surrounding it. The ionization will increase also, due to the vaporization of the electrodes. Thus, the current flow will continue to increase until such time as a balance is reached between the incoming un-ionized helium atoms and outgoing ionized atoms of helium and electrode material. This balance will define the point, for a given pressure, of maximum average ionization in the path.

As a consequence of the above, it is to be expected that, after the switch is closed, the resistance would rise from an initial value corresponding to that of the fuse wire to some relatively high value, then fall in an exponential fashion to some relatively constant lower value. This conforms well with the curve of Fig. 13.

Fig. 13

Arc Resistance Time Variation

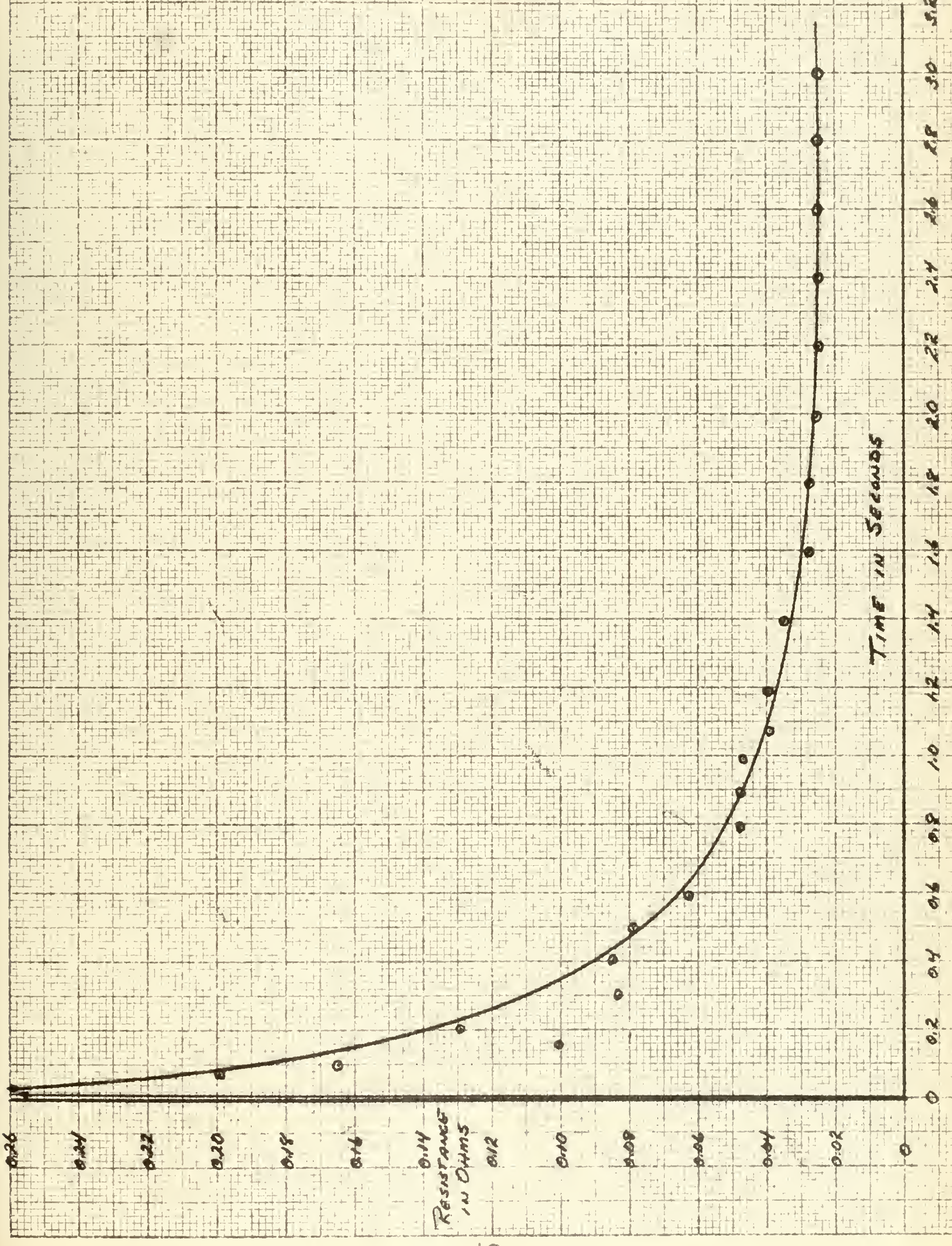

7. TEMPERATURE AND PRESSURE.

The measurement of temperature within the arc itself was not attempted. It would have been possible to obtain optical pyrometer measurements by sighting through the windows of the device, but it was felt that information so obtained would be of little use, due to the inherent inaccuracy of the method and to the limited observation time available. Spectographic measurements are to be attempted in the future, using line broadening techniques.

Measurement of the ambient temperature at the wall of the chamber during the firing period was attempted. A shielded probe containing a chromel-alumel thermocouple was introduced at the chamber wall. The results of this experiment were unsatisfactory. Radiation and convection of heat were so great that both the shield and thermocouple melted almost instantly.

Little more success was had with pressure measurements. An attempt was made to record the pressure as a function of time in order to relate it to the instantaneous power level. Toward this end, a variable reluctance pressure pickup was used to modulate a three kilocycle carrier frequency and the analog output used to drive the galvanometer. Fig. 14 presents the results of this attempt. As can be seen, the ordinate of the pressure trace is not linear and there is an objectionable oscillation. In spite of these limitations, however, certain information can be obtained. As the arc fires, the pressure at the wall increases to a relatively constant value. At the point where the pressure begins to increase from this value, the flow through the orifice was reduced

Helium Arc, Two Inch Gap

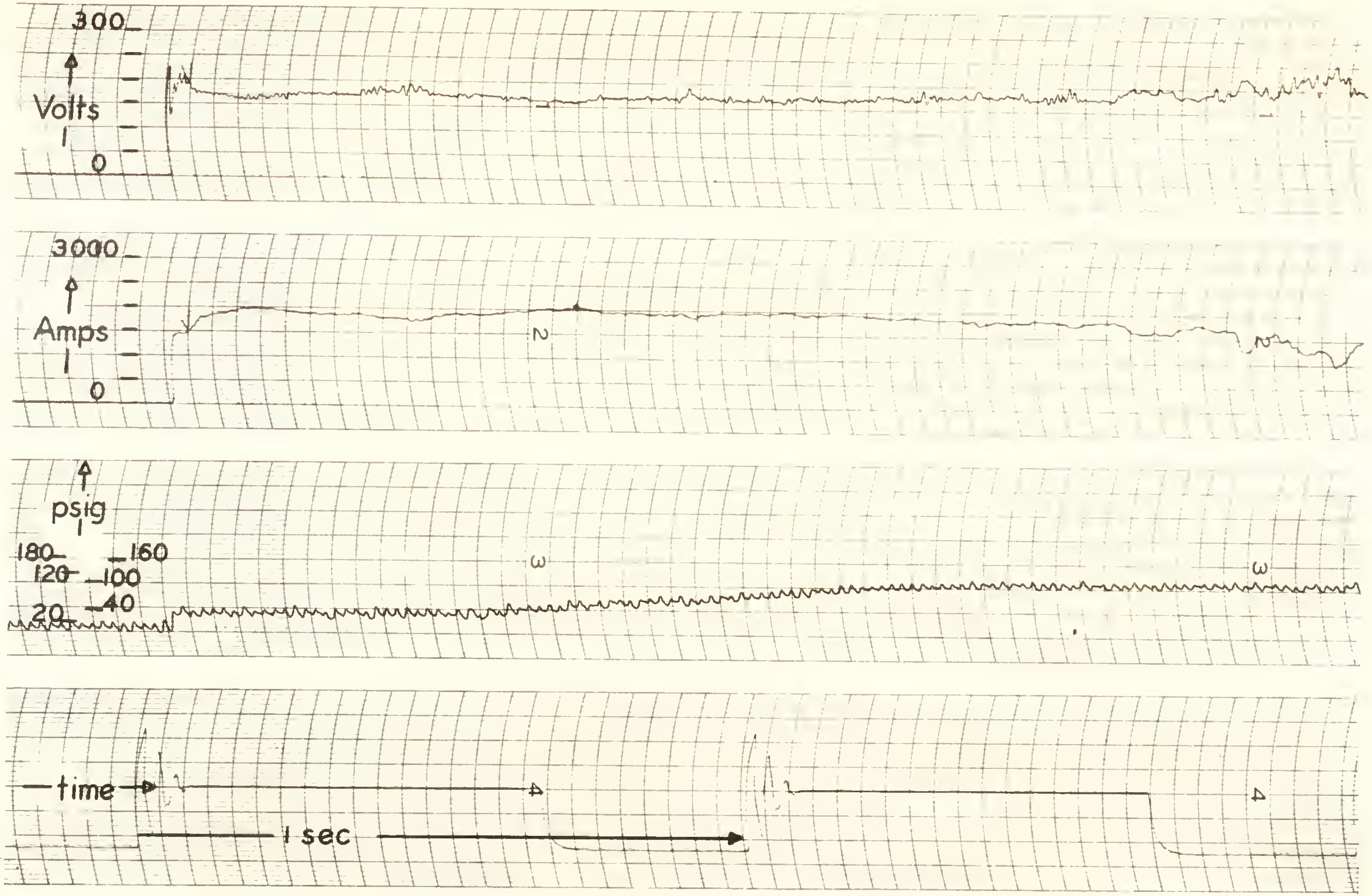

Fig. 14

due to the molten tungsten reducing the throat diameter of the anode. It can be seen that, as the pressure increases, the voltage across the arc increases and the current decreases, as would be expected. It is interesting to note that the power level remains essentially constant throughout the run. The decrease in current intensity is balanced by the increase in voltage, producing no net change in power. Future investigations of pressure versus power level will be conducted with a more satisfactory recording device.

8. CONCLUSIONS AND RECOMMENDATIONS.

In the gases helium and argon, the slope of the static arc volt-ampere characteristic is initially negative, but decreases and then becomes positive with increasing current intensity. At a given current level of operation, the minimum voltage drop across the arc is obtained, obviously, with minimum separation between electrodes. As the separation between electrodes is increased the voltage requirement is increased, but in a non-linear fashion. At large gap spacings small changes in the spacing will cause minor voltage changes. An external resistance is required for controlling the ampere level of operation of the arc jet.

Introduction of inductive reactance into the circuit of the arc jet is beneficial in stabilizing the voltage and current oscillations of the arc, and produces no objectionable effects.

Operation in argon is more stable than in helium. More energy is required by the helium arc than by the argon at a given current level of operation. However, it is possible that the energy retained through the nozzle is higher in argon than in helium.

Strong magnetic field intensities can be produced in a minimum of space by utilizing water-cooled conductors. Current densities of 10^6 amperes per square inch are possible in these conductors.

Certain tentative conclusions were reached concerning items for which insufficient data were collected to make positive statements:

For operation with a gaseous medium initially at atmospheric pressure, the operating point location on the stability curve is

independent of nozzle hole size for hole sizes less than the cathode diameter. Nozzle hole size does seem to play an important role in erosion at the anode. A large nozzle hole materially reduces erosion, but whether this is due to a reduction in the power density or a reduction in heat transfer to the nozzle needs to be determined.

A design change indicated by the experiments conducted thus far, where gaseous operation is involved, is a reduction in the ratio of the length of the arc jet chamber to its diameter in order that a more effective swirl may be developed.

The more intense arc seems to have desirable stability and erosion properties. Therefore, if it is desired to expend a given amount of energy in the arc, choice of gap and external resistance should be such as to yield a current of at least two thousand amperes.

Many experiments which had been contemplated originally were not accomplished. These will be mentioned here as recommendations for future experiment:

The static volt-ampere characteristic for different gases should be obtained for various chamber pressures. The characteristic curve obtained herein should be extended to about five thousand amperes.

The effect on the static volt-ampere characteristic of reversing the electrical polarity of the device should be observed. Also, any changes in type or amount of erosion due to this reversal of polarity should be noted.

The stability of operation with an alternating current would be of interest.

Relative ionization levels of argon and helium in the jet exhaust should be determined to ascertain which gas is the more efficient plasma agent.

An exhaustive study should be made of the effect of the magnetic nozzeling incorporated in this device. The magnetic field strengths attainable should constrict the arc, thereby causing higher temperatures and a greater degree of ionization. This should reduce both the loss of energy to the interior of the chamber and anode erosion, because of the reduced mobility of the ions and electrons normal to the magnetic field. The magnetic field should also contribute greatly to arc stability in the water configuration.

Successful light-off in the water-swirl configuration was obtained on three occasions with the higher voltage available at the Hunter's Point Plant. These runs yielded little useful information due to their short duration. In each case the water-cooled anode failed soon after light-off, and the arc extinguished. A new design is indicated for the anode, incorporating a high melting point material.

APPENDIX A

Chamber Burst Pressure Calculation

It can be shown from the flow and energy relationships that the pressure varies in the following manner:

$$p_o = \frac{P}{A^*} \frac{1}{h_o} \frac{\sqrt{R\,T_o}}{\sqrt{\gamma \left[\frac{2}{\gamma+1}\right]^{\left(\frac{\gamma+1}{\gamma-1}\right)}}}$$

Where capital P denotes the electrical energy rate in watts.

If one assumes that at 10,000°K the gas becomes completely dissociated, e.g.

$$H_2O \rightarrow H_2 + 1/2\ O_2 \longrightarrow 2H + O$$

then,

$$H_2O \rightarrow H_2 + 1/2\ O_2 \rightarrow h_1 = 57.11 \text{ K cal/gr mole } H_2O$$

$$H_2 \rightarrow 2H \rightarrow \Delta h_2 = 51.62 \text{ K cal/gr mole } H_2$$

$$O_2 \rightarrow 2O \rightarrow \Delta h_3 = 58.59 \text{ K cal/gr mole } O_2$$

Combining:

$$H_2O \rightarrow 2H + O \rightarrow \Delta h_1 + \Delta h_2 + \frac{\Delta h_3}{2} = \Delta h_{diss.}$$

$$\Delta h_{diss.} = 138.025 \text{ K cal/gr mole } H_2O$$

or:

$$\Delta h_{diss.} = 7.668 \times 10^3 \text{ BTU/\#m } H_2O$$

If one further assumes that at 50,000°K the gas becomes one hundred percent singly-ionized through the first oxygen atom, an additional relationship is introduced:

$$H \rightarrow H^+ + e \rightarrow 13.58 \text{ e.v.}$$

$$0 \rightarrow 0^+ + e \rightarrow 13.60 \text{ e.v.}$$

and:

$$1 \text{ e.v.} = 23.053 \frac{\text{K cal}}{\text{gr mole } e_i} = 23.053 \times 10^3 \frac{\text{BTU}}{\text{\#m } e_i}$$

$$H \rightarrow H^+ + e \qquad \Delta h_4 = (13.58)(23.053) = 313.06 \frac{\text{K cal}}{\text{gr mole H}}$$

$$0 \rightarrow 0^+ + e \qquad \Delta h_5 = (13.60)(23.053) = 313.52 \frac{\text{K cal}}{\text{gr mole 0}}$$

combining:

$$\Delta H_I = 2 \Delta h_4 + \Delta h_5$$

$$\Delta H_I = 939.64 \frac{\text{K cal}}{\text{gr mole } H_2O} = 52.202 \times 10^3 \frac{\text{BTU}}{\text{\#m } H_2O}$$

The value of the ratio of the specific heats at 10,000°K:

$$\gamma \doteq 1.67$$

$$C_p \doteq \frac{\overline{\gamma} \times \overline{R}}{\overline{\gamma} - 1} = 2.49 \overline{R}$$

$$\bar{R} = \frac{1545}{6} = 257.5 \quad \frac{\text{ft } \#}{\#\text{m } {}^{\circ}\text{R}}$$

$$C_p \doteq (2.49)(257.5) = 641.18 \quad \frac{\text{ft } \#}{\#\text{m } {}^{\circ}\text{R}} = 0.8241 \quad \frac{\text{BTU}}{\#\text{m } {}^{\circ}\text{R}}$$

From the above relationships it was possible to obtain the value of Δh not taking into account the dissociation and ionization factors, e.g.:

$$\Delta h' = C_p m$$

at 10,000°K :

$$\Delta h'_{10} = (.4965)(18\text{x}10^3) \quad \frac{\text{BTU}}{\#\text{m } H_2O} = 8.937\text{x}10^3 \quad \frac{\text{BTU}}{\#\text{m } H_2O}$$

at 50,000°K :

$$\Delta h'_{50} = (0.8241)(9\text{x}10^3) \quad \frac{\text{BTU}}{\#\text{m } H_2O} = 7.417\text{x}10^4 \quad \frac{\text{BTU}}{\#\text{m } H_2O}$$

With the values of Δh_{diss} , Δh_I , and $\Delta h'$ known, it becomes possible to obtain the values of h_o at the two temperatures:

$$h_{o_{10}} = \Delta h'_{10} + \Delta h_{diss.}$$

$$= 8.937\text{x}10^3 + 7.668\text{x}10^3 = 16.605\text{x}10^3 \quad \frac{\text{BTU}}{\#\text{m } H_2O}$$

$$h_{o_{50}} = \Delta h'_{50} + \Delta h_{diss.} + \Delta h_{I}$$

$$= (7.417 \times 10^{4} + 7.668 \times 10^{3} + 52.202 \times 10^{3}) \frac{BTU}{\#m\ H_2O}$$

$$= 13.404 \times 10^{4} \frac{BTU}{\#m\ H_2O}$$

The values of temperature used were based upon estimates of the operational region. Power to reach this range of temperatures was also estimated: 100 kilowatts to 3 megawatts. Based upon these values:

$$P_{100} = 94.82 \frac{BTU}{sec}$$

$$P_{3000} = 2844.6 \frac{BTU}{sec}$$

The value of $\bar{R}$ at the chosen temperatures:

$$\bar{R}_{10} = 0.1655 \frac{BTU}{\#m\ {}^{o}\bar{R}} \qquad \sqrt{\bar{R}_{10}} = 0.4068 \sqrt{\frac{BTU}{\#m\ {}^{o}\bar{R}}}$$

$$\bar{R}_{50} = 0.3309 \frac{BTU}{\#m\ {}^{o}\bar{R}} \qquad \sqrt{\bar{R}_{50}} = 0.5752 \sqrt{\frac{BTU}{\#m\ {}^{o}\bar{R}}}$$

$$T\ {}^{o}K = T\ {}^{o}\bar{R}/1.8 \qquad T_{10}\ {}^{o}K = 18{,}000\,{}^{o}\bar{R};\ T_{50}\ {}^{o}K = 90{,}000\,{}^{o}\bar{R}$$

$$\sqrt{T_{10}} = 134.2^{o} \sqrt{{}^{o}\bar{R}};\quad \sqrt{T_{50},} = 300 \sqrt{{}^{o}\bar{R}}$$

$$\sqrt{\bar{R}_{10} T_{10}} = 54.926 \sqrt{\frac{BTU}{\#m}};\quad \sqrt{\bar{R}_{50} T_{50}} = 172.56 \sqrt{\frac{BTU}{\#m}}$$

At $10,000^\circ K$:

$$\left[\frac{2}{\gamma+1}\right] = 0.8 \;; \left(\frac{\gamma+1}{\gamma-1}\right) = 5.0 \;; \quad \left[\frac{2}{\gamma+1}\right]^{\left(\frac{\gamma+1}{\gamma-1}\right)} = 0.3277$$

$$\sqrt{\left[\frac{2}{\gamma+1}\right]^{\left(\frac{\gamma+1}{\gamma-1}\right)}} = 0.7011; \; A^* = \frac{\pi D^2}{4} = \frac{\pi(3/32)^2}{4\text{x}144} = 4.794\text{x}10^{-5}\text{ft}^2$$

Substituting the values obtained in the expression for p_o , at a power rating of 100 kilowatts and $10,000^\circ K$:

$$p_a = p_{o_{100}}^{10} = \left(\frac{94.82}{4.794\text{x}10^{-5}}\right)\left(\frac{1}{16.605\text{x}10^3}\right)\frac{54.926}{0.7011}\sqrt{\frac{778}{32.2}} = 4.587\text{x}10^4 \#/\text{ft}^2$$

at the 3,000 kilowatt level; and $10,000^\circ K$:

$$p_b = p_{o_{3000}}^{10} = 1.376\text{x}10^6 \; \#/\text{ft}^2$$

Similarly, at $50,000^\circ K$:

$$\left[\frac{2}{\gamma+1}\right] = 0.749 \;; \left(\frac{\gamma+1}{\gamma-1}\right) = 3.985 \;; \quad \left[\frac{2}{\gamma+1}\right]^{\left(\frac{\gamma+1}{\gamma-1}\right)} = 0.3097$$

$$\sqrt{\left[\frac{2}{\gamma+1}\right]^{\left(\frac{\gamma+1}{\gamma-1}\right)}} = 0.7192$$

and at $50,000^\circ K$ at the 100 kilowatt power rating:

$$p_c = p_{o_{100}}^{50} = 1.740\text{x}10^4 \; \#/\text{ft}^2$$

while at 50,000°K and 3,000 kilowatts :

$$p_d = p_{o\,5000}^{\;50} = 5.220\text{x}10^5 \ \#/\text{ft}^2$$

summarizing:

$p_a = 21.67$ atmospheres $\qquad p_c = 8.22$ atmospheres

$p_b = 650$ atmospheres $\qquad p_d = 246.6$ atmospheres

It can be shown, again using the flow and energy relationships, that the flow varies as:

$$w = \frac{p_o \ A^*}{\sqrt{R \ T_o}} \sqrt{\gamma \left[\frac{2}{\gamma+1}\right]^{\left(\frac{\gamma+1}{\gamma-1}\right)}}$$

For the 10,000°K temperature, and a power rating of 100 kilowatts:

$$w_a = w_{100}^{10} = \left[\frac{9.332\text{x}10^3\text{x}4.794\text{x}10^{-5}}{54.926}\right]\left|0.7011\right| = 5.711\text{x}10^{-3} \#\text{m}$$

Similarly, at 10,000°K and 3,000 kilowatts:

$$w_b = w_{3000}^{10} = 1.713\text{x}10^{-1} \ \#\text{m}$$

At 50,000°K and 100 kilowatts: $\qquad$ At 50,000°K and 3,000 kilowatts:

$$w_c = w_{100}^{50} = 7.07\text{x}10^{-4} \ \#\text{m} \qquad w_d = w_{3000}^{50} = 2.122\text{x}10^{-2} \ \#\text{m}$$

Summarizing the results:

100 KW , $10{,}000^{0}$K $p = 21.67$ atm.; $w = 5.711 \times 10^{-3}$ #/m

100 KW , $50{,}000^{0}$K $p = 8.22$ atm.; $w = 7.07 \times 10^{-4}$ #/m

3,000 KW, $50{,}000^{0}$K $p = 246.6$ atm.; $w = 2.12 \times 10^{-2}$ #/m

3,000 KW, $10{,}000^{0}$K $p = 650.0$ atm.; $w = 1.71 \times 10^{-1}$ #/m

Reviewing the above table and taking the assumptions made in the analysis into consideration, it was felt that a maximum of 5,000 pounds-per-square inch would be encountered in practice. Stress calculations indicated that a wall thickness providing a burst pressure limit of 7,500 pounds-per-square inch would not introduce dimensional absurdities in the design. Consequently, this safety factor was introduced.

APPENDIX B

Magnetic Field Design

When the decision had been made to make provision for magnetic confinement, it became necessary to find some means of producing a strong magnetic field in the limited confines of the arc jet chamber.

From estimates made of the ionization level within the plasma, it was reasoned that magnetic field strengths ranging from 15,000 to 60,000 gauss would be necessary to produce an observable effect.

A solenoidal arrangement of turns was the obvious answer to field shape requirements. Looking at the equations for magnetic field intensity in a solenoid, it will be seen that the field intensity is directly proportional to the magnetomotive force in ampere turns. Simple calculations provide the required number of ampere turns for production of the field strengths desired. This number of ampere turns can be produced in any number of ways. However, if the number of turns is chosen the amperes through the coil are thereby fixed, and simple calculations provide the size wire necessary to carry this current. With the size of wire a known quantity, a second calculation yields the overall size of the coil. It was found that a solenoid constructed of standard wire, of sufficient diameter to carry the required current, produced a coil whose size was completely incompatible with space limitations.

Since standard wire was unsatisfactory, it was decided to make a study of the feasibility of utilizing water-cooled coils. A water cooled coil constructed of refrigeration tubing was

contemplated. This coil would clearly have few turns due to space limitations, and as a consequence would be required to carry a considerable current in order to produce the desired field strength.

At the time this study was undertaken a suitable source of high currents was unavailable, so it was not possible to conduct experiments with the refrigeration tubing itself. It was possible, however, to study the effect of water-cooling on a wire carrying the same current density which would later be required of the refrigeration tubing. A ten centimeter length of 24 gage wire was stretched along the axis of a pyrex tube which had the same inside area as the standard 3/16 inch tubing contemplated for later use. Currents of up to 325 amperes were passed through this wire with a cooling water flow rate of about two gallons per minute. This current flow produces a current density of $1.588\text{x}10^5$ amperes per square centimeter. The wire did not fail during the test. The temperature increase undergone by the water as it passed over the wire has been plotted against power and current in Fig. 1B. The fractional temperature increase corrected for flow rate has been plotted against current in Fig. 2B. This study gives the reader some idea of the increase in current carrying capacity which water cooling supplies when it is known that the maximum current normally carried by 24 gage wire is about 0.5 amperes.

If the standard 3/16 inch refrigeration tubing were used for the coil, and required to carry a current of 5,000 amperes, the current density within the tubing would be $5.22\text{x}10^4$ amperes per square centimeter. Since this figure is considerably less than

Fig. 18

Temperature Change Versus Power and Current for Water-Cooled 24 Gage Wire

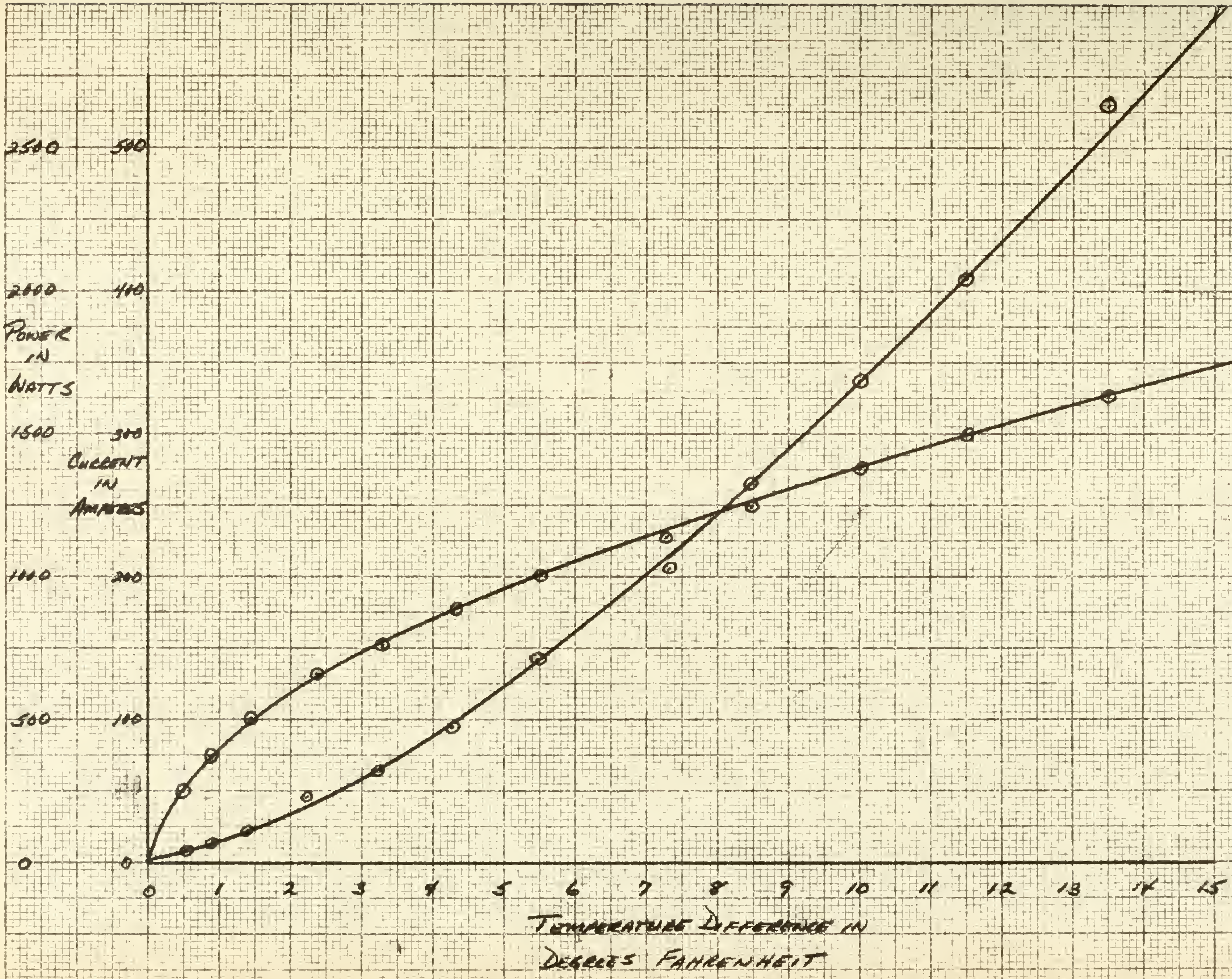

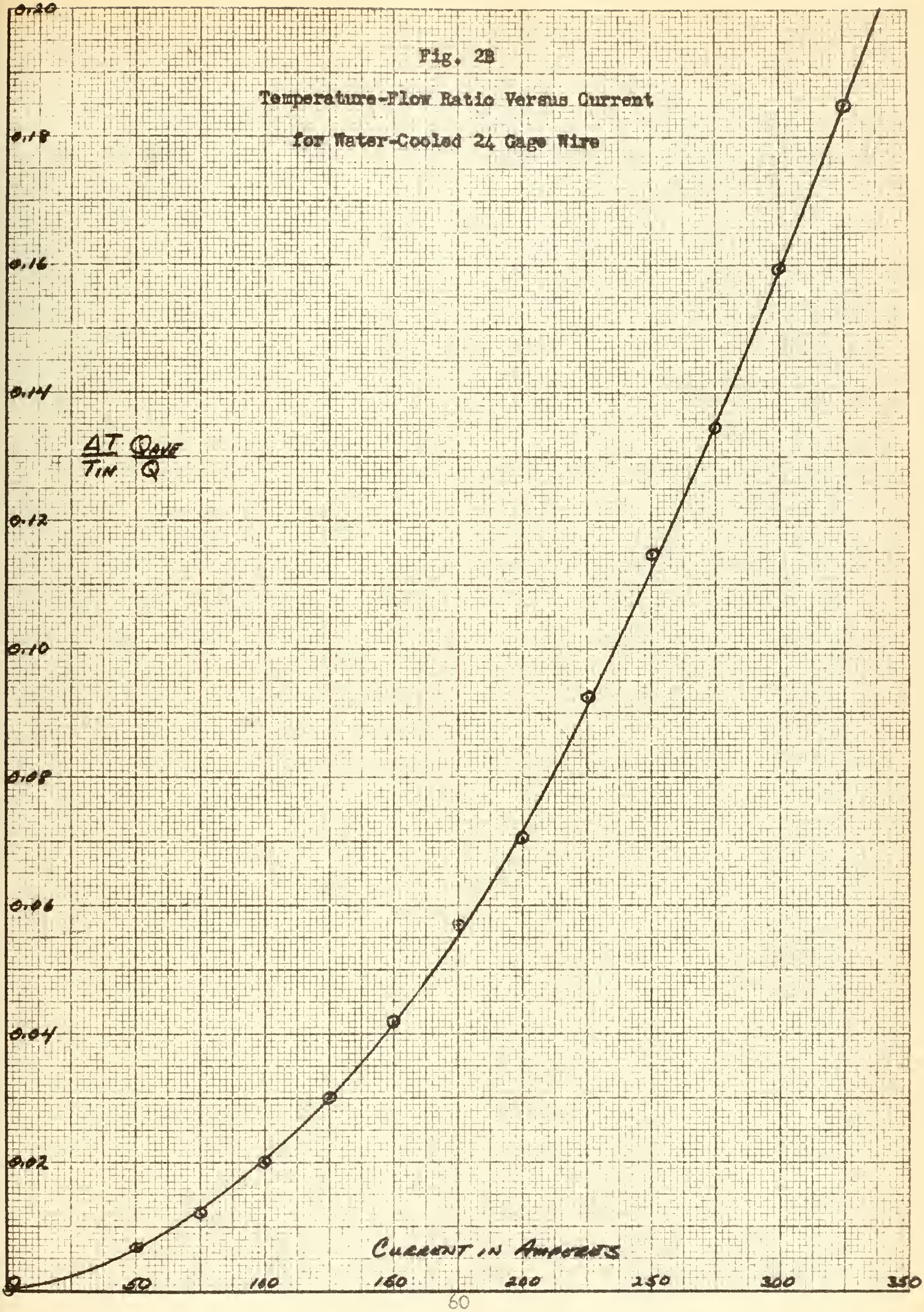

Fig. 2B

Temperature-Flow Ratio Versus Current for Water-Cooled 24 Gage Wire

that which was successfully carried by the 24 gage wire, it was felt that even though the heat transfer would be much less efficient in the refrigeration tubing, the tubing would perform satisfactorily.

Knowing the approximate inside diameter of the plasma jet, and the diameter of the swirl chamber, it was possible to compute the maximum number of helically wound turns which could be inserted in the chamber. To provide for adequate cooling of the coils, it was decided to make the solenoid a series of coils rather than a single coil. These coils would be constructed in pancake form of two layers of helically wound refrigeration tubing encased in an epoxy resin. The resin would facilitate insertion into the chamber, and would reduce turbulence in the swirl chamber. See Fig. 1a for actual size and construction features of these coils. It was found that 7.5 turns per coil of 3/16 inch tubing, 33 turns of 1/8 inch tubing, and 92 turns of 1/16 inch tubing could be used. Using a mean radius for the pancake coils in the standard equation for the magnetic flux density along the axis of the coil, it was possible to calculate the effect which each of the sections would have at the nozzle minimum section. Superposition of these individual values provided the total effect of the array of six pancake coils.

Fig. 3B is a plot of the values of flux density to be expected at the nozzle minimum section versus current intensity in three sizes of tubing. Figs. 4B and 5B show, for the six coil array, computed curves of current density versus magnetic flux density,

Fig. 3B

Computed Values of Magnetic Flux Density Versus Current

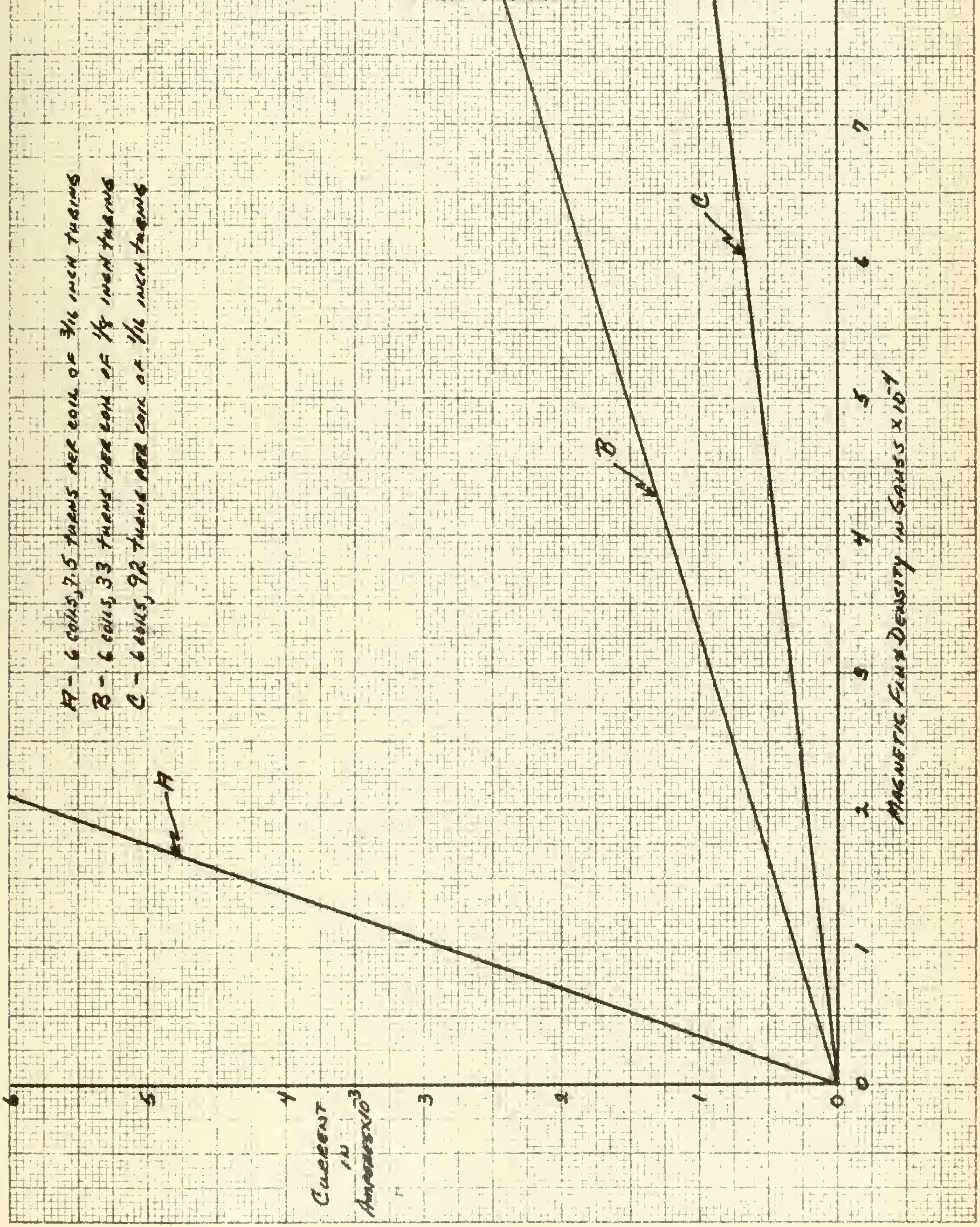

Fig. 4B

Computed Values of Magnetic Flux Density Versus Current Density

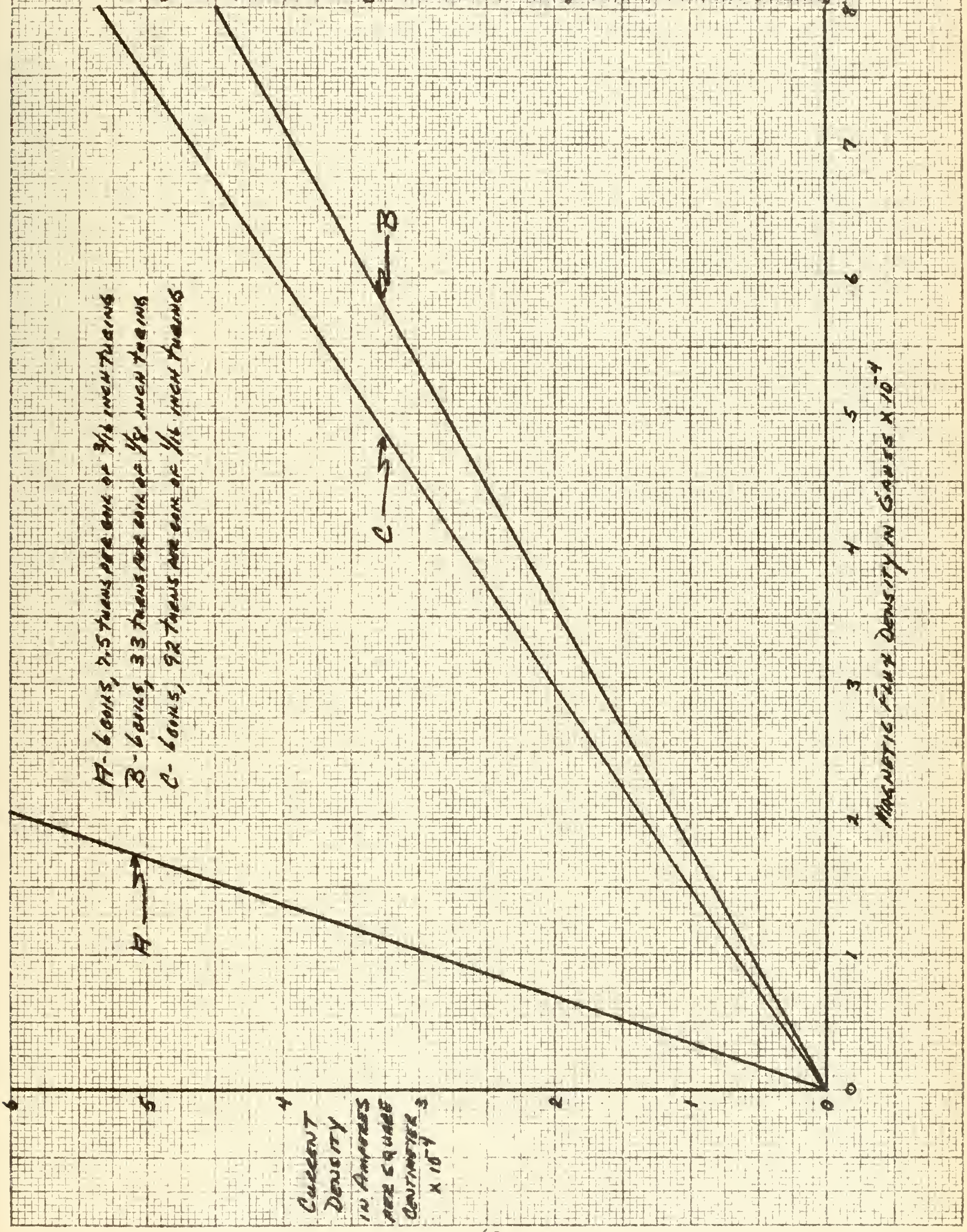

Fig. 5B

Current Versus Current Density

for Various Tube Sizes

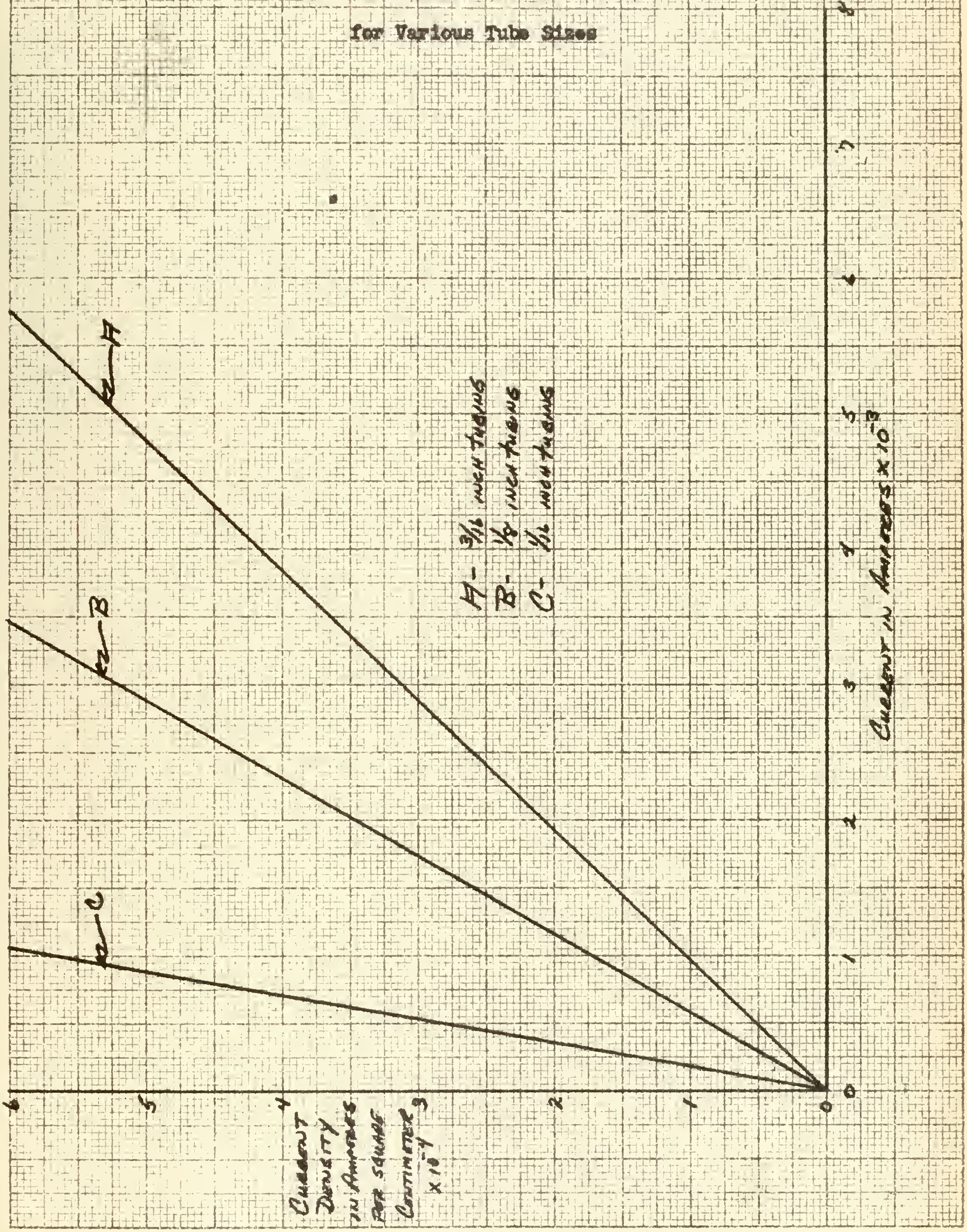

and current versus current density for the three coil sizes. From these graphs it would seem that the 1/8 inch tubing would prove to be the most satisfactory if fabrication and cooling difficulties are neglected. From the latter standpoints, however, it was felt that preliminary investigations should be made utilizing the 3/16 inch tubing.

Several coils were constructed of the 3/16 inch tubing. These coils differed slightly from the final design so that measurement could be made of the wall temperature during operation. Tests were run on these coils, and the following quantities recorded: inlet and outlet cooling water temperature; coolant flow rate; inlet and outlet tubing wall temperature; magnetic flux density at the center of the coil; current through and voltage drop across the coil. Currents up to 4,000 amperes were passed through these coils without difficulty. Various rates of coolant flow through the coil were used, and it was found that a relatively low flow rate provided adequate cooling. The measured values of magnetic flux density for the single pancake coil were surprisingly close to the calculated values, as can be seen in Fig. 6B. A plot of the temperature ratio corrected for flow rate, Fig. 7B, has been made for three coolant flow rates. From this figure it appears that by increasing the flow rate, the current could be materially increased without damage to the coils.

During the above investigation, it was obvious that the coolant pressure drip across the coil was quite large. In an attempt to determine if this drop could be materially decreased by re-designing

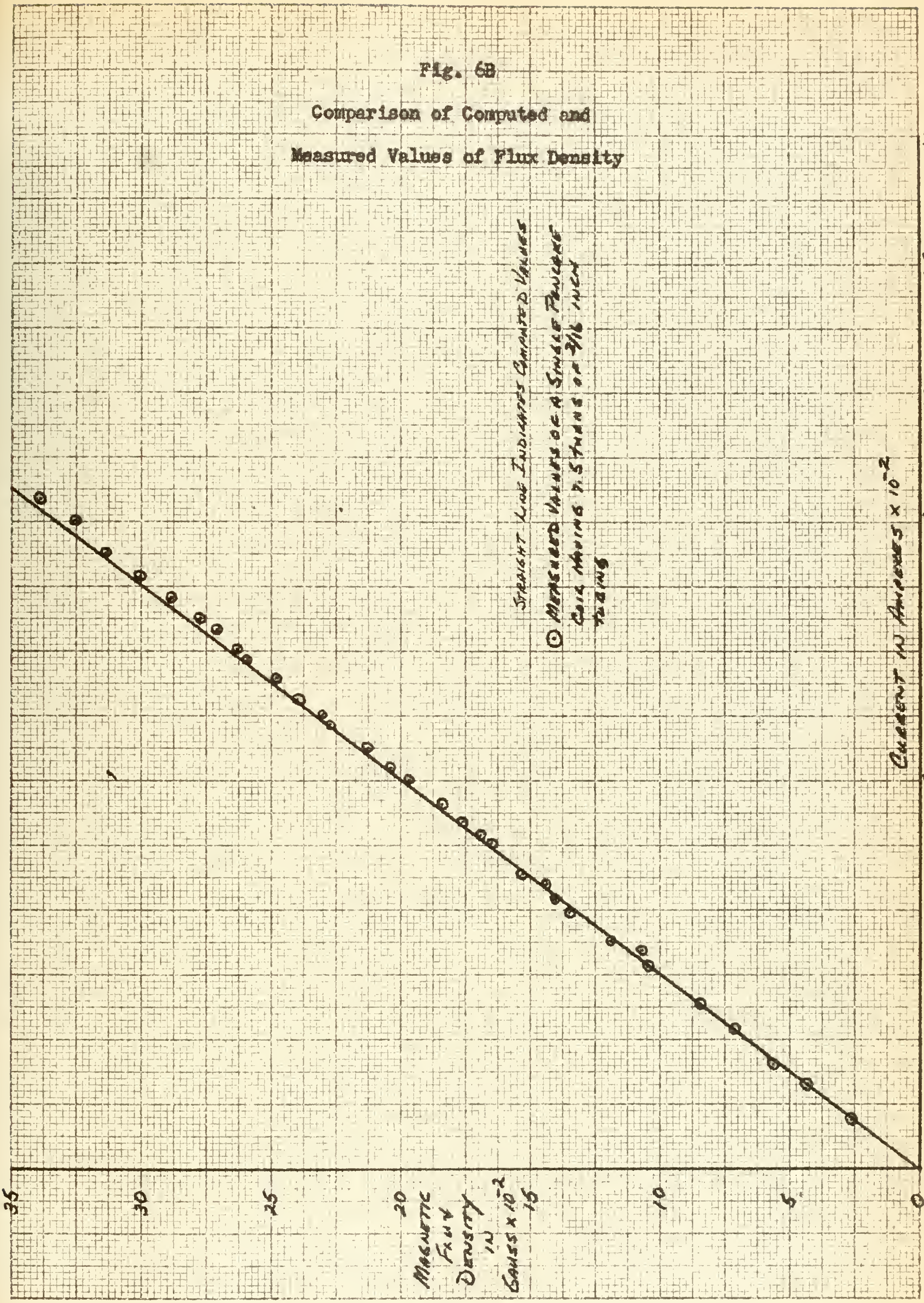

Fig. 6B

Comparison of Computed and Measured Values of Flux Density

Fig. 7B

Temperature-Flow Ratio Versus Current for Refrigeration Tubing

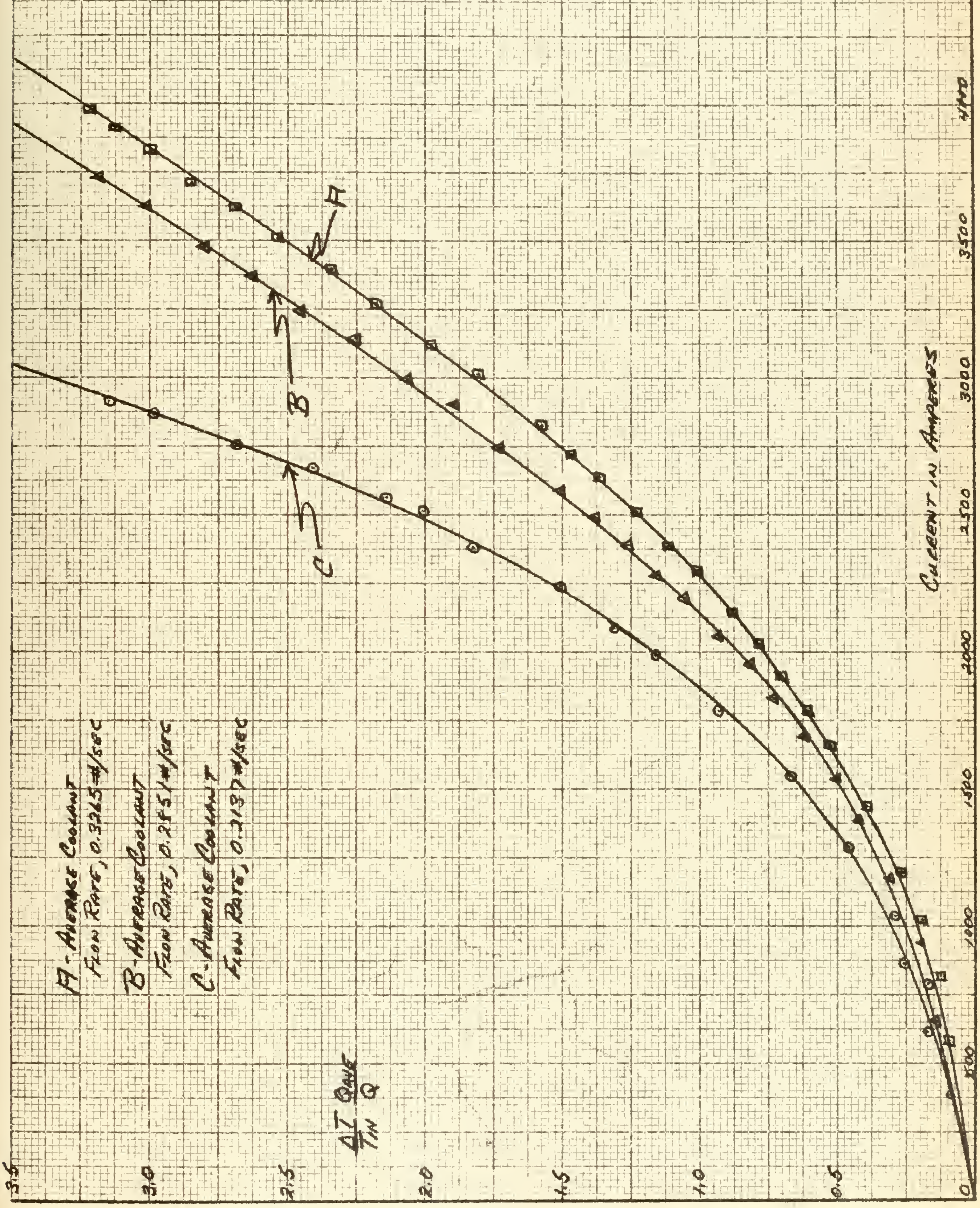

the coil connecting blocks, runs were made with the coil as designed; then with an equivalent length of straight tubing fitted with end connector blocks; and finally with a straight length of tubing having no impediments. The plotted values resulting from this investigation are shown as Fig. 8B. As can be seen from the figure, the tube itself is responsible for the major portion of the pressure drop, and the effect of coiling, and end block connectors is slight. Fig. 9B, a plot of pressure drop versus flow rate, has been included to show the pressure drop which could be expected at high flow rates. From the foregoing investigation, it can be seen that the 1/8 inch tubing would most certainly require a high pressure pump if adequate coolant flow were to be maintained.

Figs. 10B, 11B and 12B show the various set ups used in making the coil tests.

Fig. 8B

Pressure Characteristic of Water

Through 3/16 inch Refrigeration Tubing

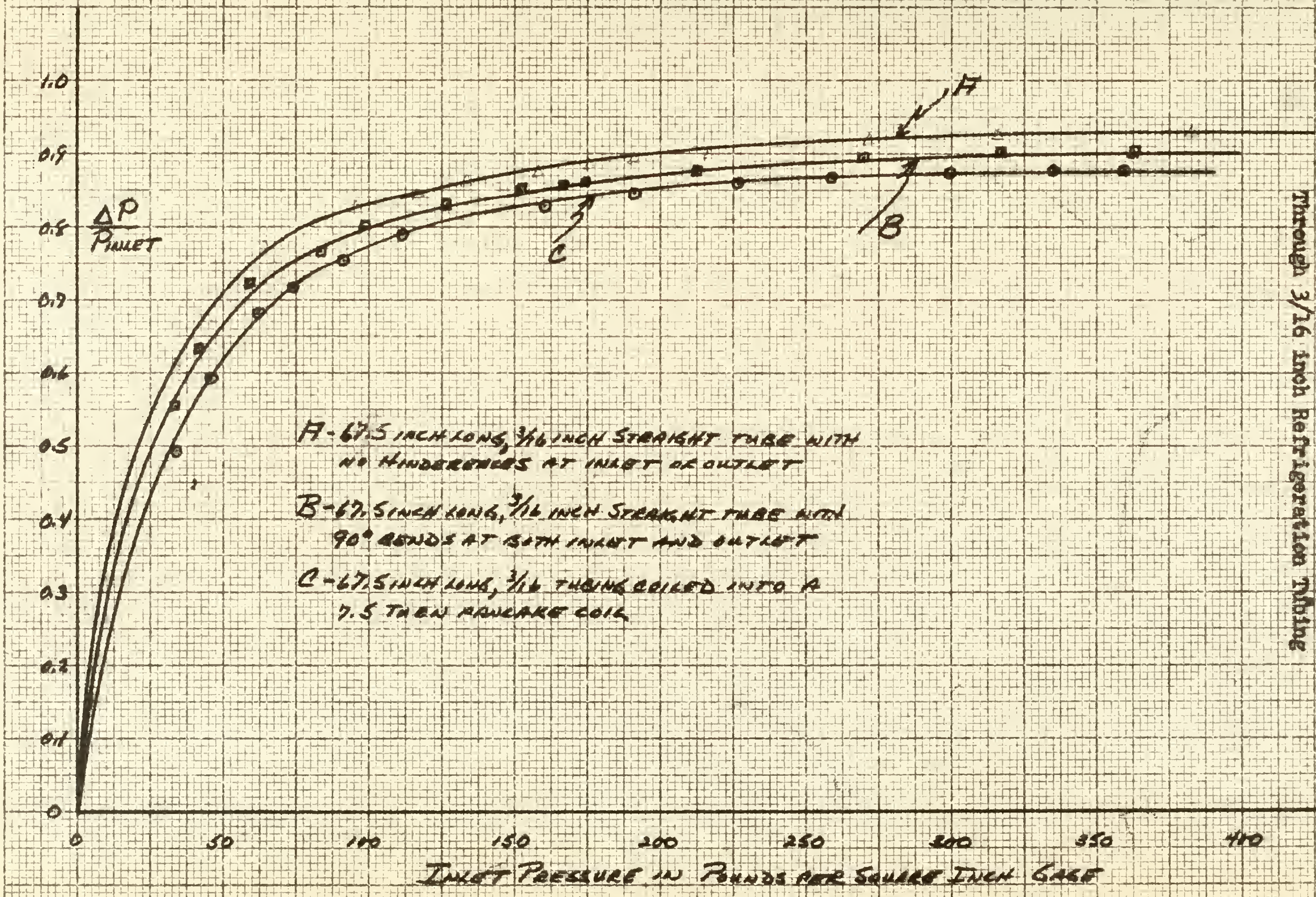

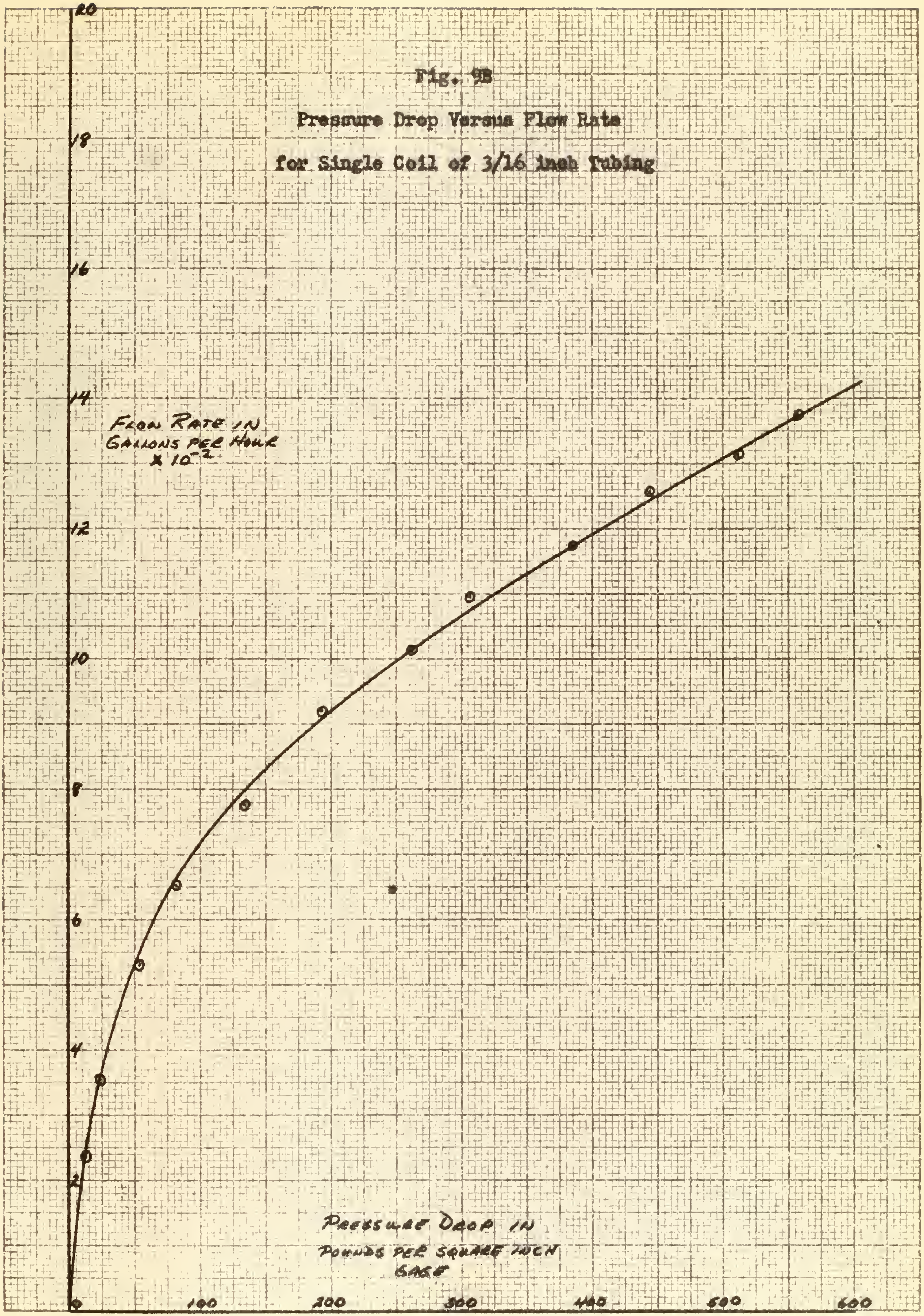

Fig. 9B

Pressure Drop Versus Flow Rate

for Single Coil of 3/16 inch Tubing

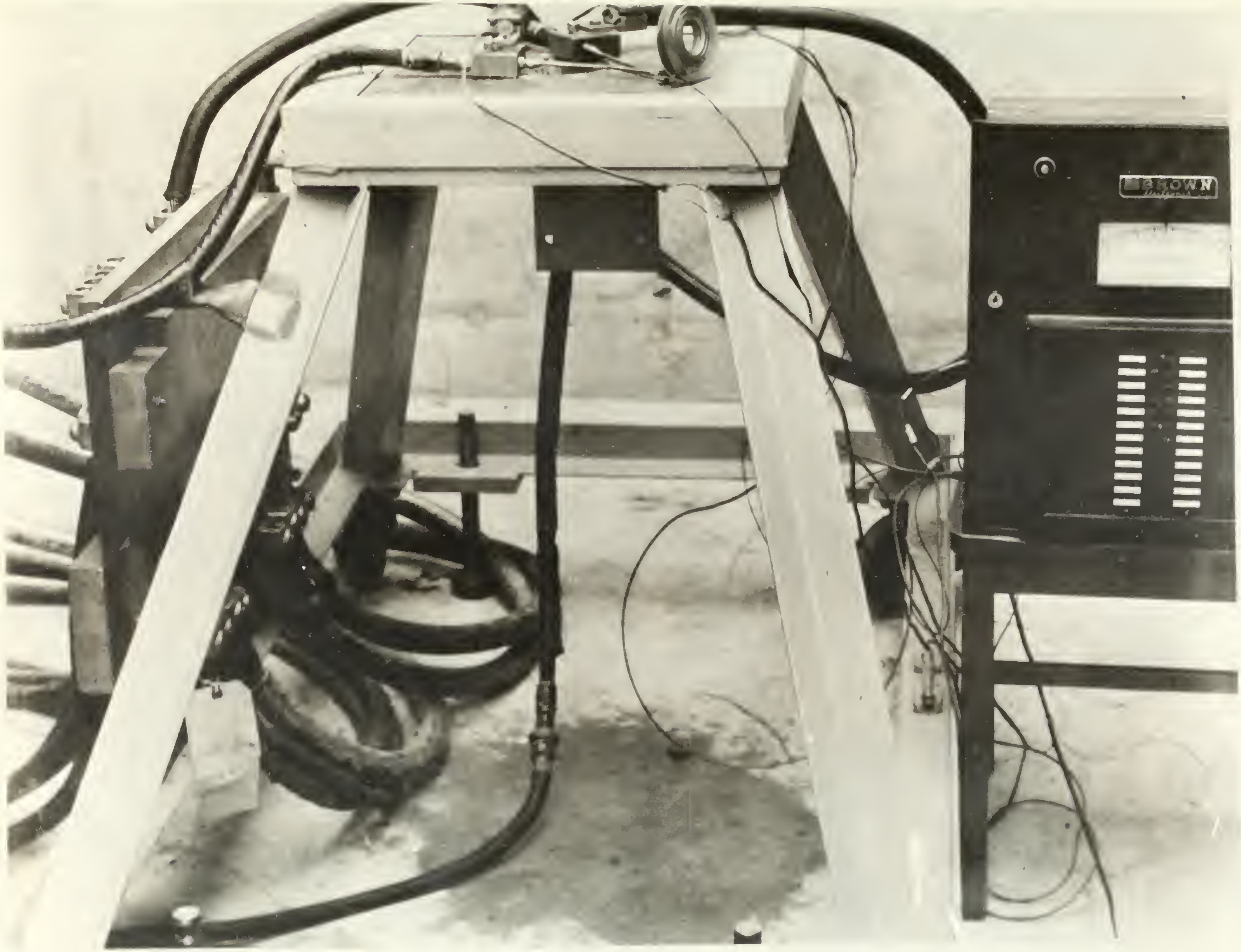

Fig. 10B Coil Test Set Up

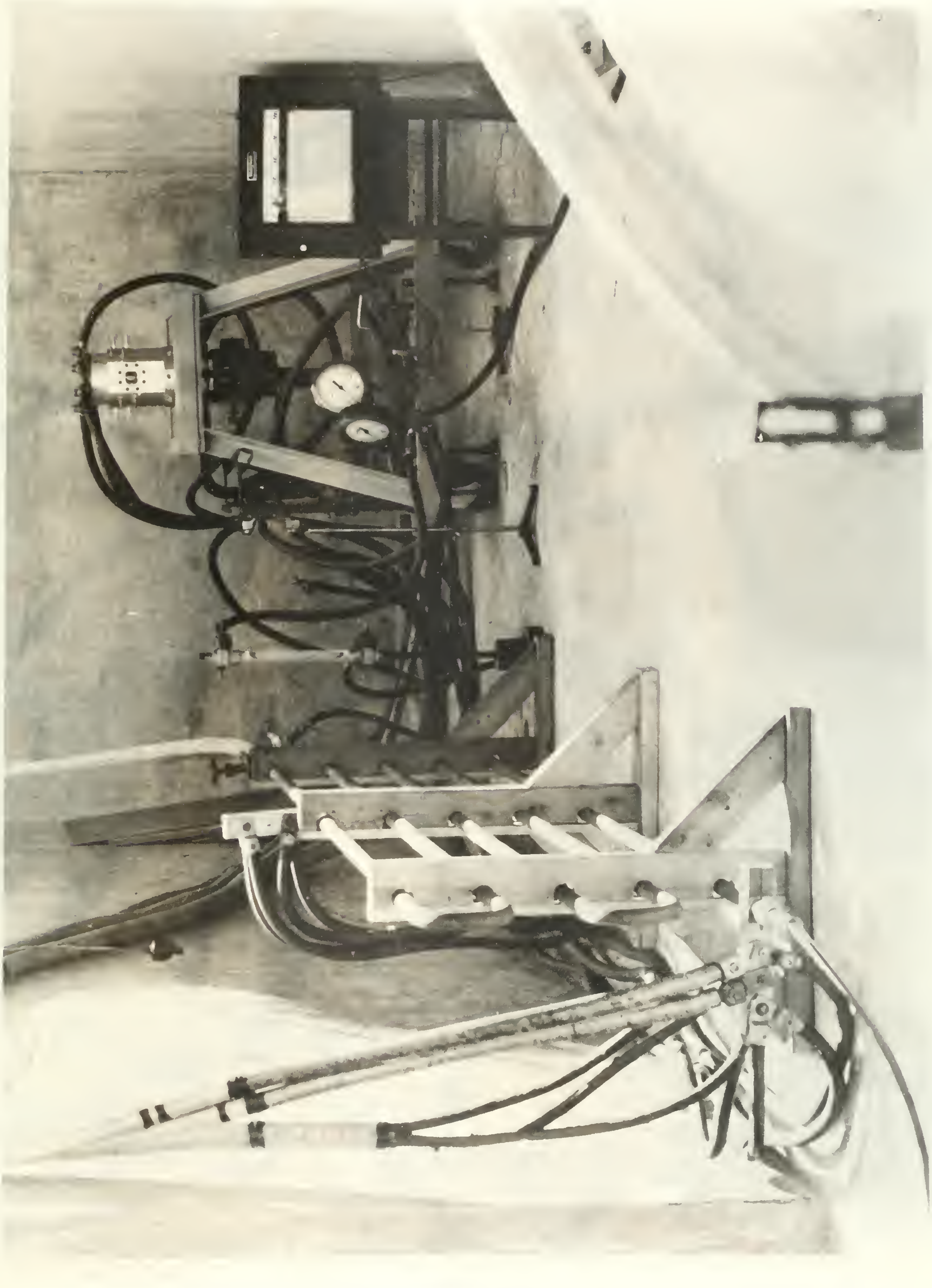

Fig. 113 Coil Test Set Up

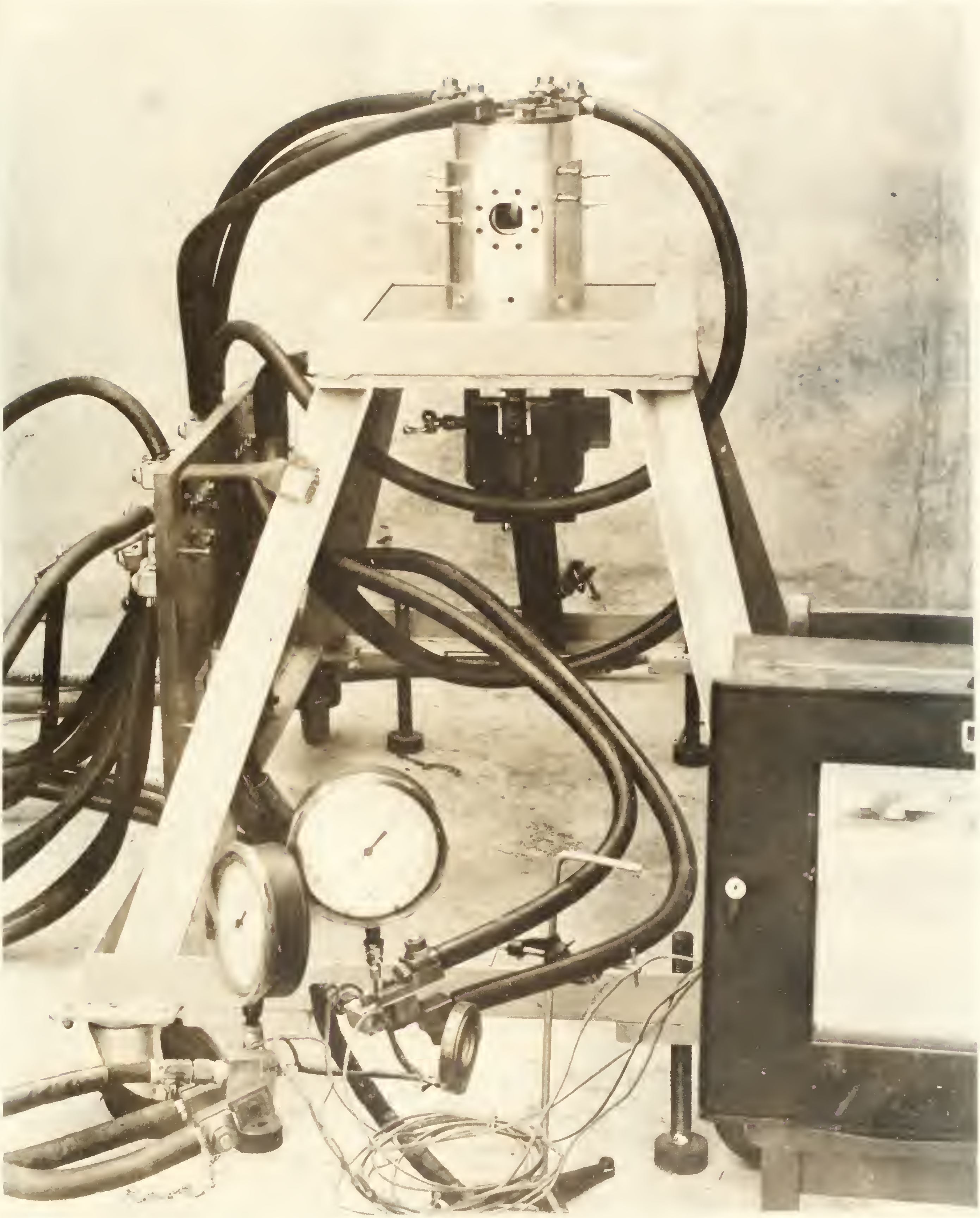

Fig. 12 [illegible] Test [illegible]

APPENDIX C

Conclusions Based Upon Model Swirl Chamber Investigation

A model of the swirl chamber was constructed to determine the conditions necessary for obtaining a satisfactory core within the plasma jet chamber. The following conclusions were arrived at for this device.

1. No core will exist if a pressure drop does not exist across the diaphragms.

2. The core will position itself along a line drawn through the axis if both holes lie along the axis.

3. The lowest flow rate which will produce a satisfactory core is a function of the hole diameters.

4. All efflux can be caused to exist at the lower hole, for a vertical core, if the ratio of hole sizes is correct. For this device, the ratio of areas upper to lower was found experimentally to be about 0.15.

5. A core will exist for horizontal mounting, but this core is not as satisfactory as the core produced when the device is mounted vertically.

6. The diameter of the core can be controlled by control of hole size and flow rate.

Since no attempt was made to vary the ratio of the length of the swirl chamber to its diameter, these conclusions cannot be said to be general; however it is felt that all but the conclusion concerning the ratio of areas will hold in any configuration.

Fig. 1C is a plot of the pressure existing at various distances from the center of the chamber. Curves have been drawn for inlet pressures ranging from 20 to 120 pounds per square inch gage, for two top hole sizes, 1/8 and 1/16 inch in diameter. From this graph it can be seen that doubling the top hole size had little effect on the pressure at any station.

Fig. 1C

Swirl Chamber Pressure Distribution

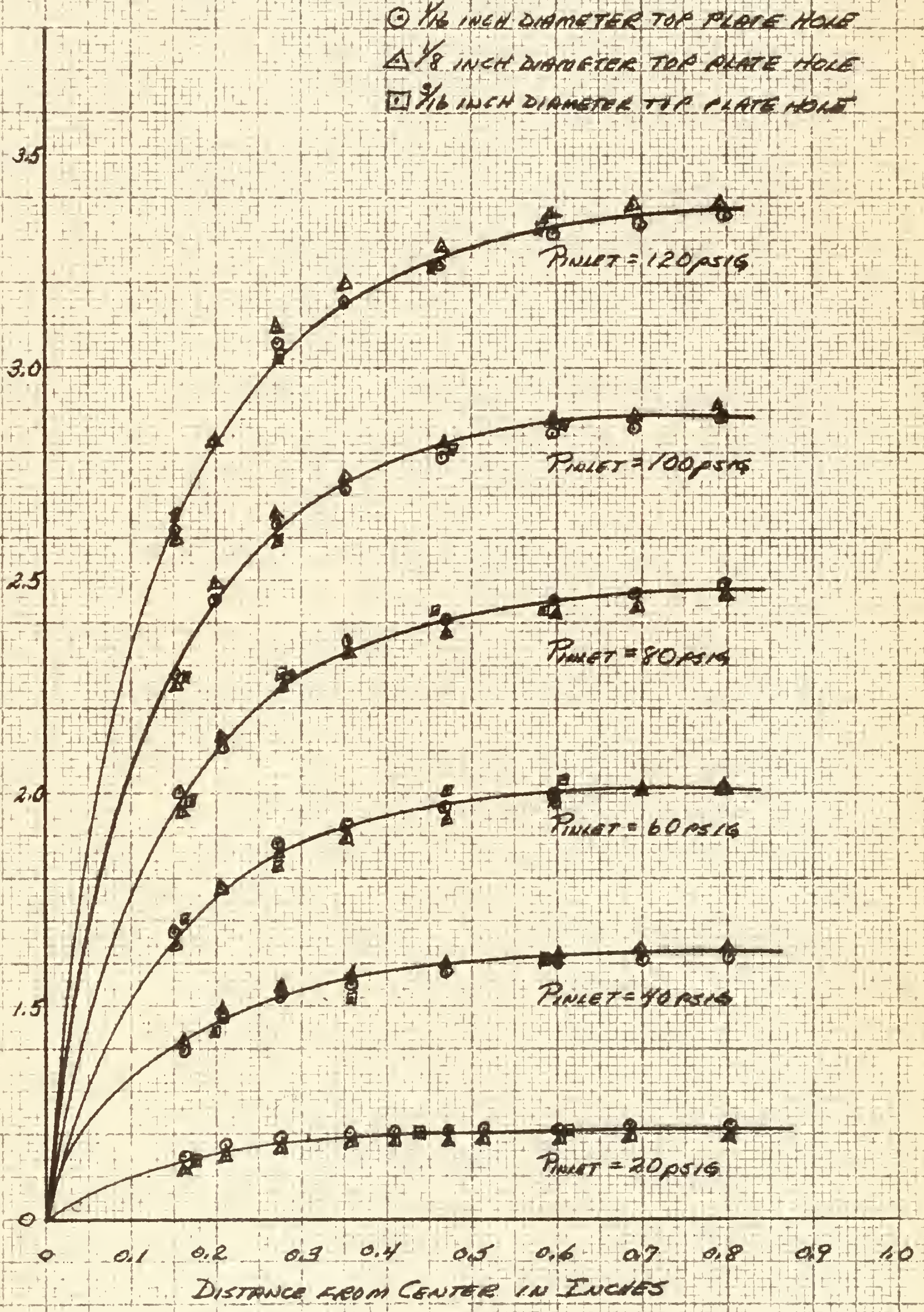

APPENDIX D

Power Generation Facilities

The electrical circuit of the plasma jet is a simple one. Fig. 1b of the main body of this report shows this circuit. Fig. 1 of this appendix is the complete wiring diagram of the plant utilized at the Naval Postgraduate School. The electrical hook-up is somewhat complicated since, in order to bring the synchronous motor on the line, it was necessary to:

1. Run the direct current generator as a motor.

2. Run the alternating current motor as an alternator.

3. Parallel the alternating current thus generated with the 440 volt supply.

4. Close the breaker shown with synchronizing lamps across its contacts.

The circuit diagram of the Hunter's Point plant differed in only two respects from that shown: the starting features of the motor driving the generator, and the fact that no external inductance was included in the arc circuit.

The electrical generating devices normally used in arc circuits are designed to have a falling volt-ampere characteristic. It is customary to connect the series field of a rotating direct current generator so as to provide differential compounding, which causes a rapid fall in the generated voltage with increasing current. In the investigation of the arc characteristic, this nonlinear variation of voltage with current would have been very

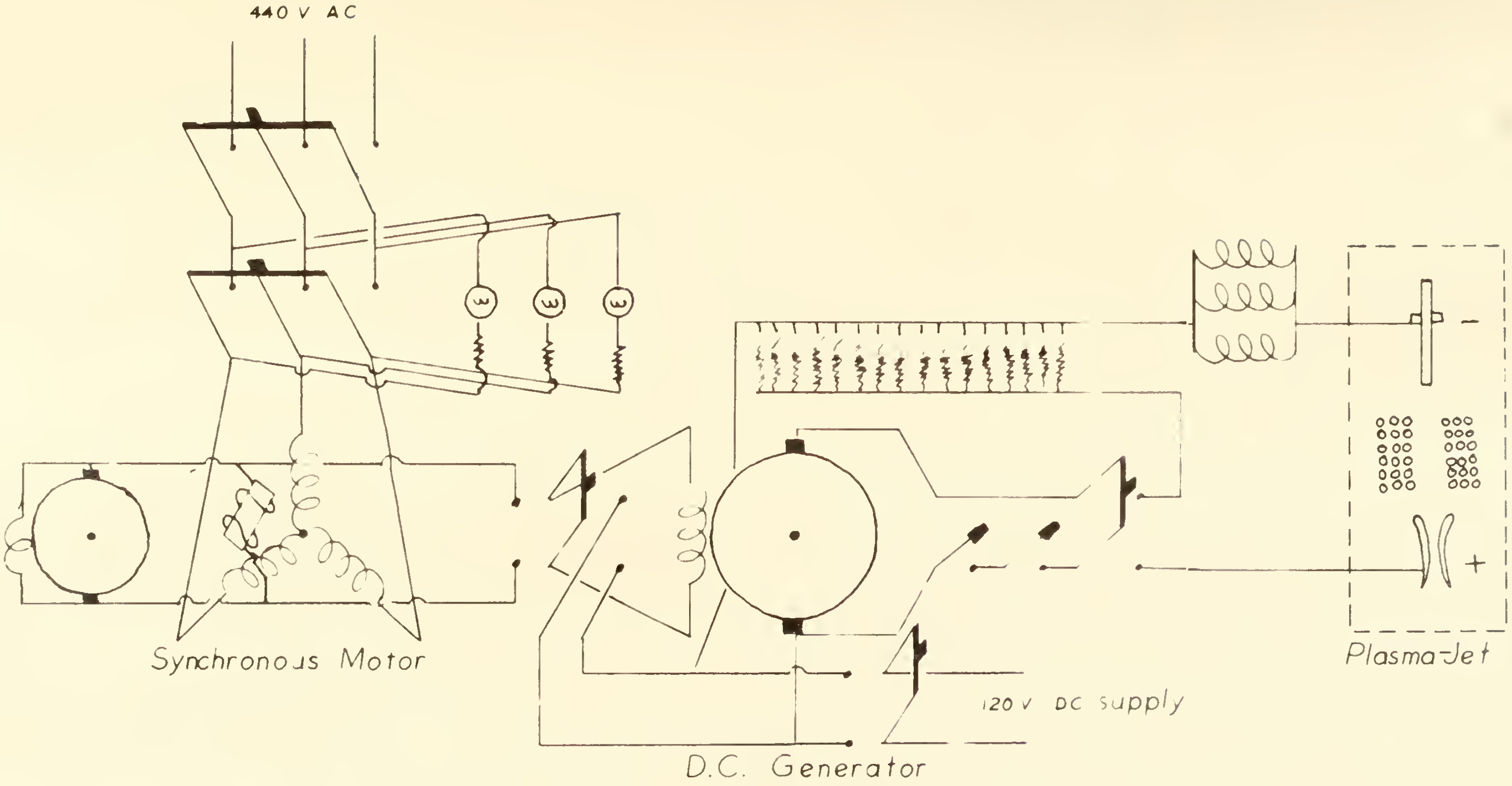

Fig 1D Wiring Diagram, Postgraduate School Power Plant

undesirable. Consequently, the series field of the generator was shunted. Figs. 2 and 3 of this appendix show the volt-ampere characteristics of the generators in the separately excited, shunted series field configuration. As can be seen the characteristic is linear, and the fall in voltage between no-load and full-load is not severe.

Figs. 4D, 5D, 6D and 7D are pictures of the Naval Postgraduate School powerplant and associated equipment. Figs. 7D, 8D, 9D, 10D and 11D are pictures of the Hunter's Point power plant, plasma jet and associated equipment.

Fig. 2D

Volt-Ampere Characteristics, Naval Postgraduate School Generator

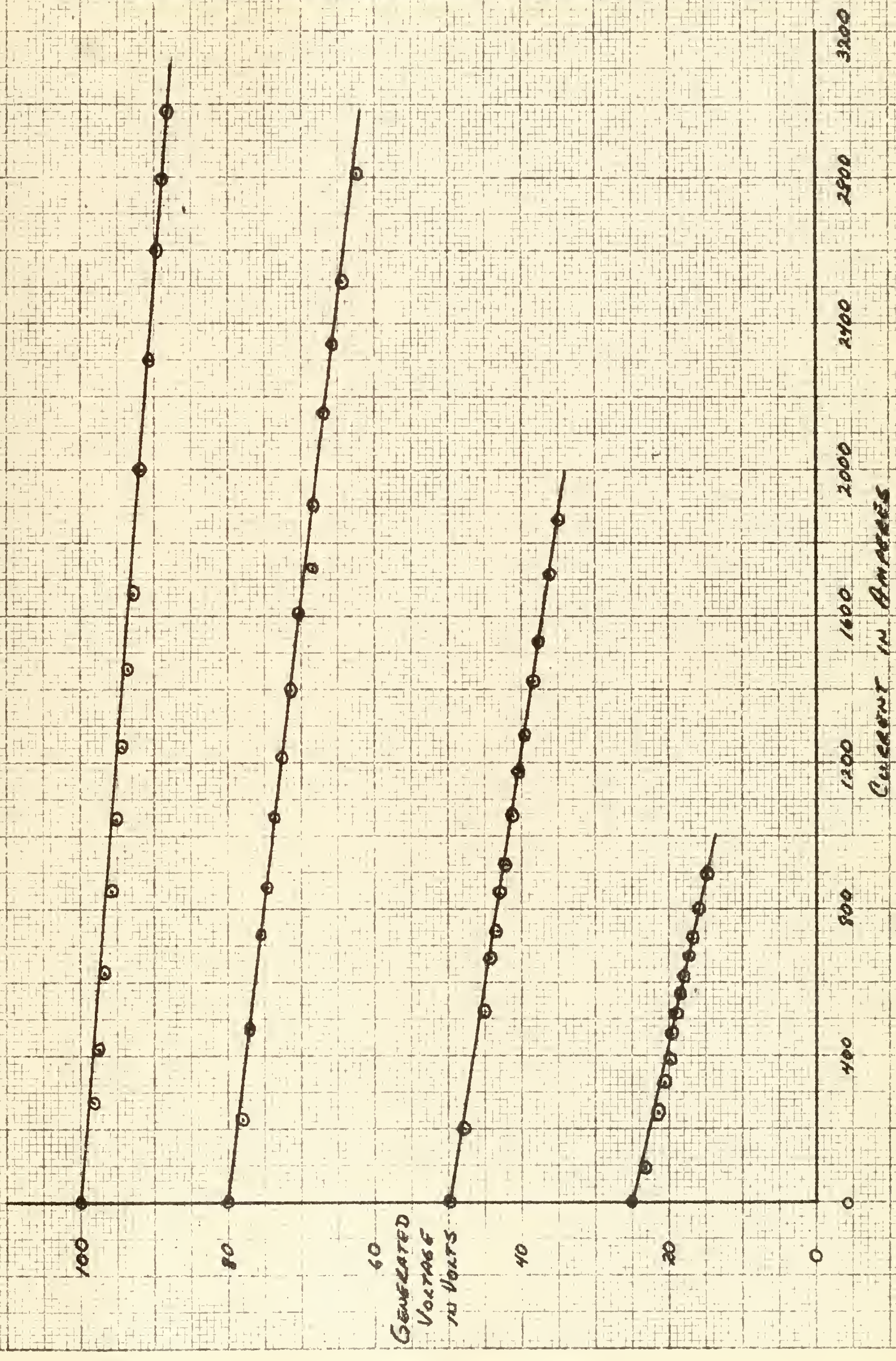

Fig. 3D

Volt-Ampere Characteristic, Hunter's Point Generator

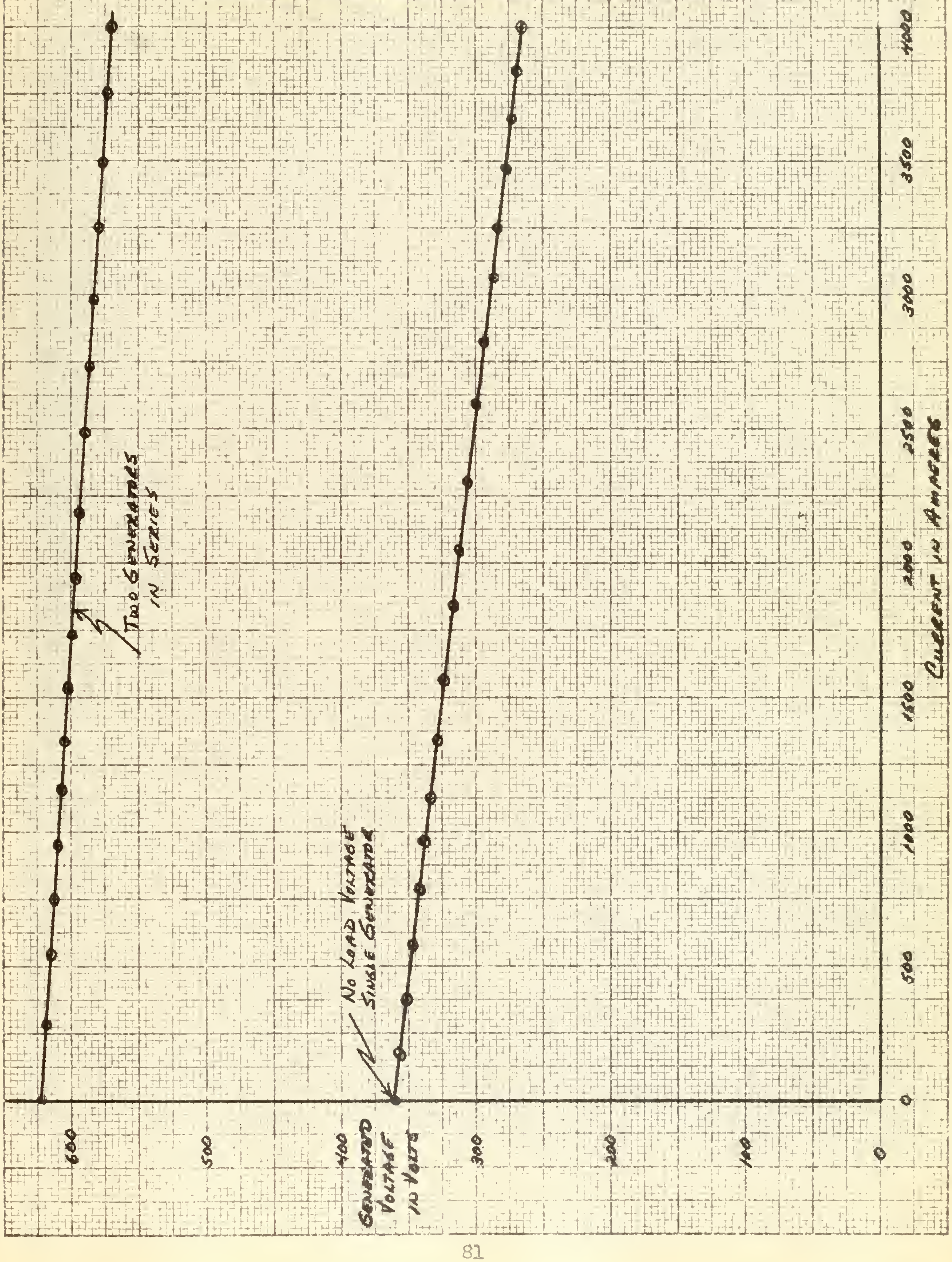

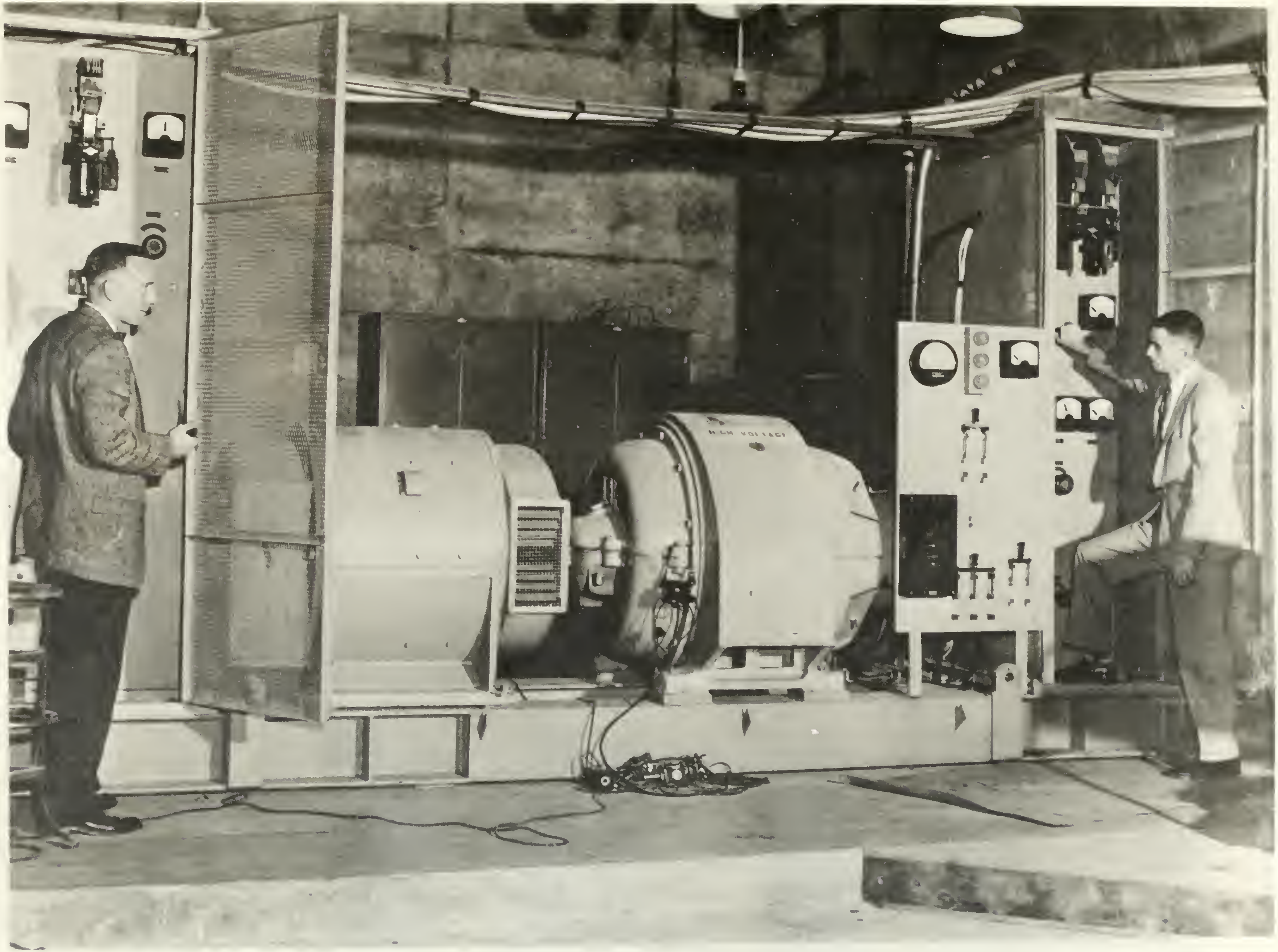

Fig. 4D Postgraduate School Power Plant

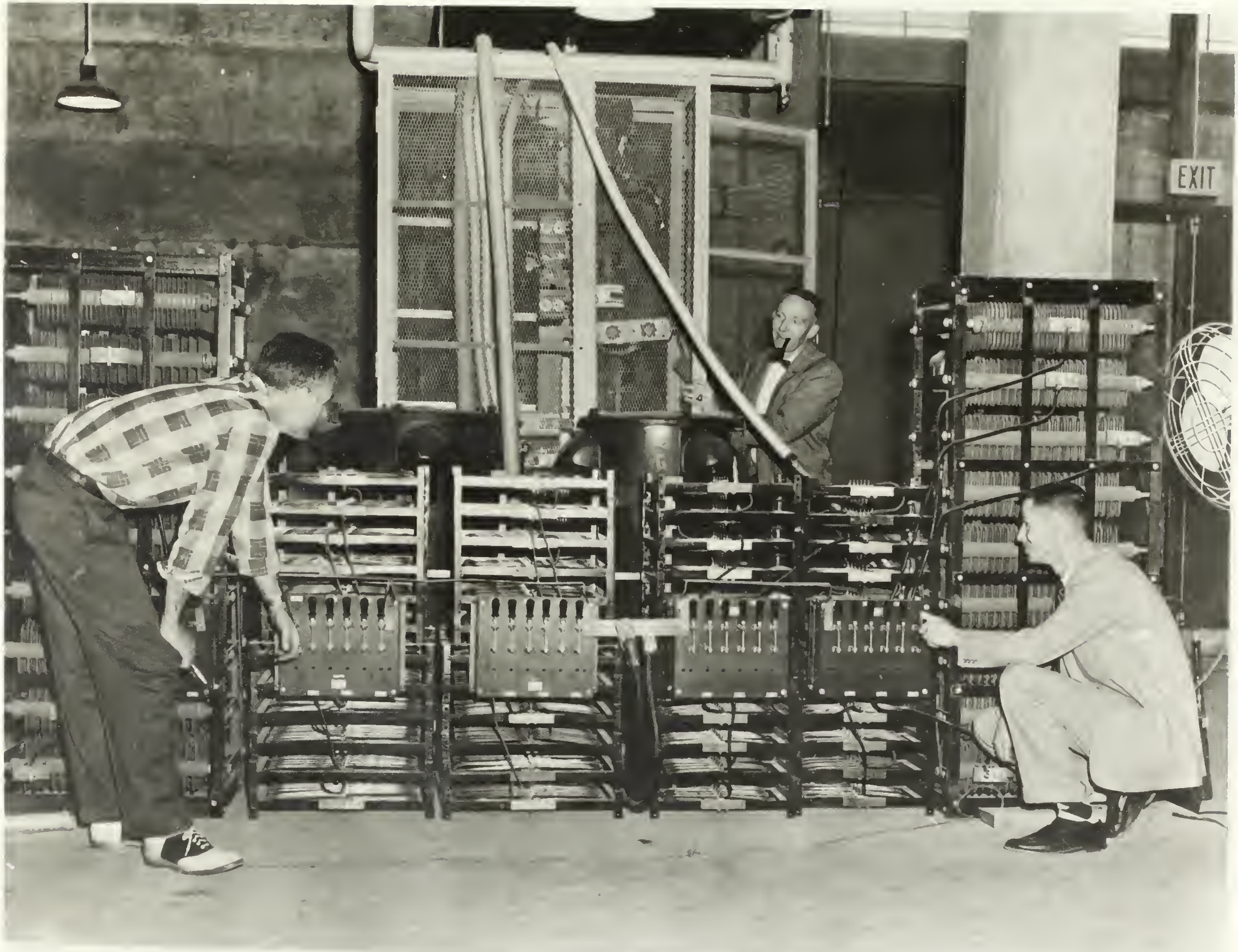

Fig. 5D Resistor Banks and Inductors
Postgraduate School Plant

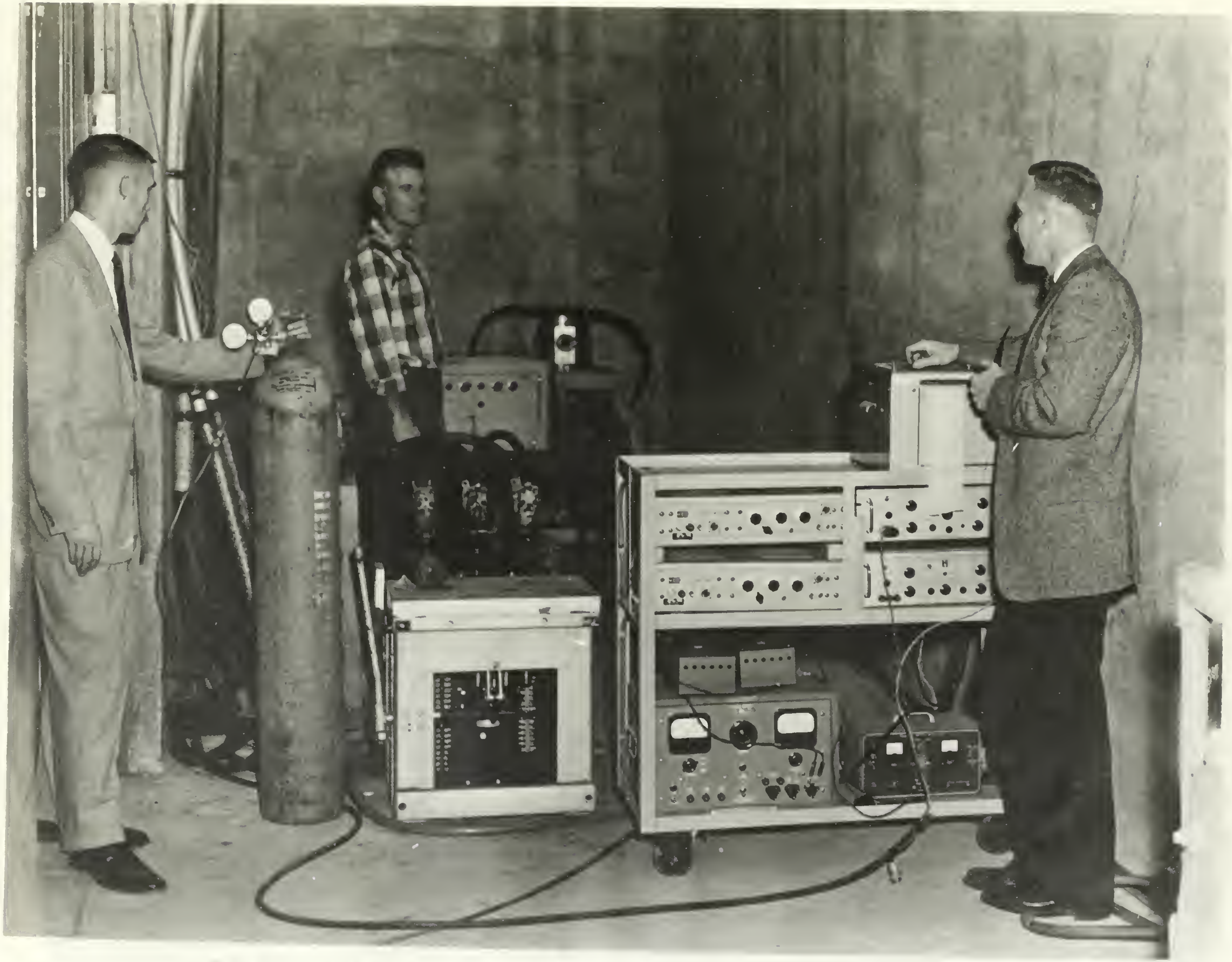

Fig. 60 Instrumentation Postgraduate School Plant

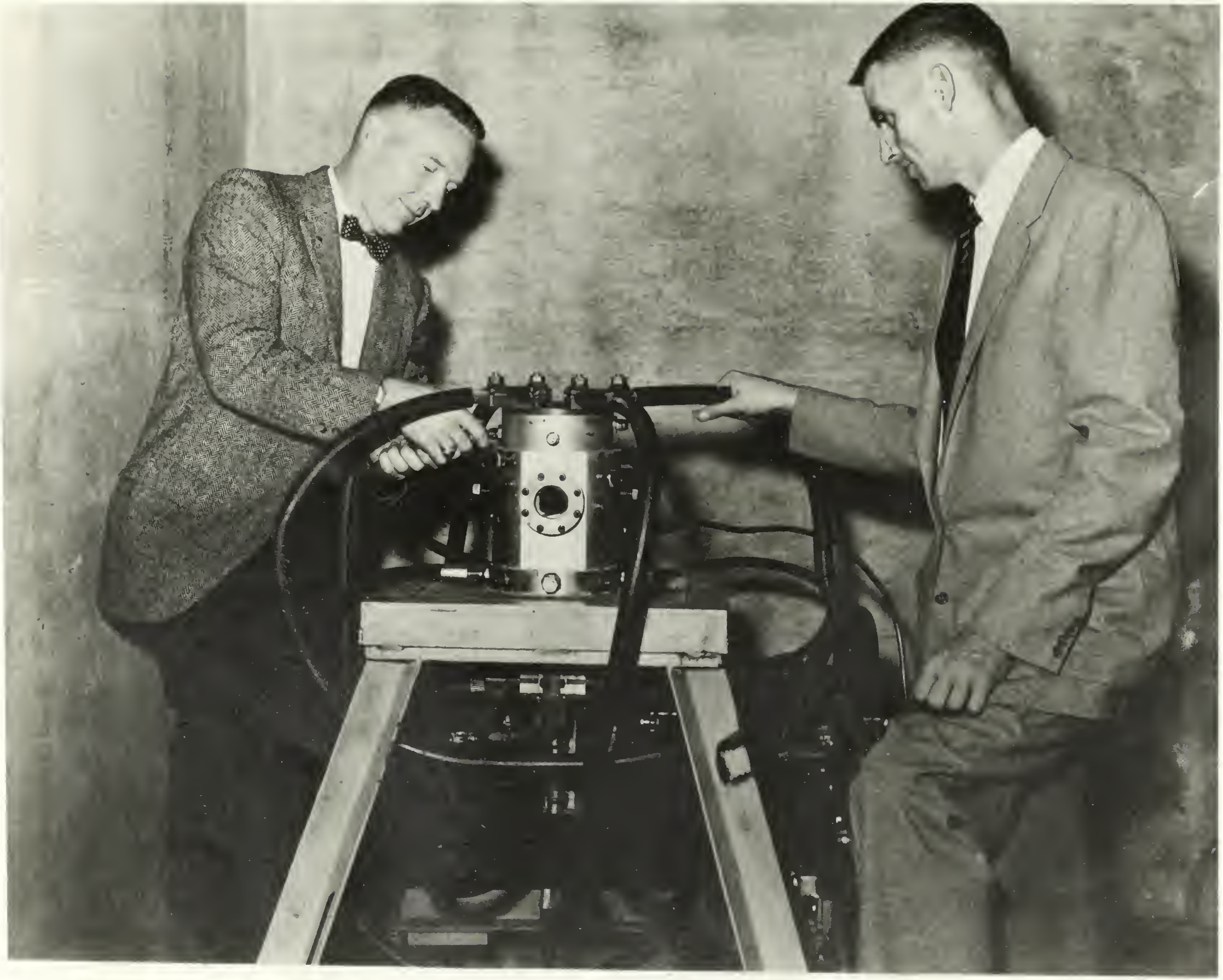

Fig. 20. Piston Jet in Current Operating Configuration

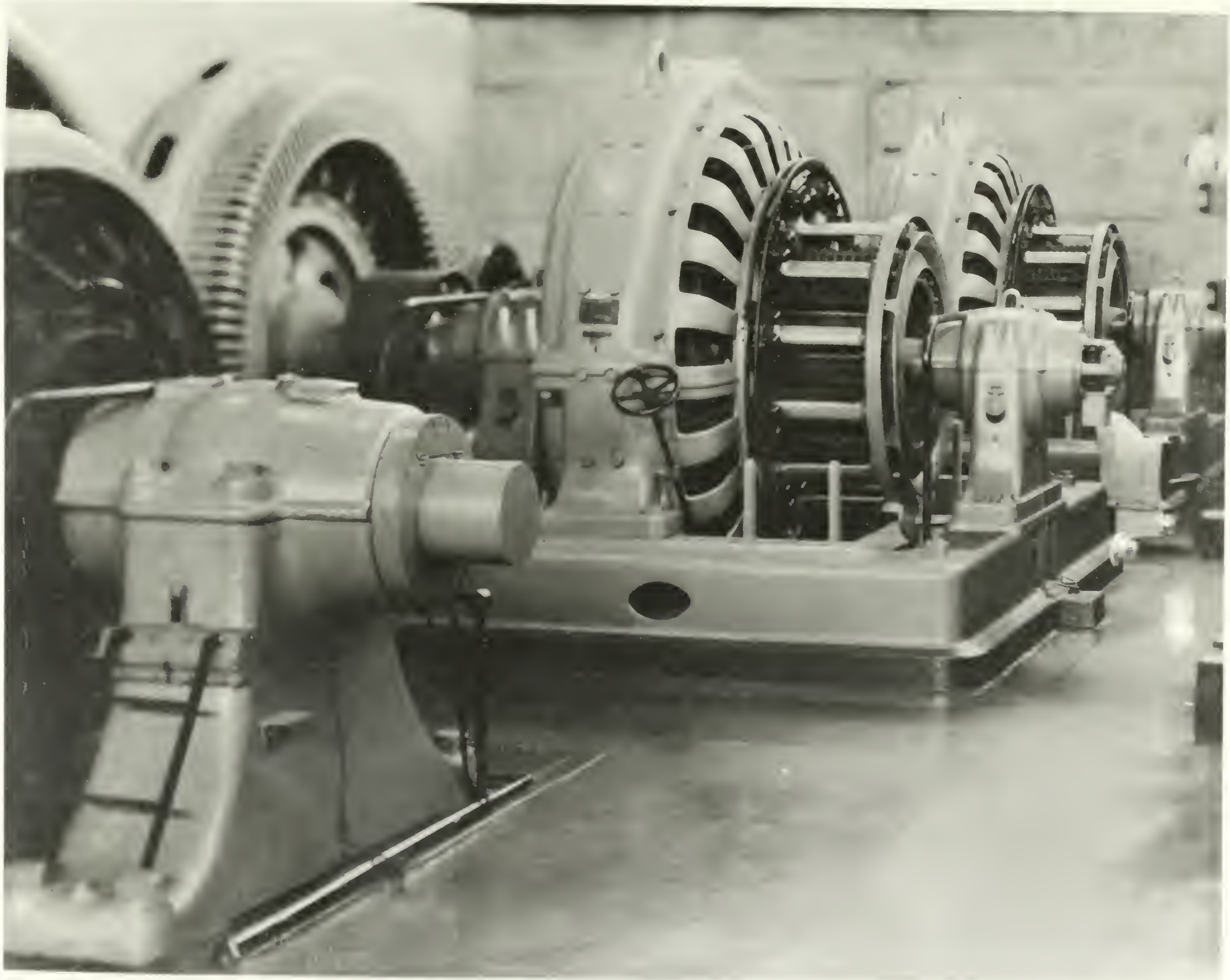

Fig. [illegible] Hunter's Point Power Plant

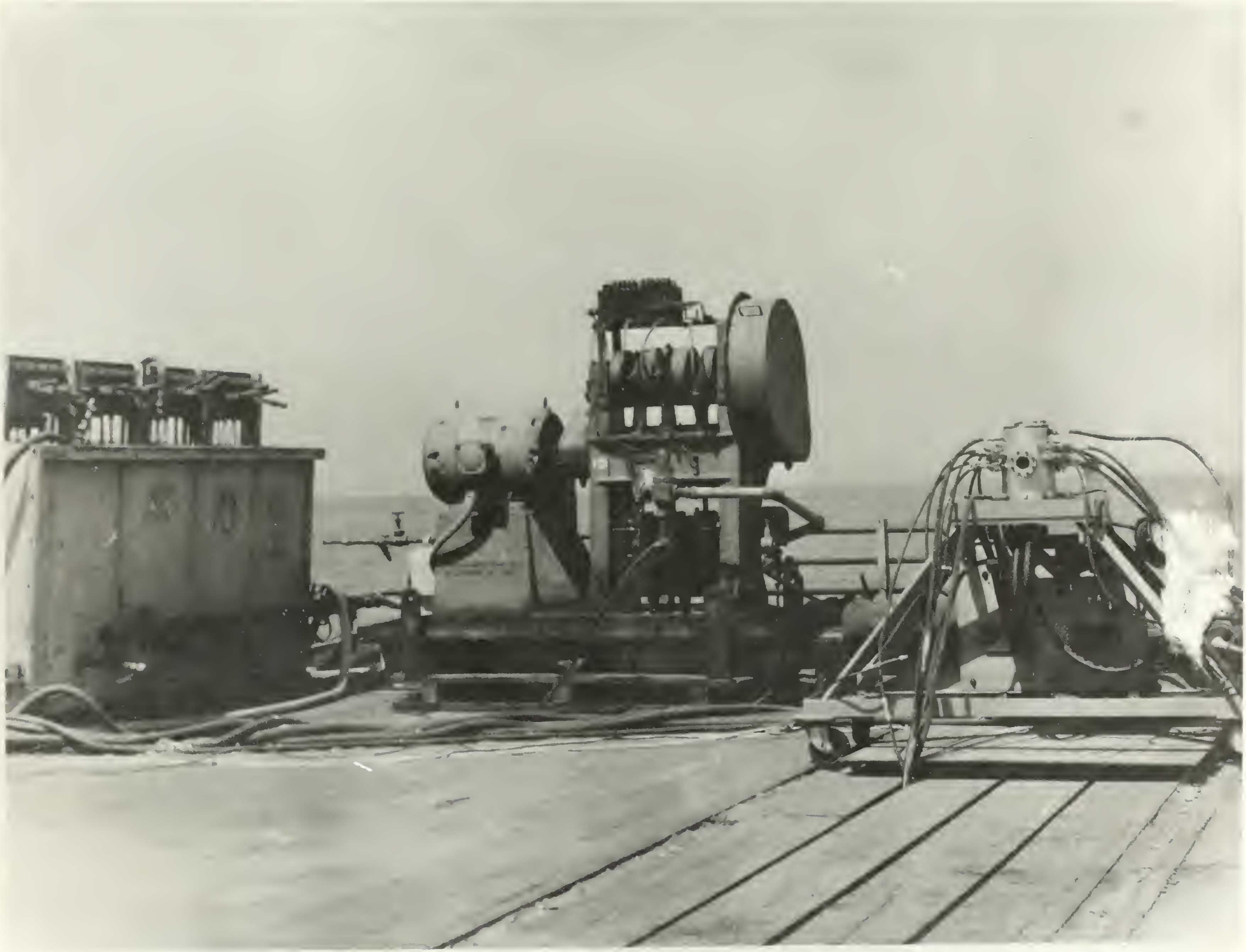

Fig. 9B Resistor Banks, Water Pump, Plasma Jet; Hunter's Point

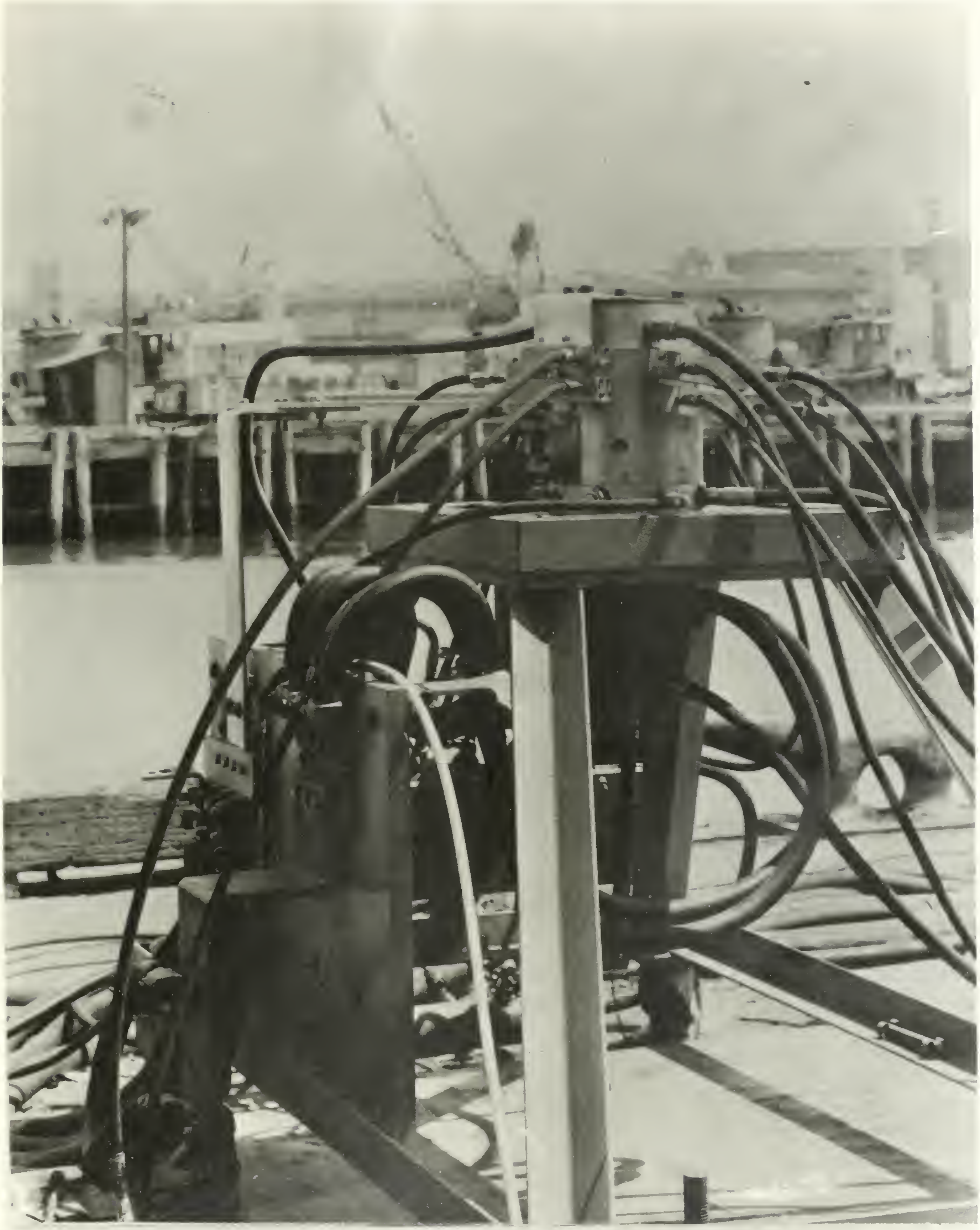

Fig. 10D Plasma Jet in Water Operation Configuration

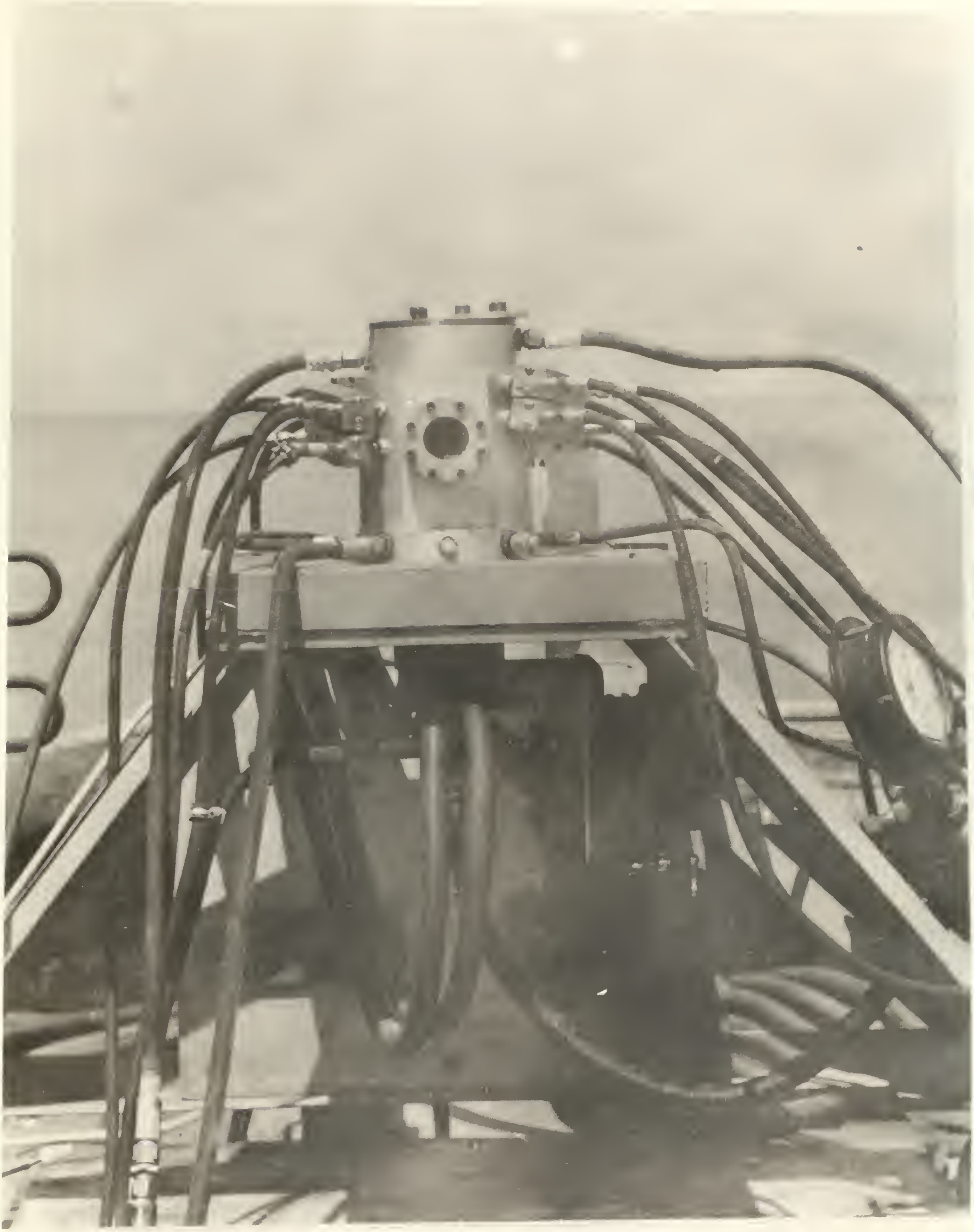

Fig. 11b Plasma Jet in Water Operating Configuration

BIBLIOGRAPHY

1. J. D. Cobine, Gaseous Conductors, Mc-Graw-Hill Book Company, New York, 1941.

2. K. K. Darrow, Electrical Phenomena in Gases, The Williams and Wilkins Co., Baltimore, 1932.

3. F. M. Penning, Electrical Discharges in Gases, Macmillan Co., New York, 1957.

4. A. von Engel, Ionized Gases, Oxford University Press, London, 1955.

5. W. Lochte-Holtgreven, Ionization Measurements at High Temperatures, Temperature, Its Measurement and Control in Science and Industry, Vol. II, H. C. Wolfe (Ed.), Reinhold Publishing Corp., New York, 1955.

6. R. W. Larenz, Temperaturmessungen in der Saule eines Gerdien-Bogens, Zeitschrift fur Physik, Band 129, Springer-Verlag, Berlin, Gottengen, Heidelberg, January-May 1951.

7. F. Burhorn and H. Maecker, Feldstarenmessungen an wasserstabilisierten Hochleistungsbogen, Zeitschrift fur Physik, Band 129, Springer-Verlag, Berlin, Gottengen, Heidelberg, January-May 1951.

8. H. Maecker, Ein zylindrischer Bogen fur hohe Leistungen, Zeitschrift fur Naturforschung, Band IIa, Verlag der Zeitschrift fur Naturforschung, Tubingen, 1956.

9. K. H. Jacobs, J. H. Bonin and P. J. Dickerman, Preliminary Investigation of Fluid-Stabilized Arcs, Summary of Available High Temperature Facilities and Some Preliminary Experimental Results, Chicago Midway Laboratories, 19 February 1958.

10. L. Spitzer, Jr., Physics of Fully Ionized Gases, Interscience Publishers, In., New York, 1956.

11. T. G. Cowling, Magnetohydrodynamics, Interscience Publishers, Inc., New York, 1957.

12. A. von Engel and M. Steenbeck, The Physics and Techniques of Electrical Discharge in Gases, University of Washington, 1950.

13. L. B. Loeb, Fundamental Processes of Electrical Discharges in Gases, John Wiley and Sons, Inc., New York, 1939.

14. K. G. Emeleus, The Conduction of Electricity through Gases, John Wiley and Sons, Inc., New York, 1951.

15. E. L. E. Wheatcroft, Gaseous Electrical Conductors, Oxford University Press, London, 1938.

16. J. S. E. Townsend, Electricity in Gases, Oxford University Press, London, 1915.

17. Sir J. J. Thomson and G. P. Thomson, Conduction of Electricity through Gases, Cambridge University Press, London, 1933.

18. L. B. Loeb and J. M. Meek, The Mechanism of the Electric Spark, Stanford University Press, Stanford University, California, 1941.

19. F. L. Arnot, Collision Processes in Gases, John Wiley and Sons, Inc., New York, 1950.

20. H. W. Liepman and A. Roshko, Elements of Gas Dynamics, John Wiley and Sons, Inc., New York, 1957.

21. A. Guthrie and R. K. Wakerling, The Characteristics of Electrical Discharges in Magnetic Fields, McGraw-Hill Book Company, New York, 1949.

22. J. M. Meek, and J. D. Craggs, Electrical Breakdown of Gases, Oxford University Press, London, 1953.

23. T. R. Hogness, Arc-Heated Plasma for Laboratory Hypersonics, Astronautics, Vol. 4, No. 3, March 1959, pp. 40-47.

24. G. M. Giannini, The Plasma Jet, Scientific American, Vol. 197, No. 2, August 1959, pp. 80-88.

25. H. P. Furth, M. A. Levine, and R. W. Wanier, Strong Magnetic Fields, Scientific American Vol. 198, No. 2, February 1958, pp. 28-33.

26. W. Lai, D. H. Sloan, and L. Talbot, Preliminary Design and Tests of a Plasma Jet, University of California, Institute of Engineering Research, Technical Report HE-150-153, 15 November 1957.

27. G. L. Cann and A. C. Ducati, Energy Content and Ionization Level in an Argon Gas Jet Heated by a High Intensity Arc, Journal of Fluid Mechanics, Vol. 4, Part 5, September 1958, pp. 529-537.

28. J. W. Reid, The Plasma Jet: Research at 25,000°F, Machine Design, 6 February 1958.

29. Ion Rockets and Plasma Jets, Air Force Office of Scientific Research, 17 April 1958.

30. W. Finkelburg and H. Maecker, Elektrische Bogen and Thermisches Plasma, Handbuch der Physik, Band XXII, Gasentladungen II, S. Flugge (Ed.), Springer-Verlag, Berlin, Gottingen, Heidelberg, 1956.

31. A. von Engel, Ionization in Gases by Electrons in Electric Fields, Handbuch der Physik, Band XXI, Gasentladungen I, S. Flugge (Ed.), Springer-Verlag, Berlin, Gottingen, Heidelberg, 1956.

32. W. P. Allis, Motions of Ions and Electrons, Handbuch der Physik, Band XXI, Gasenladungen I, S. Flugge (Ed.), Springer-Verlag, Berlin, Gottengen, Heidelberg, 1956.

33. F. Burhorn, H. Maecker and T. Peters, Temperaturmessungen am Wasserstabilisierten Hochleistungsbogen, Zeitschrift fur Physik, Band 131, Springer-Verlag, Berlin, Gottengen, Heidelberg, December 1951-March 1952.

34. E. Bagge, Gibt es angeregte Zustande bei Elementarteilchen? (Bilokale Quantentheorie des Elektrons.), Zeitschrift fur Physik, Band 135, Springer-Verlag, Berlin, Gottengen, Heidelberg, May-September 1953.

35. R. Weiss, Undersuchung des Plasmastrahles, der aus einem Hochleistubgsbogen austritt, Zeitschrift fur Physik, Band 138, Springer-Verlag, Berlin, Gottengen, Heidelberg, June-September 1954.

36. H. Maecker, Ein Lichtbogen fur hole Leistungen, Zeitschrift fur Physik, Band 129, Springer-Verlag, Berlin, Gottengen, Heidelberg, January-May 1951.

thesG253
Plasma jet electrical characteristics /
3 2768 002 02528 0
DUDLEY KNOX LIBRARY